UNCLASSIFIED

DEFENCE RESEARCH ESTABLISHMENT
CENTRE DE RECHERCHES POUR LA DÉFENSE
VALCARTIER, QUÉBEC

DREV - TR - 1999-099

Unlimited Distribution / Distribution illimitée

THE L(W)WKD MARINE BOUNDARY LAYER MODEL VERSION 7.09

by

J.L. Forand

September/septembre 1999

Approved by/approuvé par

Gabriel Ouellet

Section Head/Chef de section

16 Aug. 99

Date

SANS CLASSIFICATION

WARNING NOTICE

The information contained herein is proprietary to Her Majesty and is provided to the recipient on the understanding that it will be used for information and evaluation purposes only. Any commercial use, including use for manufacture, is prohibited. Release to third parties of this publication or of information contained herein is prohibited without the prior written consent of DND Canada.

© Her Majesty the Queen in Right of Canada as represented by the Minister of National Defence, 1999

ABSTRACT

The objective of this report is to bring up to date the present state of DREV's L(W)WKD model. Important changes to the L(W)WKD program have recently been made as a result of exchanges of both models and experimental data between Canada and France during the last few years. This has led to an agreement on a common set of equations and options that are somewhat different from those used in earlier versions of L(W)WKD and in earlier versions of the French model, PIRAM.

The first part of the report discusses changes to the basic scaling equations that are used in the L(W)WKD model, and the iterative method employed. It also discusses changes to the equations that relate the parameters produced by the basic scaling equations to meteorologically important parameters, and to the model used to calculate the refractive index profiles from the visible to the far infrared. The second part describes the additions and changes to the program's modes of operation, its new options, outputs, and compilation modes. The third part of the report presents some typical examples of the results obtainable using the program and a new analysis of the MAPTIP data. Finally, some conclusions and future improvements to the model are discussed.

RÉSUMÉ

Ce rapport a pour objectif de présenter les mises à jour récentes du modèle L(W)WKD du CRDV. Des changements importants ont été apportés au cours des dernières années, principalement à la suite du programme de coopération entre le Canada et la France portant sur la modélisation de la propagation électromagnétique à la surface de la mer. En particulier, le CRDV et le CELAR, en France, se sont entendus sur une modélisation commune qui diffère de celle que l'on retrouve dans la version originale de leurs modèles respectifs: L(W)WKD au CRDV et PIRAM au CELAR.

Dans la première partie du rapport, on présente les équations fondamentales et la méthode itérative employée dans L(W)WKD pour le calcul des paramètres physiques intermédiaires qui décrivent les propriétés de la couche de surface et des profils de température et d'humidité désirés. On y discute aussi du calcul du profil d'indice de réfractivité du visible jusqu'à l'infrarouge lointain. Dans la deuxième partie du rapport, on décrit les ajouts et les changements apportés au code informatique: modes d'opération et de compilation, options nouvelles, entrées-sorties, etc. Dans la dernière partie on presente des exemples de calcul et une nouvelle analyse des données de MAPTIP. Finalement, on discute en conclusion des améliorations futures prévues au modèle.

TABLE OF CONTENTS

ABSTRACT/RÉSUMÉ i

EXECUTIVE SUMMARY v

1.0 INTRODUCTION 1

2.0 L(W)WKD MARINE BOUNDARY LAYER MODEL 2
2.1 Scaling Equations 3
2.2 Meteorological Equations 6
2.3 Solving the Basic Scaling Equations 10
2.4 Iterative Algorithm 13
2.5 Wavy Model 18
2.6 Refractive Index 19
2.7 Structure Parameters 25

3.0 THE L(W)WKD PROGRAM 29
3.1 INTERACTIVE Program 32
3.2 BATCH Programs 51

4.0 EXAMPLES 58

5.0 MAPTIP Comparisons 62

6.0 CONCLUSIONS 70

7.0 ACKNOWLEDGEMENTS 84

8.0 REFERENCES 84

APPENDIX A 87

APPENDIX B 91

FIGURES 1 to 15

TABLES I to XVIII

EXECUTIVE SUMMARY

Due to new electro-optic (EO) sensors, such as IRST (infrared search and track) systems, that are planned for use by today's military, and the need for tactical decision aids (TDAs) for such systems, the propagation of electromagnetic radiation through the atmosphere is a question of extreme importance and relevance. As the atmosphere's refractive index varies with pressure, temperature and water vapour content, all radiation follows a curved path. Straight line propagation is only possible in non-refractive atmospheres where the index of refraction is absolutely uniform. This means that, in general, the apparent elevation angle of a target as seen by an observer is not that given by the straight line between the target and the observer. This leads to two phenomena. The first is the phenomenon commonly called sub-refraction. It occurs when electromagnetic radiation from a source is bent away from the surface of the earth. This can lead to mirage effects, where an observer can detect a single source at two different elevation angles. The second phenomenon is called super-refraction and occurs when electromagnetic radiation from a source is bent towards the surface of the earth, such that an observer can detect a source beyond the geometrically defined horizon. The strength of these phenomena is dependent upon both the meteorological conditions and the radiation's wavelength. In the maritime environment, this means that under some conditions the distance to the visible horizon for an observer can be shorter than the distance to the geometric horizon (sub-refraction), while under other conditions it can be further than the geometric horizon (super-refraction or ducting). Knowledge of the distance to the visible horizon is very important for determining the maximum distance at which an object can be detected or tracked, and consequently, for determining the maximum amount of time available for making decisions.

At DREV we have been developing the L(W)WKD model for predicting the effect of atmospheric refraction on image distortion, target detection range, ducting and mirage formation in the marine environment over the last 10 years. Recently, important changes have been made to many of the fundamental equations that make up the model as a result of exchanges between Canada and France. This exchange has culminated in our agreement on a common set of equations and options that have been integrated into Version 7.09 of Canada's L(W)WKD code and France's PIRAM code. Thus, this report is designed to document this commonality and to remark on the changes from the previous L(W)WKD versions. Changes to the operation of the program are also discussed, examples of the results obtainable using the new model, and a new analysis of the MAPTIP data are also provided along with some general conclusions and suggestions for future improvements.

1.0 INTRODUCTION

At DREV we have been developing marine boundary layer (MBL) models and programs for the last 10 years. One such model, the L(Wavy), Walmsley, KEL, DREV or L(W)WKD model (Ref. 1), has been developed to produce vertical profiles of the refractivity, the air temperature, the refractivity structure parameter, and other profiles given a specific set of meteorological parameters. These profiles, can then be used by other programs to predict the imaging characteristics of the marine boundary layer. For example, refractivity profiles can be used by ray-tracing programs to predict whether or not an imager will detect a secondary image (mirage) of a missile flying at a height of 5 m above the wave tops at a range of 15 km (Ref. 2).

DGA (France) has also been developing a MBL model called "Profils d'Indice de Réfraction en Atmosphère Marine" or PIRAM (Ref. 3, 27), whose outputs have been compared with those from L(W)WKD since the MAPTIP trial in 1993 (Ref. 2). As a result of many technical exchanges between Canada and France, an agreement has recently been obtained on a common set of equations and options that should be used in both the L(W)WKD model and the PIRAM model.

This report describes this common set of equations and options, and comments on the changes this has produced between the previous versions of L(W)WKD (prior to Ver. 7) and the current version. The first part of the report discusses the basic scaling equations that are derived from the similarity theory of Monin and Obukhov (Ref. 4 & 5) for the near-surface atmosphere, methods for their solution, and the iterative method used to determine a solution for the L(W)WKD model. It also presents the relationships between the conservative variables used by the basic scaling equations with the more commonly measured meteorological parameters. DREV's technique of incorporating the effect of waves into the model is also presented. Following this, it discusses the development and validity of a formula for the calculation of the refractive index profiles from the visible to the

far infrared (Refs. 1, 6 & 7). It ends by presenting a method to calculate various structure parameters that are useful for determining the amount of turbulence within the MBL.

The second part of the report describes, in detail, the structure and operation of the L(W)WKD program. The program can now be compiled into three different executables. The two BATCH executables are designed to be easily integrated, as separate modules, into modular programs such as IRBLEM (Infrared Boundary Layer Model)(Ref. 8); while as an INTERACTIVE executable, it is designed to allow the user to control all aspects of the program, and to generate quick graphical and textual outputs of many parameters for further analysis. The LWWKD BATCH executable produces vertical profiles of the refractive index, while the WKDCN2 BATCH executable produces vertical profiles of the refractive index structure parameter.

The report concludes with the presentation of some typical examples obtained using the L(W)WKD program, and a new analysis of some of the data obtained during the Marine Aerosol Properties and Thermal Imager Performance (MAPTIP) trial (Ref. 2,15)

Finally, it presents some conclusions, and discusses various areas for future improvements in the L(W)WKD model.

This work was carried out at DREV between May 1998 and June 1999 under work unit 1AB11, Propagation Effects in the Marine Boundary Layer.

2.0 L(W)WKD MARINE BOUNDARY LAYER MODEL

The L(W)WKD model (Ref. 1) is based on the WKD model developed for DREV by Low and Hudak (Ref. 9) and the Wavy WKD (WWKD) model developed at DREV by Beaulieu (Ref. 10). The objective in developing this model was to provide a simple and effective technique for predicting the atmosphere's refractivity profile in the marine boundary

layer at several wavelength bands using a limited set of meteorological measurements. This set includes a measurement of the sea temperature, and the wind speed at a known height, z_0, above the water level, and measurements of the air pressure, air temperature, and relative humidity at another known, but not necessarily different height, z_1. The model is based on the earlier work of Monin and Obukhov (Refs. 4& 5) using similarity theory and on more recent work by Walmsley (Ref. 11). The following sections describe the model and the recent changes that have been incorporated. In this respect Appendix A is a particularly important resource, as it provides the reader with definitions for all the defined constants and variables used in this report.

2.1 Scaling Equations

As with all MBL models, L(W)WKD assumes that the gradient of an adiabatically conservative quantity, ω, is proportional to $(1/z)\varphi_\omega(z/L)$ where z is the height above the water level and $\varphi_\omega(z/L)$ is a dimensionless function. L(W)WKD uses the three conservative quantities; wind speed (u), virtual potential temperature (θ_v), and specific humidity (q), with the following dimensionless gradient functions for the wind speed (φ_u), virtual potential temperature (φ_{θ_v}), and specific humidity (φ_q):

$$\varphi_u(\zeta) = \varphi_u\left(\frac{z}{L}\right) = \frac{\kappa z}{u_*}\frac{\partial u}{\partial z} \tag{1a}$$

$$\varphi_{\theta_v}\zeta) = \varphi_{\theta_v}\left(\frac{z}{L}\right) = \frac{\kappa z}{\theta_{v_*}}\frac{\partial \theta_v}{\partial z} \tag{1b}$$

$$\varphi_q(\zeta) = \varphi_q\left(\frac{z}{L}\right) = \frac{\kappa z}{q_*}\frac{\partial q}{\partial z}. \tag{1c}$$

u_*, θ_{v*}, and q_* are the respective scaling constants for the wind speed, virtual potential temperature and specific humidity, κ (= 0.4) is von Karman's constant, and ζ (= z/L) is a normalized height. L is called the Monin-Obukhov length and is defined by:

$$L = (u_*^2 T_{vm})/(\kappa g \theta_{v*}) \tag{2}$$

where g is the acceleration due to gravity, and T_{vm} (^{0}K) is the average virtual air temperature within the boundary layer. As required, L is positive (stable atmosphere) when θ_{v*} is positive and negative (unstable atmosphere) when θ_{v*} is negative. Furthermore, L goes to zero as u_* goes to zero, or as θ_{v*} goes to infinity. These formulations differ from that given in Ref. 1 due to the inclusion of von Karman's constant in all three functions in Eq. 1, and the use of the average virtual temperature rather than the average temperature in Eq. 2. These differences must be kept in mind when any comparisons are made between earlier versions (< Ver. 7) of L(W)WKD and later versions (≥ Ver. 7). The functional form of these equations is now also in agreement with that used by the newest version of PIRAM.

To solve Eq. 1, the following gradient functions are generally used for the wind speed, virtual potential temperature, and specific humidity. The functions are empirically derived from actual measurements and assume that both the wind scaling constant (u_*) and the Monin-Obukhov length are non-zero.

$$\varphi_u(\zeta) = \begin{cases} 1 + \gamma_1\zeta \,/\, (1 + \zeta) & , \zeta \geq 0 \; ; \; KONDO \\ 1 + \alpha_1\zeta & , \zeta \geq 0 \; ; \; WKD \\ (1 - \beta_1\zeta)^{-1/4} & , \zeta < 0 \end{cases} \tag{3a}$$

$$\varphi_{\theta_v}(\zeta) = \begin{cases} 1 + \gamma_2\zeta \,/\, (1 + \zeta) & , \zeta \geq 0 \; ; \; KONDO \\ 1 + \alpha_2\zeta & , \zeta \geq 0 \; ; \; WKD \\ (1 - \beta_2\zeta)^{-1/2} & , \zeta < 0 \end{cases} \tag{3b}$$

$$\varphi_q(\zeta) = \begin{cases} 1 + \gamma_3\zeta \,/\, (1 + \zeta) & , \zeta \geq 0 \; ; \; KONDO \\ 1 + \alpha_3\zeta & , \zeta \geq 0 \; ; \; WKD \\ (1 - \beta_3\zeta)^{-1/2} & , \zeta < 0 \end{cases} \tag{3c}$$

where the coefficients, α_i, β_i, and γ_i (i = 1, 2 ,3), are constants. ζ (or L) greater than zero gives the appropriate functions for a stable atmosphere, and ζ (or L) less than zero gives the functions for an unstable atmosphere. Following Beaulieu (Ref. 10), and Kondo (Ref. 12),

Eq. 3 is used with the following values for the coefficients: $\alpha = \alpha_1 = \alpha_2 = \alpha_3 = 5$, $\beta = \beta_1 = \beta_2 = \beta_3 = 16$, and $\gamma = \gamma_1 = \gamma_2 = \gamma_3 = 6$. Two equations (KONDO & WKD) are given for the stable case. The first formulation is that originally proposed by Kondo (Ref. 12) and is now the default form used in both PIRAM and L(W)WKD. Earlier versions of L(W)WKD used the WKD formulation proposed by KelResearch (Ref. 9) as the default, and it is still provided as an option by L(W)WKD.

Combining Eqs. 1 and 3, and performing the integration gives the following solutions for u(z), $\theta_v(z)$ and q(z):

$$u(z) = u_0 + (u_*/\kappa)[\ln(z/z_{0u}) + \Psi_u(z;L) - \Psi_u(z_{0u};L)] \tag{4a}$$

$$\theta_v(z) = \theta_{v0} + (\theta_{v*}/\kappa)[\ln(z/z_{0\theta_v}) + \Psi_{\theta_v}(z;L) - \Psi_{\theta_v}(z_{0\theta_v};L)] \tag{4b}$$

$$q(z) = q_0 + (q_*/\kappa)[\ln(z/z_{0q}) + \Psi_q(z;L) - \Psi_q(z_{0q};L)] \tag{4c}$$

where the integrated gradient functions, Ψ, are given by

$$\Psi_u(z;L) = \begin{cases} \gamma \ln(1+\zeta) & , \zeta \geq 0 \ ; \ KONDO \\ \alpha\zeta & , \zeta \geq 0 \ ; \ WKD \\ 2\tan^{-1}x - 2\ln(1+x) - \ln(1+x^2) & , \zeta < 0 \end{cases} \tag{5a}$$

$$\Psi_{\theta_v}(z;L) = \Psi_q(z;L) = \begin{cases} \gamma \ln(1+\zeta) & , \zeta \geq 0 \ ; \ KONDO \\ \alpha\zeta & , \zeta \geq 0 \ ; \ WKD \\ -2\ln(1+x^2) & , \zeta < 0 \end{cases} \tag{5b}$$

and

$$x = (1-\beta\zeta)^{1/4}. \tag{5c}$$

z_{0u}, $z_{0\theta v}$, and z_{0q} are the respective roughness lengths for the wind speed, virtual potential temperature and specific humidity. u_0, θ_{v0}, and q_0 are constants of integration for the wind speed, virtual potential temperature and specific humidity evaluated at their respective roughness length. This set of equations is composed of three equations with 10 unknowns

(including L). Before presenting any methods for their determination, it is important that we first define some important meteorological concepts and their relationships.

2.2 Meteorological Equations

Before discussing definitions of potential temperature, virtual temperature, water vapour pressure, etc., it is important to comment on the conceptual reason for many of the changes that have been made with respect to those presented in the previous L(W)WKD report (Ref. 1). In the previous report, a system at a given temperature, total atmospheric pressure, and specific humidity is moved adiabatically to a dry-air pressure of 1000 mb, with the resultant temperature of this new system being the potential temperature. Then the specific humidity was added to this system, and it was treated as if it were an ideal gas of the same density as dry-air. This results in an equivalent dry-air system at approximately the same pressure at a temperature given by the virtual potential temperature. This procedure has several conceptual and physical problems, particularly with respect to the total atmospheric pressure and the dry-air pressure, that have led to its replacement by the following conceptual process. For a system at a given temperature, specific humidity, and total atmospheric pressure, the virtual temperature is calculated for an equivalent dry-air system at the same total atmospheric pressure. This equivalent dry-air system is then adiabatically moved to a new system at a uniform pressure of 1000 mb at a new temperature defined as the virtual potential temperature.

2.2.1 Virtual Temperature and Specific Humidity

The virtual temperature, T_v, is the temperature at which a volume of dry air has the same density, ρ, as moist air with specific humidity, q, at the same total atmospheric pressure (P). Equation 6 shows the relationship between the virtual temperature and the temperature of moist air (T), and how this is applied to the ideal gas law (Eq. 6c):

$$T_v = [1 + (1 - \mu)q/\mu]\ T \qquad (6a)$$

$$\mu = M_w/M_a = 0.622 \qquad (6b)$$

$$P = \rho R_a T_v = \rho R_m T\ . \qquad (6c)$$

In these equations, M_w is the molecular mass of water, M_a is the molecular mass of dry air, R_m is the gas constant for moist air, R_a (= R/M_a) is the gas constant for dry air, and R is the universal gas constant. In turn, the specific humidity can be expressed in terms of the total atmospheric pressure ($P=P_a+P_w$), the dry air pressure (P_a), and the water vapour pressure (P_w) by

$$q = \mu P_w/[P-(1-\mu)P_w] \qquad (7a)\ ,$$

$$= \mu P_w/[P_a+\mu P_w] \qquad (7b)$$

$$= \omega/(1+\omega)\ ;\omega = \mu P_w/P_a\ . \qquad (7c)$$

where ω is called the mixing ratio. The new PIRAM model also follows these definitions.

2.2.2 Virtual Potential Temperature

The virtual potential temperature of dry air (θ_v) is defined as the temperature that a volume of dry air at virtual temperature, T_v, assumes when brought adiabatically from its existing pressure, P, to a standard reference pressure, P_{ref}. The resultant virtual potential temperature is related to the virtual temperature by

$$\theta_v = T_v(P_{ref}/P)^{(\gamma-1)/\gamma} \qquad (8)$$

where γ (= c_p/c_v =1.40 for dry air at room temperature) is the ratio of the specific heat at constant pressure (c_p) and the specific heat at constant volume (c_v) for dry air. By default and by convention P_{ref} is taken to be 1000 mb although L(W)WKD does allow it to be modified. In earlier versions of L(W)WKD, the dry-air pressure was used by default in Eq. 8

instead of the total air pressure. While L(W)WKD still provides this as an option, the total air pressure is now the default option. The PIRAM model uses the same formulation.

2.2.3 Water Vapour Pressure

As the water vapour pressure is not generally available from meteorological measurements, L(W)WKD calculates it using the following empirical relationship for the saturated water vapour pressure obtained from a variation of the Clausius-Clapeyron equation (Ref. 1):

$$\ln(P_w^s(T)) = 19.32 - 4223/(T - 32) \qquad (9)$$

Thus, Eq. 9 provides a relationship between either the saturated water vapour pressure (P_w^s) and the air temperature (T), or using Eq. 10b, the water vapour pressure (P_w) and the dew-point temperature (T_d). Thus, given the dew-point temperature, the water vapour pressure is easily determined. However, as the relative humidity (H_r) is more commonly quoted than the dew-point temperature, use must be made of Eq. 10a, which relates the water vapour pressure to the relative humidity, and the saturated water vapour pressure:

$$P_w(T) = H_r(T)\, P_w^s(T) \qquad (10a)$$

$$P_w(T) = P_w^s(T_d). \qquad (10b)$$

The PIRAM model uses a different formulation of Eq. 9 (see Ref. 27) for the saturated water vapour pressure; however, this shouldn't produce any significant differences.

At the surface of a sea with salinity, S, and at temperature T_s, the relative humidity is not 100% as was previously used by default in most earlier versions of both L(W)WKD and PIRAM. Instead, it is given by

$$H_r(T_s, S) = \frac{P_{sw}^s(T_s, S)}{P_w^s(T_s)} \approx \frac{P_w^s(T_s)(1 - \varepsilon S)}{P_w^s(T_s)} = (1 - \varepsilon S) \qquad (11a,b)$$

where P^s_{sw} is the saturated water vapour pressure above salt water (sw), P^s_w is the saturated water vapour pressure above fresh water, and ε is taken to be 5.37×10^{-3} (Ref. 13). Thus, for a standard salinity of 34g of salt per kilogram of water, the relative humidity at the surface is 98.2 %. This is now the default value for the relative humidity at the sea surface for both L(W)WKD and PIRAM.

2.2.4 Vertical Atmospheric Pressure Profile

The final required equation is that relating the total air pressure ($P = P_a + P_w$) to the height above the ground. These equations are different from those in the earlier versions of L(W)WKD due to the change in conception of the physical processes discussed earlier. Assuming that the forces on an equivalent slab of dry-air are balanced, and using Eq. 6c for the perfect gas law, gives the hydrostatic equation:

$$\frac{dP}{P} = -\frac{g}{R_a T_v} dz, \tag{12}$$

where dP is the pressure differential across the slab, dz is the width of the slab, g is the acceleration due to gravity near the surface, T_v is the virtual temperature of the slab, and R_a is the gas constant for dry-air. Assuming that g and R_a do not vary much near the surface, integrating Eq. 12 gives;

$$P(z)/P(z_1) = e^{-\frac{g}{R_a}\int_{z_1}^{z}\frac{dz'}{T_v(z')}} \approx e^{\frac{-g(z-z_1)}{R_a T_v(z_1)}} \approx 1 - \frac{g(z-z_1)}{R_a T_v(z_1)} \tag{13a,b,c}$$

where $P(z_1)$ is the total atmospheric pressure, and $T_v(z_1)$ is the virtual air temperature at the height z_1. The approximation, Eq. 13b, is used by L(W)WKD, and is obtained by assuming that the temperature profile is uniform (constant temperature within the MBL). The further simplification of Eq. 13c is obtained by using the first term of the Taylor series expansion of the exponential in Eq. 13b. This final form is used in PIRAM; however, it should not

produce any significant differences between the models. The air density profile can be obtained from Eq. 13b and Eq. 6c, such that

$$\rho(z) = \frac{P(z_1)}{R_a T_v(z_1)} e^{\frac{-g(z-z_1)}{R_a T_v(z_1)}}. \qquad (14)$$

Again PIRAM expands the exponential and only uses the first term in z.

2.3 Solving the Basic Scaling Equations

To solve Eq. 4 requires the determination of ten unknown parameters. Six of these parameters can be determined using boundary conditions, while the other four need to be determined using other techniques. The current differences between the previous L(W)WKD versions and the PIRAM model are highlighted in the following sections.

2.3.1 Boundary Conditions

At sea level, the following three boundary conditions allow the following definitions to be made for the three roughness lengths. First, let z_{ou} be the height at which the wind speed is zero ($u(z_{ou}) = 0$), z_{0q} the height at which the water vapour pressure is equal to the sea surface water vapour pressure, and $z_{0\theta_v}$ the height at which the virtual potential temperature of the air is equal to that given by air at the temperature of the sea (T_s), and the water vapour pressure is given by the sea surface water vapour pressure. Applying these definitions to Eq. 4, and using Eqs. 6, 7, and 8 gives:

$$u_0 = u(z_{0u}) = 0 \qquad (15a)$$

$$q_0 = q(z_{0q}) = \mu H_r(T_s) P_w^s(T_s) / [P_a(0) + \mu H_r(T_s) P_w^s(T_s)] \qquad (15b)$$

$$\theta_{v0} = \theta_v(z_{0\theta_v}) = T_s[1 + (1-\mu) q_0/\mu][1000/P(0)]^{(\gamma-1)/\gamma} \qquad (15c)$$

where $P_a(z=0)$ is the dry-air atmospheric pressure in millibars, $P(z=0)$ is the total atmospheric

pressure, $H_r(T_s)$ is the relative humidity, and $P_w^s(T_s)$ is the saturated water vapour pressure at the water level for water at temperature, T_s.

Three more boundary conditions are given using measurements of the wind speed $u(z_0)$ at the height z_0, and measurements of the air temperature, $T(z_1)$, total atmospheric pressure, $P(z_1)$, and relative humidity, $H_r(z_1)$ at the height, z_1. Applying these conditions to Eq. 4, and using Eqs. 6, 7 and 8 gives:

$$\Delta u(z_0) = u(z_0) = (u_*/\kappa)[\ln(z_0/z_{0u}) + \Psi_u(z_0;L) - \Psi_u(z_{0u};L)] \quad (16a)$$

$$\Delta\theta_v(z_1) = \theta_v(z_1) - \theta_{v0} = (\theta_{v*}/\kappa)[\ln(z_1/z_{0\theta_v}) + \Psi_{\theta_v}(z_1;L) - \Psi_{\theta_v}(z_{0\theta_v};L)] \quad (16b)$$

$$\Delta q(z_1) = q(z_1) - q_0 = (q_*/\kappa)[\ln(z_1/z_{0q}) + \Psi_q(z_1;L) - \Psi_q(z_{0q};L)] \quad (16c)$$

where

$$q(z_1) = \mu H_r(z_1) P_w^s(T(z_1))/[P_a(z_1) + \mu H_r(z_1) P_w^s(T(z_1))] \quad (17a)$$

$$\theta_v(z_1) = T(z_1)[1 + (1-\mu) q(z_1)/\mu][1000/P(z_1)]^{(\gamma-1)/\gamma}. \quad (17b)$$

$q(z_1)$ is the specific humidity, $\theta_v(z_1)$ is the virtual potential temperature, and $P_w^s(T(z_1))$ is the saturated water vapour pressure at height z_1. Furthermore, $\Delta\theta_v(z_1)$ is known as the virtual potential air-sea temperature difference (VPASTD), and $\Delta q(z_1)$ is known as the air-sea specific humidity difference (ASSH).

The two sets of boundary conditions provide six equations for the determination of the 10 unknowns and are used by both L(W)WKD and PIRAM. The following two sections provide the remaining four equations.

2.3.2 Roughness Lengths

The following empirical relationships have been developed by Businger et. al. (Ref. 14)

and Smith (Ref. 15). They relate $z_{0\theta_v}$ to z_{0u}, and z_{0q} to z_{0u} by;

$$\ln(z_{0\theta_v}/10) = -\kappa^2/[C_{TN}\ln(10/z_{0u})] \quad (18a)$$

$$\ln(z_{0q}/10) = -\kappa^2/[C_{EN}\ln(10/z_{0u})] \quad (18b)$$

where C_{TN} is the 10 m neutral heat flux coefficient whose value has been established to be 1.0×10^{-3} for wind speeds ranging from 6 to 22 m/s, and C_{EN} is the 10 m moisture flux coefficient defined by Smith (Ref. 15) and evaluated to be 1.2×10^{-3}. To solve Eq. 18, use is made of the following wind dependent relation (Ref. 1,9,10 & 15);

$$z_{ou} = (\alpha_c/g)u_*^2 + \frac{\nu_d}{u_*} e^{-C\kappa} \quad (19a)$$

$$= (\alpha_c/g)u_*^2 + \frac{a_d\theta_v + b_d}{u_*} e^{-C\kappa} \quad (19b)$$

where κ is von Karmen's constant, C is a constant equal to -5.5, g is the acceleration due to gravity, α_c (= 0.011) is Charnock's constant, and ν_d is the dynamic viscosity for dry air. As with the previous versions of L(W)WKD, these values have been chosen according to Walmsley (Ref. 11). The difference with the earlier versions is that the dynamic viscosity is now taken to be a function of the virtual potential temperature (K), where a_d is 9.267×10^{-8} and b_d is 1.346×10^{-5} (see Eq. 19b). These values are obtained from a linear fit of the data given in Table A3 of Ref. 16 for temperatures from 0 to 40°C at a pressure of 1000 mb. Both L(W)WKD and PIRAM now use this functional form. However, L(W)WKD uses the average virtual potential temperature, given by;

$$\theta_{vm} = [\theta_{vs} + \theta_v(z_1)]/2 \approx \theta_v \,, \quad (20)$$

where θ_{vs} is the virtual potential temperature at the sea surface, and $\theta_v(z_1)$ is the virtual potential temperature at height z_1, in place of the virtual potential temperature given in Eq. 19b. The exact formulation used by PIRAM is not known; however, it is doubtful that any significant differences would result in a slightly different interpretation.

2.3.3 Monin-Obukhov Length

With the addition of Eqs. 18 and 19 there are now 9 equations for 10 unknowns with the remaining unknown being the Monin-Obukhov length (L). Equation 2 provides the required 10th equation provided a definition is given for the average virtual temperature, T_{vm}. As in previous versions of L(W)WKD, this average is taken between the respective temperature at the sea surface, and that measured at the height z_1;

$$T_{vm} = [T_{vs} + T_v(z_1)]/2. \tag{21}$$

Here, again as for Eq. 20, L(W)WKD and PIRAM may have slightly different interpretations; however, again, no significant differences are expected.

2.4 Iterative Algorithm

The algorithm described below is the one used by the new L(W)WKD program to provide solutions for any set of atmospheric parameters of interest and has been slightly modified from the earlier versions (before Ver. 7.0). The algorithm is enumerated as a series of steps, with each step accompanied by a descriptive comment. For simplicity the algorithm is divided into three parts. The first part describes the steps required to determine the measured virtual potential air-sea temperature difference (VPASTD = $\Delta\theta_v$) and the air-sea specific humidity difference (ASSHD = Δq), while the second part describes the steps used to initialize the variables used during the iteration algorithm described in the third section. The iterative algorithms used by L(W)WKD and PIRAM still remain different as they have not been part of any discussions to bring them into agreement.

2.4.1 Part 1 - Measurements

1) Calculate the water vapour pressure, $P_w(z_1)$, using Eqs. 9 and 10a with the measured relative humidity and air temperature at the height z_1.

2) Calculate the specific humidity, $q(z_1)$, using Eq. 7a with the measured air pressure at the height z_1, and the water vapour pressure from Step 1.

3) Calculate the virtual temperature, $T_v(z_1)$ using Eq. 6a, the measured air temperature at the height z_1, and the specific humidity from Step 2.

4) Calculate the virtual potential temperature, $\theta_v(z_1)$ using Eq. 8, the measured air pressure at the height z_1, $P(z_1)$, and the virtual temperature from Step 3. If the dry-air option has been chosen then the air pressure is replaced by $P(z_1) - P_w(z_1)$, where $P_w(z_1)$ is obtained from Step 1.

5) Calculate the total atmospheric pressure at sea level, $P(z=0)$, using Eq. 13b, the total air pressure at height z_1, and the virtual temperature from Step 3.

6) Calculate the water vapour pressure at sea level, $P_w(z\approx0) = P^s_{sw}(z\approx0)$, using Eqs. 9 and 11a with the sea surface relative humidity and sea surface temperature.

7) Calculate the specific humidity at sea level, $q(z\approx0)$, using Eq. 7a with the air pressure from Step 5 and the water vapour pressure from Step 6.

8) Calculate the virtual temperature at sea level, $T_v(z\approx0)$ using Eq. 6a, the measured sea temperature and the specific humidity from Step 7.

9) Calculate the virtual potential temperature, $\theta_v(z\approx0)$ using Eq. 8, the air pressure from Step 5, and the virtual temperature from Step 8. If the dry-air option has been chosen then the air pressure is replaced by $P(z\approx0) - P_w(z\approx0)$, where $P_w(z\approx0)$ is the result from Step 6.

10) Calculate the average virtual temperature in the layer, T_{vm}, using Eq. 21 and the results from Steps 3 and 8.

11) Calculate the average virtual potential temperature in the layer, θ_{vm}, using Eq. 20 and the results from Steps 4 and 9.

2.4.2 Part 2 - Initialization

1) Set the number of iterations parameter, N, equal to zero. This parameter keeps track of the number of iterations required to obtain a stable solution.

2) Set the iteration precision parameter, ε, equal to 0.001. This is one of the two arbitrarily set parameters that can stop the iteration procedure. Its significance is discussed further in Step 10 of Part 3.

3) Set the maximum number of iterations parameter, MAXN, equal to 100. This is the second arbitrary set parameter that can stop the iteration procedure.

4) Set the following parameter, S(0), equal to a large number. It is currently set arbitrarily to 1×10^{10}. The significance of this parameter is discussed in Step 10 of Part 3.

5) Calculate the air-sea specific humidity difference (ASSHD = $q(z_1) - q_0$) using the results from Steps 2 and 7 of Part 1.

6) Calculate the virtual potential air-sea temperature difference (VPASTD = $\theta_v(z_1) - \theta_{v0}$) using the results from Steps 4 and 9 of Part 1.

7) Set the wind speed measured at the height z_0 to $u(z_0)$.

8) Set the initial wind roughness height, $z_{0u}(0)$ equal to 1.5×10^{-4} m. This is a generally accepted approximate value (Ref. 1).

9) Set the initial virtual potential temperature roughness height, $z_{0\theta v}(0)$, using Eq. 18a.

10) Set the initial specific humidity roughness height, $z_{0q}(0)$, using Eq. 18b.

11) Set the initial wind scaling constant, $u_*(0)$, using only the first term in Eq. 19 and the value of z_{0u} from Step 8:

$$u_* = [z_{0u}/1.12x10^{-3}]^{1/2} = 0.3660 \ m/s. \qquad (22)$$

12) Set the initial virtual potential temperature scaling constant, $\theta_{v*}(0)$, to (κ x VPASTD)/z_1 where κ is von Karmen's constant and VPASTD is obtained from Step 6.

13) Set the initial specific humidity scaling constant, $q_*(0)$, to (κ x ASSHD)/z_1 where κ is von Karmen's constant and ASSHD is obtained from Step 7.

14) Set the initial Monin-Obukhov length, L(0), using Eq. 2 and the results from Steps 11 and 12, and Step 10 from Part 1.

2.4.3 Part 3 - Iteration

1) Using the wind speed roughness height, $z_{0u}(0)$, the Monin-Obukhov length, L(0), and $u(z_0)$, solve Eq. 16a for a new value of the scaling constant, $u_*(1)$.

2) Using the virtual potential temperature roughness height, $z_{0\theta_v}(0)$, the Monin-Obukhov length, L(0), and the VPASTD, solve Eq. 16b for a new value of the scaling constant, $\theta_{v*}(1)$.

3) Using the specific humidity roughness height, $z_q(0)$, the Monin-Obukhov length, L(0), and the ASSHD, solve Eq. 16c for a new value of the scaling constant, $q_*(1)$.

4) Calculate a new value for the wind speed roughness height, $z_{0u}(1)$, using Eq. 19b, $u_*(1)$ from Step 1, and θ_{vm} from Step 11 of Part 1.

5) Calculate a new value for the virtual potential temperature roughness height, $z_{0\theta_v}(1)$, using Eq. 18a and $z_{0u}(1)$ from Step 4.

6) Calculate a new value for the specific humidity roughness height, $z_{0q}(1)$, using Eq. 18b and $z_{0u}(1)$ from Step 4.

7) Calculate a new value for the Monin-Obukhov length, L(1), using Eq. 2, T_{vm} from Step 10 of Part 1, and the new scaling constants $u_*(1)$ and $\theta_{v*}(1)$ calculated from Steps 1 and 2.

8) Calculate the absolute relative differences for the three scaling constants and the three roughness heights. The absolute relative difference is defined to be:

$$D_A = \begin{cases} |[A(1) - A(0)]/A(0)| & ; A(0) \neq 0 \\ |[A(1) - A(0)]/A(1)| & ; A(0) = 0, A(1) \neq 0 \\ 0 & ; A(0) = A(1) = 0 \end{cases} \qquad (23)$$

where A represents any of the six parameters.

9) Calculate the sum, S(1), of the six absolute relative differences calculated in Step 8. S is the measure used to describe the goodness of the solution.

10) The final step in the iteration loop is the following IF block which decides whether to continue or stop the iterative procedure. The procedure is stopped and the solution is valid if S(1) is less than ε and N is less than MAXN. The significance of S(1) being less than ε is that the sum of the relative differences is less than 100*ε % (i.e. the maximum possible value that any of the individual relative differences can have is 100*ε %). Thus, a value of 0.001 translates into a maximum difference of 0.1% for any of the parameters. The IF block used by L(W)WKD is constructed as follows:

IF (S(1) < ε) THEN
- solution found; stop the iteration procedure and return the results

ELSE IF (N > MAXN) THEN
- no solution found within MAXN iterations; stop the iteration procedure and return an error flag

ELSE IF ((N ≤ 5) OR (S(1) < S(0)) THEN
- solution not yet found; continue the iteration procedure as either less than 6 iterations have been performed (N ≤ 5) or the goodness of the solution is improving (S(1) < S(0))
- increment N to N+1
- set $z_{0u}(0) = z_{0u}(1)$; $z_{0\theta v}(0) = z_{0\theta v}(1)$; $z_{0q}(0) = z_{0q}(1)$
- set $u_*(0) = u_*(1)$; $\theta_{v*}(0) = \theta_{v*}(1)$; $q_*(0) = q_*(1)$
- set L(0) = L(1)
- GOTO Step 1

ELSE
- no solution found because N > 5 and S(1) ≥ S(0)
IF (mode is INTERACTIVE[1]) THEN
- stop the iteration procedure and return an error flag
ELSE (mode is BATCH[1])
IF (wind speed < 25 m/s) THEN
- increase the wind speed by 0.5 m/s and return to Step 1
ELSE
- stop the iteration procedure, return an error flag, and output uniform profiles

[1] The INTERACTIVE and BATCH modes of operation are discussed in Section 3.

2.5 Wavy Model

The Wavy WKD model developed at DREV by Beaulieu (Ref. 10) was an attempt to mimic the effect that water waves would have on the vertical profiles generated by the WKD model (flat sea). The L(W)WKD model also incorporates this effect on the profiles it generates. This feature is not present in PIRAM and will only be discussed briefly in this report as Ref. 1 discusses it in detail.

If one assumes that the action of the waves is to turn a flat surface into a sinusoidal surface with a wave height (trough to peak) of H_w and a wavelength of λ_w, then the height of any part of the wave (H) above the mean sea level is given by

$$H(x) = (H_w/2)\cos(2\pi x/\lambda_w), \tag{24}$$

where x is between 0 and λ_w. Thus, assuming that the instantaneous vertical profile, Φ_α, for parameter α, above every point of the wave is that given by L(W)WKD for a flat sea, the average effect of this wave action can be calculated by averaging the vertical profile over one wavelength. This gives:

$$\Phi_\alpha^w(z) = \begin{cases} (1/H_w)\displaystyle\int_{z-H_w/2}^{z+H_w/2} \Phi_\alpha(z')dz' \; ; \; z \geq z_{max} + H_w/2 \\ (1/H_w)\displaystyle\int_{z_{max}}^{z+H_w/2} \Phi_\alpha(z')dz' \; ; \; z_{max} \leq z < z_{max} + H_w/2 \end{cases} \tag{25}$$

where Φ_α^w is the averaged vertical α-profile, z is the height above the mean sea level or flat sea, z′ is the instantaneous height above a point on the wave, and z_{max} (=max(z_{ou}, $z_{o\theta v}$, z_{oq})) is the maximum of the wind speed, virtual potential temperature, and specific humidity roughness heights. The first function in Eq. 25 is used for heights above the peak of the wave, while the second function is used for heights between the mean sea level and the wave's peak. The function is not calculated for heights below the mean sea level.

Equation 25 can easily be calculated using the rectangular integration rule such that

$$\Phi_\alpha^w(z) = \begin{cases} \sum_{i=0}^{n-1} \Phi_\alpha(z_i')/n & ; z \geq z_{max} + H_w/2;\ i = 0,1,..n-1 \\ \sum_{i=m}^{n-1} \Phi_\alpha(z_i')/(n-m) & ; z_{max} \leq z < z_{max} + H_w/2;\ i = 0,1,..n-1 \end{cases} \tag{26}$$

$$z_i' = z - (H_w/2)\cos(2\pi i/n) \tag{27}$$

and

$$m = (n/\pi)\cos^{-1}[2(z - z_{max})/H_w]. \tag{28}$$

The above procedure is only valid for profiles that are linear combinations of the four fundamental vertical profiles given by Eqs. 4a, 4b, 4c and 13b for the wind, virtual potential temperature, specific humidity, and total atmospheric pressure respectively. Any nonlinear combinations of these profiles must first calculate the wavy profile for each of these four profiles before combining their results. This is an extremely important point (see Ref. 1), as many of the desired quantities, involve nonlinear combinations of these profiles.

2.6 Refractive Index

Discussion of the functional form for the index of refraction or refractivity will be relatively brief as it is fully discussed in Ref. 1. While the functional form used by L(W)WKD and PIRAM is the same, the same is not true for the various coefficients and this has not been part of any common agreement.

Following Ref. 1, the refractivity ($Z = (n-1) \times 10^6$, where n is the refractive index), of the atmosphere at a wavelength, λ, can be approximated by

$$Z(\lambda)x10^{-6} = \left[D_a(\lambda,T)\frac{P_a}{kT} + D_w(\lambda,T)\frac{P_w}{kT}\right](100\ Pa/mb) \tag{29a}$$

$$= \left[A(\lambda,T)\frac{P_a}{T} + B(\lambda,T)\frac{P_w}{T}\right] x\ 10^{-6} \tag{29b}$$

where k is Boltzmann's constant, Z is the refractivity, P_a is the dry-air pressure, P_w is the water vapour pressure, T is the temperature, D_a is the dry-air molecular refractivity, D_w is the water vapour molecular refractivity, A is the dry-air coefficient, and B is the water vapour coefficient. In all future discussions it will be assumed that all pressures are in millibars, all temperatures are in Kelvin, all densities are in grams per cubic metre, and all wavelengths are in micrometers. This leads to various transformation constants in many of the equations, including the factor of 100 Pascal/1 millibar given in Eq. 29a.

2.6.1 Dry-Air Refractivity

Using measured refractivities for standard air (defined as containing 0.03% CO_2 per volume at 101.3 mb and 15 ^{0}C), many authors have determined the A coefficient of Eq. 29. As discussed in Ref. 1, L(W)WKD uses the following Sellmeier function (Ref. 17) developed by Edlén in 1953 (Ref. 18) for A:

$$A(\lambda) = \left[64.328 + \frac{29498.10}{146 - 1/\lambda^2} + \frac{255.40}{41 - 1/\lambda^2}\right]\frac{288.2}{1013} \tag{30a}$$

$$= a(\lambda)\frac{288.2}{1013} \tag{30b}$$

where

$$a(\lambda) = \left[64.328 + \frac{29498.10}{146 - 1/\lambda^2} + \frac{255.40}{41 - 1/\lambda^2}\right]. \tag{31}$$

λ is the wavelength in vacuum in μm and k is Boltzmann's constant. It has simple poles at

0.083 μm (=[1/146]$^{1/2}$) and 0.156 μm (=[1/41]$^{1/2}$) which simulate the effects of resonances due to bound states, states near the ionization limit, and dissociative states. Edlén has shown that this fit is good to within 0.04 units (~ .05%) down to 0.2 μm.

2.6.2 Water Vapour Refractivity

For water vapour, L(W)WKD uses the results of Hill and Lawrence (Ref. 7), which separates the molecular refractivity into the following sums over the IR and UV resonances (λ_i);

$$D_w(\lambda,T) = \sum_{IR} S_i(T)/(1/\lambda_i^2 - 1/\lambda^2) + \sum_{UV} S_i(T)/(1/\lambda_i^2 - 1\lambda^2)$$
$$= D_w^{IR}(\lambda,T) + D_w^{UV}(\lambda,T) , \qquad (32)$$

where Sellmeier's dispersion function (Ref. 17) is used, and the S_i's are the line strengths. Using dispersion data from Erickson (Ref. 19) for eight visible wavelengths between 0.644 and 0.361 μm, they give the UV molecular refractivity to be

$$D_w^{UV}(\lambda) = \frac{37.47}{124.40 - 1/\lambda^2} \frac{k}{R_w} = b^{UV}(\lambda) \frac{k}{R_w} , \qquad (33a)$$

where

$$b^{UV}(\lambda) = \frac{37.47}{124.40 - 1/\lambda^2} , \qquad (33b)$$

and R_w (=R/M_w=0.4619) is the gas constant for water vapour. There is a simple pole at 0.090 μm which simulates the resonances from bound states, states near the ionization limit, and dissociation states. As for dry-air, this implies that Eq. 33 should be good down to 0.2 μm. The claimed accuracy is less than 0.5%. A plot of $b^{UV}(\lambda)$ is given in Fig. 1.

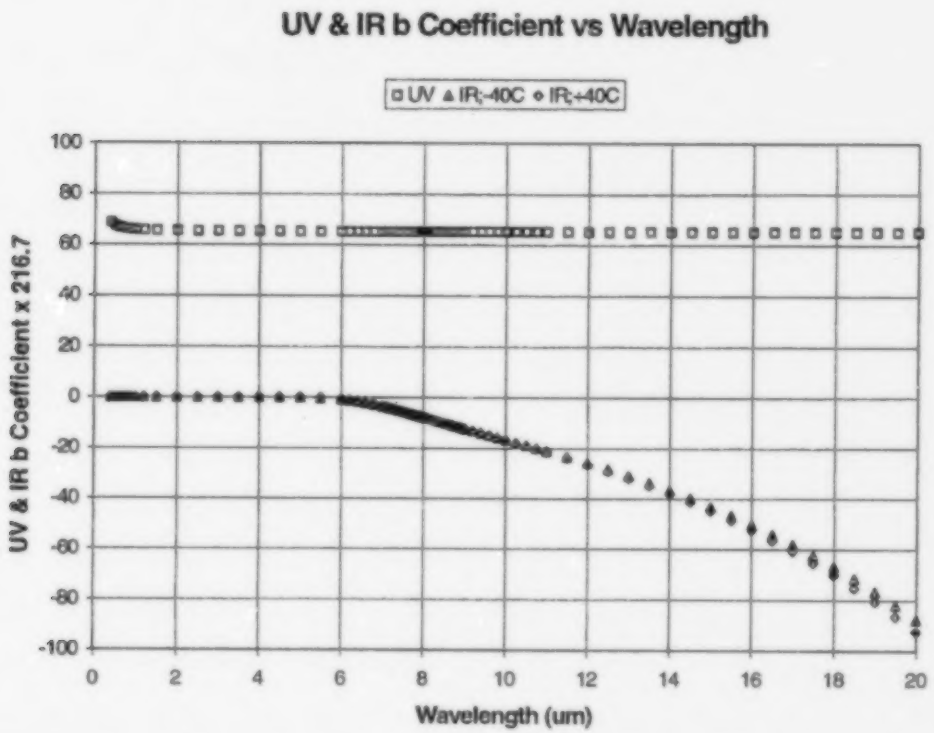

FIGURE 1 - Plot of b coefficients (x $100/R_w = 216.7$)

To determine the refractivity due to the IR resonances, Hill and Lawrence (Ref. 7) calculated $D_w^{IR}(\lambda,T)$ by performing the summation over more than 40,000 water-vapour resonances extending from radio frequencies to the visible for nine wavelengths and temperatures from -40 to 40 °C in 10 °C steps. The wavelengths were 18.83, 17.82, 15.43, 13.11, 11.60, 10.37, 9.341, 8.562 and 7.837 μm. After fitting the calculations and scaling the results to agree with measurements near 10.6 μm, the following IR refractivity function was found,

$$D_w^{IR}(\lambda,T) = \left[\frac{0.957 - 0.928\delta^{0.4}(x-1)}{1.03\delta^{0.17} - 19.8x^2 + 8.1x^4 - 1.7x^8}\right]\frac{k}{R_w} = b^{IR}(\lambda,T)\ \frac{k}{R_w} \qquad (34a)$$

where

$$b^{IR}(\lambda,T) = \left[\frac{0.957 - 0.928\delta^{0.4}(x-1)}{1.03\delta^{0.17} - 19.8x^2 + 8.1x^4 - 1.7x^8}\right], \qquad (34b)$$

$\delta = T/273.15$, and $x = 10/\lambda$. The plot of $b^{IR}(\lambda,T)$, in Fig. 1, shows the effect of changing the temperature. As can be seen, the effect of temperature is not very important, so that using $\delta = 1$ does not significantly affect the output of Eq. 34. This graph is different from that given in the previous report (Ref. 1) due to an error of sign that was introduced when creating the graph. Fortunately, this error does not produce a significant effect on the values of the A and B coefficients (see Table 1) in the regions of interest. Adding the UV and IR contributions together, we get the following result for the refractivity of water vapour;

$$Z_w(\lambda,T) = [D_w^{UV}(\lambda) + D_w^{IR}(\lambda,T)]\frac{1x10^8 P_w}{kT} = B(\lambda,T)\frac{P_w}{T}, \qquad (35a)$$

where

$$B(\lambda,T)x10^{-8} = [D_w^{UV}(\lambda) + D_w^{IR}(\lambda,T)]/k = [b^{UV}(\lambda) + b^{IR}(\lambda,T)]/R_w = b(\lambda)/R_w\ , \qquad (35b)$$

and

$$b(\lambda) = [b^{UV}(\lambda) + b^{IR}(\lambda,T)]\ . \qquad (35b)$$

Equation 35 is applicable for wavelengths between 0.2 and 19 μm when they are sufficiently far from any significant resonances. In particular, this means that Eq. 35 should work very well in the visible, the 3-5 μm and the 8-12 μm windows.

2.6.4 The A & B Coefficients

Figure 2 shows a plot of the A and B coefficients defined in the preceding sections for

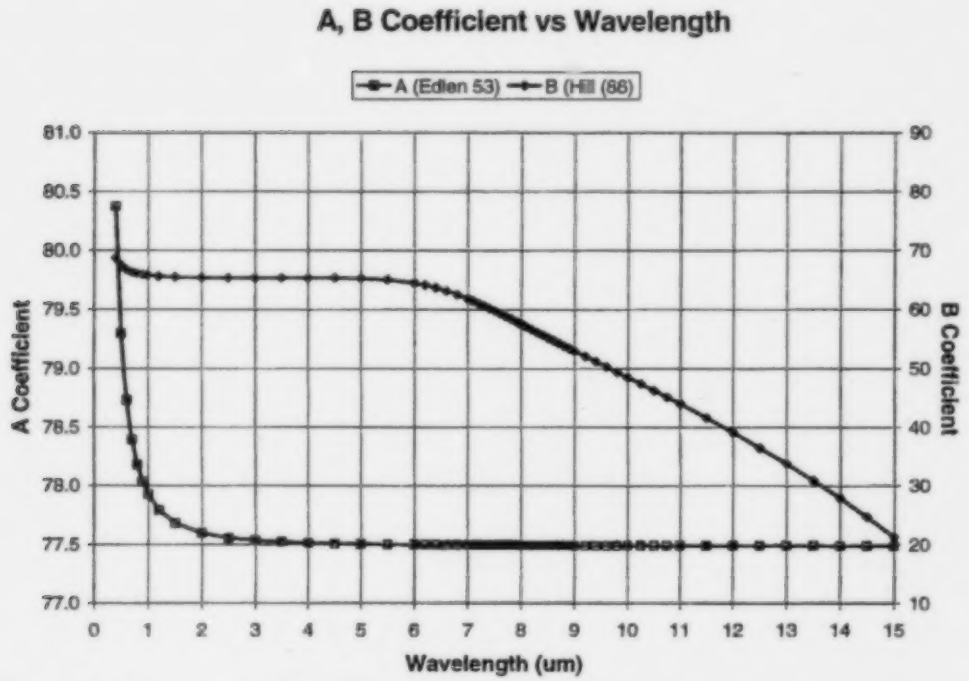

FIGURE 2 - Plot of A and B coefficients versus wavelength

0 ^{0}C; however, the L(W)WKD program does not compute these coefficients for any desired wavelength. Instead, it uses precomputed averages over both temperature and wavelength for four bands between 0.4 and 12 μm, and for the microwave/radar band. Table I shows the values for A and B along with a measure of their uncertainty. These values are essentially those given by Ref. 1 except for some minor changes in the B coefficient. For ease of comparison, its values from Ref. 1 are given in the last column. The PIRAM model is very similar except that it does not use band averages for the visible and IR. Instead, it calculates the A coefficient for a specified wavelength, and the B coefficient from the A coefficient using B = A - 12.79. As can be seen from Table 1, this does not cause any significant differences except in the far-infrared. The values used in the RF band are taken from Ref. 20.

TABLE I[1]
A & B Wavelength Coefficients

Wavelength Band	λ (μm)	A (K/mb)	B (K/mb)	B (K/mb) (Ref. 1)
Visible	0.4 - 1.0	78.6 ± 0.6	66.6 ± 0.8	67.0 ± 0.8
Near-IR	1.0 - 3.0	77.6 ± 0.1	65.5 ± 0.1	65.5 ± 0.1
Mid-IR	3.0 - 5.0	77.52 ± 0.01	65.33 ± 0.01	65.0 ± 0.2
Far-IR	8.0 - 12.0	77.491 ± 0.001	48.5 ± 5.4	40.0 ± 7.7
RF & MicroWave	< 50 GHz	77.6	$72 + 3.75 \times 10^5/T$	$3.734 \times 10^5/T$

2.7 Structure Parameters

The L(W)WKD model also calculates profiles for the refractive index structure parameter, C_n^2, the refractivity index structure parameter, C_Z^2, and other structure parameters. Differences with PIRAM continue to exist in this area as it was not part of our common agreement. As such, this section is relatively brief as the reader is referred to Ref. 1 for more detailed information.

As shown in Ref. 1, the refractive index structure parameter at an elevation, z, is given by

$$\begin{aligned} C_n^2(z) &= h^{-2/3}\langle[n(z) - n(z+h)]^2\rangle_{avg} \\ &= 1x10^{-12}\, h^{-2/3}\langle[Z(z) - Z(z+h)]^2\rangle_{avg} = 1x10^{-12} C_Z^2(z) \end{aligned} \tag{36}$$

where h is some incremental height, Z is the refractivity, and C_Z^2 is the refractivity structure parameter. Using Eq. 29b, the refractivity structure parameter can be expressed as

$$h^{2/3} C_Z^2(z) = \langle[(K_A(z,\lambda,T)(T(z) - T(z+h)) + K_B(\lambda,T)(\rho_w(z) - \rho_w(z+h))]^2\rangle_{avg} \tag{37}$$

where

$$K_A(z,\lambda,T) = \frac{A(\lambda)P_a(z)}{T^2(z)} \; ; \; K_B(z,\lambda,T) = B(\lambda,T)\frac{R_w}{100\ Pa/mb} \; . \qquad (38a,b)$$

Carrying out the square in Eq. 37, gives

$$h^{2/3}C_{Z^2}(z) = < K_A^2\ [T(z)-T(z+h)]^2 + K_B^2\ [\rho_w(z)-\rho_w(z+h)]^2 + 2K_A K_B\ [T(z)-T(z+h)][\rho_w(z)-\rho_w(z+h)] > \qquad (39)$$

and finally

$$C_{Z^2}(z) = K_A^2\ C_{T^2}(z) + K_B^2\ C_{\rho_w^2}(z) + 2K_A K_B\ C_{T\rho_w}(z) \; , \qquad (40)$$

where C_{T^2} is the temperature structure parameter, $C_{\rho_w^2}$ is the water vapour density structure parameter, and $C_{T\rho_w}$ is the temperature-water vapour density structure parameter.

Following the parametrization of Monin-Obukhov, the virtual potential temperature structure parameter, the specific humidity structure parameter, and the virtual potential temperature-specific humidity structure parameter can be expressed in terms of the scaling parameters, θ_{v*} and q_*, such that

$$C_{\theta_v^2}(z) = \theta_{v*}^2\ z^{-2/3}\ f_1(z/L) \qquad (41a)$$

$$C_{q^2}(z) = q_*^2\ z^{-2/3}\ f_2(z/L) \qquad (41b)$$

$$C_{\theta_v q}(z) = r_{\theta_v q}\ \theta_{v*}\ q_*\ z^{-2/3}\ f_3(z/L) \qquad (41c)$$

where $r_{\theta_v q}$ is the virtual potential temperature-specific humidity correlation coefficient, and the f_i's are experimentally determined functions. As the water vapour density is related to the specific humidity by $\rho_w = \rho q$, where ρ is the total air density, we can express the water vapour density structure parameter, and the virtual potential temperature-water vapour density structure parameter by

$$C_{\rho_w}^2(z) = \rho^2(z)\ C_q^2(z) \qquad (42a)$$

$$C_{\theta,\rho_w}(z) = \rho(z)\ C_{\theta,q}(z)\,, \qquad (44b)$$

where we have assumed that the total density changes very little between z and z+h. Similarly, using Eqs. 6a and 8, and assuming that the specific humidity and the pressure change very little between z and z+h, the temperature structure parameter and the virtual temperature structure parameter are given by

$$C_T^2(z) = C_{T_v}^2(z)/[1 + (1 - \mu)q(z)/\mu]^2 \qquad (43a)$$

$$C_{T_v}^2(z) = (P(z)/1000)^{2(\gamma-1)/\gamma}\ C_{\theta_v}^2(z). \qquad (43b)$$

These results also imply the following two relations:

$$C_{Tq}(z) = C_{T,q}(z)/[1 + (1 - \mu)q(z)/\mu] \qquad (44a)$$

$$C_{T,q}(z) = (P(z)/1000)^{(\gamma-1)/\gamma} C_{\theta,q}(z)\ . \qquad (44b)$$

Subsequent substitution of the results from Eqs. 41 thru 44 into Eq. 40 allows one to easily calculate either the refractive index structure parameter, or the refractivity structure parameter once we have some knowledge about the correlation coefficient, $r_{\theta_v q}$, and the structure parameter functions, f_i's, in Eq. 41.

2.7.1 Structure Parameter Functions

Several expressions for the structure parameter function, f_1, have been proposed. Edson et al. (Ref. 21) proposed a modified version of that given by Wyngaard et al. (Ref. 22), while F.F.O.[1] (see Ref. 23) has proposed an independent function. These three functions are given

[1]Forschuninstitut Für Optik (Germany)

below:

$$(Wyngaard)\quad f_1(z/L) = \begin{cases} 4.9[1-7(z/L)]^{-2/3} & ;\ z/L<0 \\ 4.9[1+2.75(z/L)] & ;\ z/L\geq 0 \end{cases} \tag{45}$$

$$(Edson)\quad f_1(z/L) = \begin{cases} 5.8[1-7(z/L)]^{-2/3} & ;\ z/L<0 \\ 5.8[1+2.4(z/L)^{2/3}] & ;\ z/L\geq 0 \end{cases} \tag{46}$$

$$(F.F.O.)\quad f_1(z/L) = \begin{cases} 6.3[1-7(z/L)+75(z/L)^2]^{-1/3} & ;\ z/L<0 \\ 6.3[1+7(z/L)+20(z/L)^2]^{1/3} & ;\ z/L\geq 0\ . \end{cases} \tag{47}$$

L(W)WKD uses that of Edson et al.; however, the other two functional forms may be equally valid. The PIRAM model uses the F.F.O. functional form.

As it is difficult to determine the function f_2, most authors have worked under the assumption that it is proportional to f_1. This hypothesis implies that

$$\frac{C_{q^2}}{C_{\theta_v^2}} = A_{21}\frac{q_*^2}{\theta_{v*}^2} \tag{48}$$

where the structure parameter ratio $A_{21}(=f_2/f_1)$, is the proportionality constant to be determined, and which must always be positive. Similarly, using the following definition for $r_{\theta_v q}$:

$$r_{\theta_v q} = \frac{C_{\theta_v q}}{\sqrt{C_{\theta_v^2}\ C_{q^2}}}, \tag{49}$$

it follows that

$$f_1(z/L) = f_2(z/L)/A_{21} = f_3(z/L)/A_{21}^{1/2}. \tag{50}$$

The correlation coefficient can be either positive or negative depending upon whether the atmosphere is unstable or stable, respectively. Generally, it is accepted to have an absolute value between 0.6 and 1. Following Claverie et al. (Ref. 3), L(W)WKD uses an absolute value of 0.8 as the exact value has been shown to have little influence on the final result. Claverie et al. (Ref. 3) state that the constant of proportionality, A_{21}, can vary from 1 to 10^4 in the case of strong vapour pressure fluctuations. Neglecting the strong fluctuations, they assume it has a value of 1, even though this may not be entirely realistic. Davidson et al. (Ref. 24) suggest a value for A_{21} of 0.6. For the moment L(W)WKD will follow the recommendations of Claverie et al. until more experimental data have been collected. In this respect, A_{21} can be thought of as another experimental parameter to be determined. Consequently, both PIRAM and L(W)WKD use the same values for A_{21}, and the correlation coefficient.

3.0 THE L(W)WKD PROGRAM

Version 7.09 of the L(W)WKD program has seen a number of important changes since Version 6.1 was discussed in DREV's earlier report (Ref. 1). The principal changes include:

1) changes to the modular structure and their functions so as to satisfy the Canada-France agreement on a common set of fundamental equations and options

2) the capability for the user to modify certain global parameters within the program

3) the capability to compile the program in three different modes for easier integration into modular programs such as IRBLEM (Ref. 8)

and

4) the ability to calculate and output refractivity profiles for multiple sets of meteorological data taken at differing horizontal ranges.

Apart from these four changes, which are discussed in more detail below, many other changes have been made since Version 6.1. These changes are listed in the C file "LWWKD.C", of which its relevant section is given for reference in Appendix B.

To adapt the previous L(W)WKD program so as to integrate the common set of equations and options agreed upon thru an exchange between Canada and France, and for other reasons as well, the modular structure of the program, and many of its functions were modified. Most of the changes relevant to the Canada-France agreement were made to the PROFILE.C and WEATHER.C modules and their header files, as these files contain all of the profile and meteorological (weather) functions.

In order to give greater flexibility to the program, the program now looks for the initialization file "LWWKD.INI". If it doesn't exist the program uses default values for certain global parameters, while if it does exist the program will use the user defined parameters contained within the file. This addition required the addition of the module READINI.C and its header file. Further detail about the use of the initialization file are give in a later section.

Earlier versions of L(W)WKD have been able to operate in BATCH mode. That is, the user could run the program, select a METDATA file, and the program would output files containing the vertical refractivity profiles for a desired wavelength band, and various vertical meteorological (temperature, pressure, etc.) profiles. However, in recent years, a variants of the program have been produced so that they could be integrated as modules into modular programs such as IRBLEM. As a result, in order to reduce the amount of effort required to update these versions of the program, the same seventeen C modules and eighteen header files that currently make up L(W)WKD, can be compiled into three different programs by simply changing the INTERACT and WKDCN2 definitions within the LWWKD.H header file. If INTERACT is set to 1 and WKDCN2 set to 0, the INTERACTIVE version of the program LWWKD is created; however, when INTERACT is set to 0, two different BATCH programs, both of which are designed to be integrated into IRBLEM (Ref. 8) as separate modules, are created depending upon whether WKDCN2 is set to 0 or 1. If WKDCN2 is set to 0, a BATCH version of the program is created that outputs a file containing the vertical profile of the refractive index and its gradients, while if WKDCN2

is set to 1, a batch version of the program is created that outputs a file containing the vertical profile of the refractive index structure parameter. Both BATCH programs operate in a similar fashion to the BATCH mode of operation within the INTERACTIVE program, in that they look for a METDATA file (Ref. 1), processes it, and create appropriate output files for use in modular programs such as IRBLEM. More details about the three compilation modes are given in a later section.

The ability to calculate multiple vertical refractivity profiles using meteorological data at differing horizontal ranges is not an addition to Version 7.09; however, it wasn't present in Version 6.1. This additional feature is only currently available with the INTERACTIVE version of the program. It is useful when the vertical refractivity profiles are saved as an L(W)WKD binary data file and that file is used with a compatible ray-tracing program that can accept two-dimensional (vertical elevation and horizontal range) refractivity data. Ref. 25 shows an example of its use with the DREV program REFRACT.

Version 7.09, is written for DOS using Version 3.0 of Borland's TURBO C/C++. The program can also be run as a DOS program in WINDOWS or OS/2. Presently, the code is composed of seventeen C modules and eighteen user defined header files containing approximately 360 kb of code. All three compilations are compiled and linked using the large memory model and produce about 260 kb of executable code. The names of the modules are LWWKD.C, LWWKDBAT.C, LWWKDINT.C LWWKDSCR.C, GRAPHMET.C, GRAPHREF.C, GRAPHOTH.C, PROFILE.C, WEATHER.C, READINI.C, LIBERROR.C, LFILE.C, L_GRAPH.C, WIN.C, MENU.C, VALUEX.C, and MISC.C. Similarly, the header files are LWWKD.H, LWWKDBAT.H, LWWKDINT.H, LWWKDSCR.H, GRAPHMET.H, GRAPHREF.H, GRAPHOTH.H, PROFILE.H, WEATHER.H, READINI.H, LIBERROR.H, LFILE.H, L_GRAPH.H, WIN.H, MENU.H, VALUEX.H, CDEF.H, and IBMKEYS.H. LWWKD.C is the entrance module and contains two different **main** routines whose use depends upon the setting of the INTERACT definition within the LWWKD.H header file. Figures 3a,b and c show the flow of the L(W)WKD program in

both INTERACTIVE and BATCH compilation modes.

3.1 INTERACTIVE Program

If the INTERACTIVE program is compiled, the user can interactively control and monitor the program's operation. This interactivity is achieved through the use of menus whose options are selected using the keyboard, and windows that can either display information to the user, request input from the user, or allow the user to edit/modify information used by the program. The modules WIN.C, MENU.C and MISC.C along with the header files IBMKEYS.H, WIN.H, MENU.H and CDEF.H contain all the routines that manage these interactive resources. Further information regarding these resources can be found in Ref. 1.

3.1.1 L(W)WKD's Main Screen

Upon executing the L(W)WKD INTERACTIVE program, a copyright page informs the user of the owner's proprietary rights, the program's version and creation date. After reading the warning, the user can press any key to enter the program. The program starts by looking for the LWWKD initialization file "LWWKD.INI", and reading it if it exists. Table II shows the general format for the initialization file and the default values for all the user-definable parameters. It also shows the minimum and maximum permissible values. Any improper value causes the program to display a warning message, and to use the default values instead of those contained within the initialization file. Subsequently, it initializes other default structures within the program, calculates a default profile parameter, and displays the **Main** screen and the **Program** menu.

The **Main** screen is composed of two **text** windows and a **menu** window (see Fig. 4). The top-left "Weather Measurements" window shows the default weather parameters used by L(W)WKD to calculate the profile parameters that are shown in the top-right "Weather

TABLE II
General format for the LWWKD.INI file

Line #	Variables	Default	Minimum	Maximum	Comment/Example
1	Comment				- all comment lines must be at the beginning of the file, and they must start with a #. - for example: # This is a comment.
2	kel_cel	273.15	273	274	- variable to go between Celsius and Kelvin - for example: kel_cel 273.1
3	Mair	28.9	28	30	- variable giving the mass of dry air - for example: Mair 28.8
4	Mwater	18	17	20	- variable giving the mass of water - for example: Mwater 18.1
5	R	8.3145	8	9	- variable giving the Gas Constant - for example: R 8.31
6	g	9.806	9.5	10	-variable giving the acceleration due to gravity - for example: g 9.8
7	gamm	1.4	1.35	1.45	- variable giving the ratio of specific heat at constant pressure to that at constant volume for dry air -for example: gamm 1.41
8	cp	1004	1000	1010	- variable giving the specific heat at constant pressure - for example: cp 1004.1
9	Kconst	0.4	0.35	0.45	- variable giving von Karman's constant - for example: Kconst 0.41
10	p_adiab	1000	950	1050	- variable giving the adiabatic reference pressure - for example: p_adiab 1010.0
11	max_height	50	5	100	- variable giving the maximum output height for vertical profiles - for example: max_height 20.0
12	pot_mode	1	0	1	- variable giving the potential temperature mode (0 - use dry air pressure; 1 - use total air pressure) - for example: pot_mode 0
13	scale_mode	1	0	1	- variable giving the scaling function mode for stable conditions (0 - LWKD; 1 - KONDO) - for example: scale_mode 0
Note: all 12 variables do not have to be listed and they do not have to be listed in the above order. Thus the user only has to include those variables for which he does not want to use the default values.					

Profiles" window. Three changes from Ver. 6.1 can be noticed on the **Main** screen. These are the inclusion of multiple weather parameter data sets at different horizontal ranges, the addition of a sea surface relative humidity to each data set, and the addition of the ability to choose among three different model options. Table III shows the default weather parameters (**not tested** means that no bounds test is made). Figure 4 also shows these same parameters along with the resultant vapour pressure for the chosen data set as shown by the title "WEATHER PARAMETERS - 1" on the left side of the screen. At the bottom of the figure, the three default modes for the options **Scaling** (Scaling Equations), **Pot. Temp.** (Potential Temperature), and **Pressure** (Reference Adiabatic Pressure) are also shown. By default, the **KONDO** version of the scaling equations is used under stable conditions (see Eq. 3), and the total atmospheric pressure (**Tot.**) with a reference pressure of **1000 mb** are used in Eq. 8 to determine the potential temperature.

TABLE III
Parameter Bounds and Defaults in Interactive Mode

Parameter/Units	Minimum Bound	Maximum Bound	Default
Horizontal Range (km)	0	100	0
Wave Height (m)	0	10	0.25
Wind Sensor Height (m)	0	50	15
Wind Speed (m/s)	0	not tested	5
T/P/RH Sensor Height (m)	0	50	15
Air Temperature (°C)	not tested	not tested	10
Sea Temperature (°C)	not tested	not tested	5
Atmospheric Pressure (mb)	0	not tested	1010
Relative Humidity	0	1	0.8
Sea Surface Relative Humidity (%)	0	1	0.982

The L(W)WKD pr ofile parameters calculated using these initial values are displayed in the right-hand side window of Fig. 4. It shows the calculated roughness heights and scaling constants used for the wind speed, virtual potential temperature and the specific

humidity profiles. It also shows the wind speed, air temperature, relative humidity, and water vapour pressure calculated using these profiles, along with the Monin-Obukhov length and the number of iterations that were required for L(W)WKD to obtain the solution.

The **Program** menu (Fig. 3a) is the point of entry into the L(W)WKD program and is composed of three function keys F1-Interactive, F2-Batch and F5-EXIT. Pressing the F5 key opens a **dialog** window that requires a user response to the following question: "Exit program (Y/N)?". A **N**o response leaves the user inside the program while a **Y**es response clears the screen, closes the program, and returns the user to the operating system. Using the F1-Interactive function key opens a **message** window that displays "Use the Arrow keys to cycle between data sets" for several seconds before the user is presented with the **Main** menu and finds himself in the **Interactive** mode of operation. Likewise, pressing the F2-Batch function puts the user in the **Batch** mode of operation. The details of using either operational mode are fully described in the following two sections.

3.1.2 Interactive Mode

After the F1-Interactive function key of the **Program** menu has been selected, another window is added to the screen and the **Program** menu is replaced by the **Main** menu (see Fig. 5). The new, initially empty window is the "Other Weather Measurements" window. The purpose of the window is to display any other weather measurements that the user wishes to have included in any of the meteorological graphs. More details related to this window, along with the actions initiated by the four function keys; F1-Modify, F2-Load Data, F3-Save Data, and F4-Output Data, of the **Main** menu are given in the following subsections. The F5-RETURN key returns the user to the **Program** menu.

3.1.2.1 F1-Modify

The F1-Modify function key allows the user to modify the measured parameters so as to produce new profile parameters, to modify the three options, and to add/delete/modify values displayed in the "Other Weather Measurements" window. Upon pushing the key a new menu, the **Modify** menu, appears. It is composed of the four function keys F1-Weather, F2-Options, F3-Other;Wind, F4-Other;Temp and F5-RETURN (see Fig. 3b). Pressing the F5-RETURN key returns the user to the **Main** menu. The F1-Weather key allows the user to modify the weather parameters, the F2 key allows the user to modify the various options, while the F3 and F4 keys allow the user to modify the wind parameters or the temperature/relative humidity parameters belonging to the "Other Weather Measurements" window.

3.1.2.2 F1-Weather

Pressing the F1-Weather key presents the user with the **Weather** menu (see Fig. 3b). It is composed of the following four function keys: F1-Edit, F2-Add, F3-Delete, F4-RESET, F5-ABORT, and F6-RETURN. The F2-Add key is only displayed while the number of data sets is less than 10, and the F3-Delete key is only displayed when there is more than 1 data set. The F4-RESET and F5-ABORT keys are only present after a weather set has been edited. Pressing the F6-RETURN key opens the following **dialog** window: "Return to Main Menu? (Y/N):". A **No** response leaves the user at the same place within the program, while a **Yes** response returns the user to the **Modify** menu.

Pushing the F1-Edit key opens an **edit** window through which the user can modify the horizontal range for the measurements, the $H_{1/3}$ wave height, the wind speed and the wind sensor height, the sea temperature, sea surface relative humidity, and the air pressure, air temperature, relative humidity, and their sensor height. After the user has accepted the changes to these weather parameters, the program verifies that they are within the accepted bounds given by Table III. Any parameters outside these limits are reset to their previously

held values, new profile parameters are calculated, and the new weather and profile parameters are displayed on the main screen. On the other hand, if the profile parameters cannot be calculated, the following message, "Could not fit new weather parameters!!", is displayed in a **message** window for two seconds, and the newly edited weather parameters are reset to their previous values.

After accepting the modifications and returning to the **Weather** menu, the F4-RESET and F5-ABORT keys are available. The F4-RESET key allows the user to reset the weather parameters to the values they had before they were last edited, while the F5-ABORT key opens the **dialog** window: "Reset parameters and QUIT? (Y/N):". A **No** response leaves the user at the same place within the program, while a **Yes** response resets the weather parameters and returns the user to the **Modify** menu (i.e., it does a RESET and a RETURN).

Pushing the F2-Add key, when it is available, displays the **message**, "New weather parameter set added!!", for two seconds. The new data set is created using the default weather parameters at a horizontal range of 0 km. To edit or delete the new data set, use the left/right arrow keys to select the correct data set and push F1-Edit or F3-Delete, respectively. The operator has to select the proper weather parameter set as the program automatically reorders the sets by increasing horizontal range.

Pushing the F3-Delete key, when it is available, displays the **dialog** window: "Delete current weather parameter set? (Y/N):". If the correct set has not been chosen, make a **No** response, choose the correct data set using the left/right arrow keys, and push the F3-Delete key again. Choosing the **Yes** response automatically deletes the current data set, reorders the data sets, and displays one of the remaining data sets on the screen. This process can not be undone.

3.1.2.3 F2-Options

Pressing this new function key presents the user with an **edit** window that allows the user to modify the three modes for the **Scaling Equations**, the **Potential Temperature**, and the **Reference Pressure**. By default the **Scaling Equations** parameter is set to 1, which corresponds to the Kondo version of the gradient (scaling) equations used under stable conditions (see Eq. 3), the **Potential Temperature** parameter is set to 1, which corresponds to using the total atmospheric pressure in Eq. 8, and the **Reference Pressure** is set to 1000 mb for use in Eq. 8. Changing the **Scaling Equations** parameter to 0 allows the user to use the WKD version under stable conditions, changing the **Potential Temperature** parameter to 0 allows the user to use the dry-air atmospheric pressure in Eq. 8 instead of the total air pressure, and the **Reference Pressure** can take any value greater than 0 for use in Eq. 8. Any parameters outside these limits are reset to their previously held values, new profile parameters are calculated, and the new weather and profile parameters are displayed on the main screen. On the other hand, if the profile parameters cannot be calculated, the following message, "Could not fit using new options!!", is displayed in a **message** window for two seconds and the newly edited option parameters are reset to their previous values.

After accepting the modifications and returning to the **Options** menu, the F2-RESET and F3-ABORT keys are available. The F2-RESET key allows the user to reset the option parameters to the values they had before they were last edited while the F3-ABORT key opens the **dialog** window: "Reset options and QUIT? (Y/N):". A **No** response leaves the user at the same place within the program while a **Yes** response resets the weather parameters and returns the user to the **Modify** menu (i.e., it does a RESET and a RETURN).

3.1.2.4 F3-Other;Wind & F4-Other;Meteo

Selecting either of these two function keys presents the user with either the **Wind** menu

or the **Meteo** menu (see Fig. 3b). Both menus are identical and are composed of the following four function keys: F1-Edit, F2-Add, F3-Delete and F4-RETURN. However, the F1, F2 and F3 keys are not always displayed. Pressing the F4-RETURN key opens the following **dialog** window: "Return to Main Menu? (Y/N):". A **No** response leaves the user at the same place within the program while a **Yes** response returns the user to the **Modify** menu. The functions of the other keys are given in the following subsections.

3.1.2.4.1 F1-Edit

The F1-Edit key is only displayed when there is data that can be edited. Pushing the key opens an **edit** window which requests the user to enter the number (1 to 8) associated with the data set to be modified. An illegal entry produces the following two second **message** window, "Input out of range!!", and then allows the user to enter a new number. Once the data set has been selected, an **edit** window is opened and the user can modify the associated data. If the Other;Wind function key had previously been selected, the user can modify the wind speed and the wind sensor height, while if the Other;Meteo function key had previously been selected, the user can modify the air temperature, relative humidity, and the sensor height. After the user has accepted the changes to the edited parameters, the program verifies that they are within the same bounds given by Table III, before accepting them and displaying them on the main screen. The data sets are always displayed in increasing order with respect to their sensor heights.

3.1.2.4.2 F2-Add

The F2-Add key is only displayed when there is still space for another data set (the maximum number is 8). If there is, pushing the key opens an **edit** window through which the user can modify the parameters belonging to the appropriate default data set. If the Other;Wind function key had previously been selected, the user can add a new wind speed and wind sensor height, while if the Other;Meteo function key had previously been selected,

the user can add a new air temperature, relative humidity and meteo sensor height. After the user has accepted the new data set, the program verifies that they are within the limits given by Table III, and displays them on the main screen. Again, the data sets are listed in increasing ordered with respect to the sensor heights.

3.1.2.4.3 F3-Delete

The F3-Delete key is only displayed when there is data that can be deleted. Pushing the key opens an **edit** window which requests the user to enter a number, from 1 to 8, of the data set to be deleted. An illegal entry produces the following two second **message** window, "Input out of range!!", and then allows the user to enter a new number. Once the data set is selected, the following **dialog** window is displayed: "Delete data set (Y/N)?". A **No** response aborts the delete and returns the user to the preceding menu (**Wind** or **Meteo**) while a **Yes** response deletes the data set before returning the user to the preceding menu. The data sets are then reordered with respect to the sensor heights before they are redisplayed on the main screen.

3.1.2.5 F3-Save Data

The F3-Save Data function key allows the user to save certain information to a special L(W)WKD binary file having the extension "lwd". The file's most recent structure is shown in Table IV where the first column gives the data type (integer, float, etc.), the second gives the number of bytes it requires, and the third column describes the data type's significance. This file is a general purpose file that includes each set of measured weather parameters, and their associated profile parameters and refractivity profiles. The refractivity profiles are designed for use as input into ray-tracing algorithms. The file can be extended to contain other data while remaining backward compatible by changing the file identification number. In this way each file identification number can be uniquely associated with a specific L(W)WKD version's file format such that any program using such files always know exactly

how to retrieve the required data.

Upon pressing the key, the user is presented with the **Wave Selection** window (see Fig. 3a). It is a **selection** window from which the user can choose from one of five wavelength bands (Visible, Near-IR, Mid-IR, Far-IR, or Radar). After choosing the wavelength band, the user is presented with the **Model Selection** window. This is a **selection** window from which the user must choose to incorporate, or not, the Wavy Model for calculating the refractivity profiles. Once both selections are made, a **Save File** window is produced showing a listing of all the files in the current directory having the extension "lwd". Scroll through this listing until an **edit** window appears and enter a filename. Do not include the extension, as the extension "lwd" is automatically appended. Once the filename has been accepted, the user is presented with a second **edit** window. This window allows the user to create a unique file header for every L(W)WKD file. After creating the file header, the file is created, saved to the current directory, and the program displays the message: "Writing to file.....". Each file requires at least 4.5 kb.

TABLE IV
Format for the L(W)WKD binary file

Data Type	Bytes	Comments
1. Integer	2	File identification number = 4. Previous versions used 0, 1,2, & 3.
2. Integer	2	# of bytes in the file header including the null character = N.
3. String	N	N characters belonging to the file header.
4. Integer	2	# of bytes in the wavelength band's name including the null character = M.
5. String	M	M characters belonging to the wavelength band's name - VISIBLE, NEAR-INFRARED, MID-INFRARED, FAR-INFRARED or RADAR.
6. Integer	2	# of weather sets (maximum is 10)
7. Character	1	Scaling Equation Option (default is 1)
8. Character	1	Potential Temperature Option (default is 1)
9. Double	8	Reference Pressure Option (default is 1000 mb)
The following 4 outputs (10 to 13) are written for each weather set.		

10. Integer	2	# of bytes in the weather parameter structure (PARAM).
11. PARAM (11 floats)	32	PARAM contains the following 11 weather parameters - horizontal range, $H_{1/3}$ wave height, wind sensor height, wind speed, meteo sensor height, air temperature, sea temperature, air pressure, relative humidity, sea surface rel. humidity, and the sea surface wind speed (= 0).
12. Integer	2	# of bytes in the weather profile structure (W_STRUCT).
13. W_STRUCT (1 unsigned) (10 double)	81	W_STRUCT contains the following profile parameters - number of iterations (unsigned int), Monin-Obukhov length, wind speed scale and roughness height, wind speed, virtual potential temperature scale and roughness height, air temperature, water vapour density scale and roughness height, and relative humidity.
14. Float	4	Minimum height = $H_{1/3}/2$.
15. Float	4	Maximum height = 50.
16. Integer	2	# of bytes in the Other Wind weather structure (W_PARAM).
17. Integer	2	# of Other Wind weather structure data sets.
Output 18 is done for each Other Wind data set.		
18. W_PARAM	8	W_PARAM contains a wind sensor height and a wind speed.
19. Integer	2	# of bytes in the Other Meteo weather structure (M_PARAM).
20. Integer	2	# of Other Meteo weather structure data sets.
Output 21 is done for each Other Wind data set.		
21. M_PARAM	12	M_PARAM contains a meteo sensor height, an air temperature and a relative humidity.
The following output is written for each weather set.		
22. Data Record (2 float) (3 double)	32	Each data record contains the range (L = 0 km), the height (m) above the MWL (h), the refractivity (Z), and two derivatives (dZ/dh and dZ/dL(=0)) at the height h. The height (h) is calculated iteratively as follows: h = h + 0.05 + 0.025*h and records are written until h = max. height. The refractivities are calculated for the chosen wave band.

3.1.2.6 F2-Load Data

The F2-Load Data function key allows the user to load the meteorological parameters previously saved in an L(W)WKD binary file from the current directory. When the key is pressed, the user is presented with a **Load File** window showing a numbered list of all the

files in the current directory with the extension "lwd". Make a note of the number associated with the file to be loaded while scrolling through the listing. When the **edit** window appears, enter the number. If the number is valid, the file is loaded, and displays the file's header and the wavelength band for two seconds each before displaying the message "File Loaded....". It should be noted, that all previous binary file formats can be read, and that the refractivity profile data records are neither read nor required by the program.

3.1.2.7 F4-Output Data

Pressing the F4-Output Data key of the **Main** menu presents the user with the **Output** menu (see Fig. 3c). This menu consists of the five function keys: F1-Meteo Screen, F2-Meteo Profile, F3-Ref. Profile, F4-Other Graphs, and F5-RETURN. Pressing the F5-RETURN key returns the user to the **Main** menu while use of the other keys allows the user to produce various textual or graphical outputs. These outputs are discussed in the following subsections.

3.1.2.7.1 F1-Meteo Screen

Choosing the F1-Meteo Screen key allows the user to output the data displayed on the **Main** screen to a file in either ASCII or PostScript format. These files can then be sent to a printer to produce a hardcopy of the **Main** screen or as input for other software. Upon pressing the key, the user is presented with a **File Selection** window. This **selection** window contains two choices: PostScript or ASCII File. After selecting the file type, a **Save File** window is produced showing a listing of all the files in the current directory with the appropriate extension ("psc" or "asc"). Scroll through the list until the **edit** window appears and enter a filename without an extension. Once the filename is accepted, the file is created, saved to the current directory, and the program displays the message: "File Written.....", before returning to the **File Selection** window. The PostScript file requires 5.5 kb, and the

ASCII file 1.5 kb.

3.1.2.7.2 F2-Meteo Profile

Choosing the F2-Meteo Profile key allows the user to graphically output various vertical profiles, for six different meteorological parameters, to the monitor or a PostScript file. Upon pressing the key, the user is presented with the **Meteo Selection** window. This **selection** window has the following options: Wind Speed, Air Temp., Virt. Pot. Temp., Total Pressure, Rel. Humidity, Vapour Pressure, Spec. Humidity, Vapour Density, and ALL-ASCII. The ALL-ASCII option allows the user to create an ASCII file containing the profiles for all eight parameters. The file's general format is given in Table V. After selecting any of the above choices, the user is presented with the **Model Selection** window. Once the model (Non-Wavy or Wavy) for the profile calculation is chosen, the **Height Edit** window appears. It is an **edit** window requiring the user to enter the maximum height to which the profiles are to be calculated. The default value is given by **max_height** as given by Table II. After entering this parameter the program follows one of two paths.

TABLE V
General format for all ASCII files

Line #	Variable (Format)	Comment
1.	File identification number (integer)	Identifies the file's origins (= 10)
2.	File description (string)	States the type of file and L(W)WKD version
3.	Waveband descriptor (string)	This line is optional. Not all files use it.
4.	Min. and max. height (reals)	This line is optional. Not all files use it.
5.	Fixed profile height (real)	This line is optional. Not all files use it.
6.	Headers for each column (string)	The headers describe the structure of each data record
7.	Underline for each header (string)	
8.	Data record (all real)	Currently, the largest record contains 9 consecutive real parameters

If the ALL-ASCII option was chosen, a **Save File** window is displayed showing a listing of all the files in the current directory with the extension "asc". Scroll through the listing until the **edit** window appears, and enter a filename without an extension. After the filename is accepted, the file is created, saved to the current directory, and the program displays the message: "File Written.....", before returning to the **Meteo Selection** window. The ASCII file requires about 9 kb for the default height of 50 m with a step size of 0.5 m.

If any of the other options were chosen, the user is shown the **Display Selection** window. It is a **selection** window with the following two display options: Monitor or PostScript. Choosing Monitor will create a graphical display on the screen. To remove the graph from the screen and be returned to the **Meteo Selection** window, the user may strike any key on the keyboard. If PostScript is chosen, a **Save file** window is produced showing a listing of all the files in the current directory with the extension "psc". Scroll through the list until the **edit** window appears and enter a filename without an extension. Once the filename is accepted, the graph is written to the file and saved to the current directory, before returning the user to the **Meteo Selection** window. The PostScript file requires close to 5 kb under the default conditions. Any weather data present in the "Other Weather Measurements" window is also plotted on these graphs; however, they are not included in the ASCII files.

3.1.2.7.3 F3-Index Profile

Choosing the F2-Ref. Profile key allows the user to graphically output XY plots of either the refractivity (Z), the derivative of the refractivity with height (dZ/dh), or the second derivative of the refractivity with height (d^2Z/dh^2) for any of the wavelength bands to the monitor, or to a PostScript file for different X-parameters. The possible X-parameters are the height above the MWL, the ASTD (sea temperature fixed), the wind speed, and the relative humidity. All plots can also be done with or without the Wavy model.

Upon pressing the key, the user is presented with the **Refractivity Y Selection** window. This is a **selection** window having the following options: Refractivity, d(Ref.)/d(H), dd(Ref.)/dd(H), and ALL-ASCII. The ALL-ASCII option allows the user to create an ASCII file containing the values for all three refractivity profiles using the same general format shown in Table V. After pressing the key, the user is presented with the **Refractivity X Selection** window. It's a **selection** window with the following options: Height, ASTD (sea fixed), Wind Speed, and Rel. Humidity. Once it has been selected, the **Wave Selection** window, and then the **Model Selection** window are displayed to the user. After choosing both the wave band and whether or not to use the Wavy model, the **Height Edit** window appears. If the X-dependent parameter is "Height", enter the maximum height ($\leq$ **max_height** given by Table II) to which the appropriate Y-parameter profile is to be plotted. Otherwise, enter the height ($\leq$ **max_height**) at which the appropriate Y-parameter is to be calculated for the chosen X-dependent parameter. After choosing this height, the program follows one of the two following paths.

If the ALL-ASCII option was chosen, a **Save File** window is displayed showing a listing of all the files in the current directory with the extension "asc". Scroll through the list until the **edit** window appears, and enter a filename without an extension. After the filename is accepted, the file is created, saved to the current directory, and the program displays the message: "File Written.....", before returning to the **Ref. Y Selection** window. The ASCII file usually requires less than 10 kb.

If any other option was chosen, the user is shown the **Display Selection** window. Choosing Monitor creates a graphical display on the screen. To remove it from the screen and be returned to the **Wave Selection** window, the user may strike any key on the keyboard. If PostScript is chosen, a **Save File** window is produced showing a listing of all the files in the current directory with the extension "psc". Scroll through the list until the **edit** window appears, and then enter a filename without an extension. Once the filename is accepted, the

graph is written to the file and saved to the current directory before returning the user to the **Ref. Y Selection** window. The PostScript file usually requires less than 6 kb.

3.1.2.7.4 F4-Other Graphs

Choosing the F4-Other Graphs key allows the user to graphically output various XY plots to the monitor, or to a PostScript file using either the Non-Wavy or Wavy model. ASCII files, using the same general format given in Table V, can also be created. Upon pressing the key, the user is presented with the **Graphic Selection** window (see Fig. 3c). It's a **selection** window with the following two general options for the Y-axis: Structure Parameters and Profile Parameters.

Choosing Structure Parameters allows the user to create XY plots for four structure parameters as functions of six different parameters for any of the five wavelength bands. The possible structure parameters are the refractivity structure parameter, the temperature structure parameter, the vapour density structure parameter, and the temperature-vapour density structure parameter. The possible dependent X-axis parameters are the height above the MWL, the ASTD (sea temperature fixed), the ASTD (air temperature fixed), the wind speed, the relative humidity, and the $H_{1/3}$ wave height.

Choosing Profile Parameters allows the user to create XY plots of the various weather profile parameters versus the ASTD (sea temperature fixed), the ASTD (air temperature fixed), the wind speed, the relative humidity, the reference pressure (adiabatic pressure), or von Karmen's constant. The possible weather profiles are the Monin-Obukhov length, the wind scale parameter, the wind roughness height, the temperature scale parameter, the temperature roughness height, the humidity scale parameter, and the humidity roughness height. As the process involved in creating these graphs or files are nearly identical to that for creating graphs of the refractivity profiles, only their differences will be described.

If the user chooses to create graphs of a structure parameter, the user will discover that the process is nearly identical to that for creating graphs of the refractivity profiles. The differences are only with respect to the available choices for the Y-axis and X-axis parameters. On the other hand, if the user chooses to create graphs of a profile parameter, the user will notice the following differences. After having entered a choice for the Y-parameter and the X-parameter, the user will not be asked to select a wave band or whether or not to use the Wavy model. This is because these parameters are independent of these two options. After displaying the selected XY plot on the monitor, saving the selected XY plot to a PostScript file, or saving the entire set to an ASCII file, the program returns to the appropriate **Y Selection** window. The PostScript files use less than 5 kb while the ASCII files use less than 10 kb.

3.1.3 Batch Mode

Pressing the F2-Batch function key of the **Program** menu allows the user to produce weather, structure parameter, and refractivity output files from an input file containing up to 999 sets (records) of weather measurements. Upon selecting this mode, three new windows are added to the bottom of the **Main** screen. These are the "Warnings", "Status" and "METDATA File" windows (see Fig. 6). The "Warnings" window informs the user of any problems associated with analyzing a specific weather record while the "Status" window shows the user which weather record is currently being processed. The "METDATA File" window is an **edit** window containing the name of the default input ASCII file: "METDATA". The user may change the name or accept it. The format of this file is given in Table VI. If a valid METDATA file is not entered, the user is returned to the **Program** menu; otherwise, the user is presented with the **Wave Selection** window, and then the **Model Selection** window. After having selected both the wavelength band, and whether or not to incorporate the Wavy model, the **Processing** menu (see Fig. 3a) is displayed and the program begins to process the weather records belonging to the METDATA file. The **Processing**

TABLE VI

General format for a METDATA ASCII file - a space separates each item

Line #	Variables	Comment/Example
1	String comment line	-each comment line must start with a # - for example: #This is a comment.
2	5 integers	-day, month, hour, minute, and measurement interval (min.) - for example: 20 2 8 20 5 (they are often set to zero)
3	Integer (N_w)	-number of weather conditions in the file - for example: 10
4...	Read weather condition (read 1 line at a time)	-each line contains 22 variables in the following order: air temperature measurement height (m), atmospheric pressure (mbar), air temperature (° C), relative humidity (%), solar radiation*, wind speed, wind direction*, water temperature (°C), wind speed measurement height (m), $H_{1/3}$ wave height (m), visibility (km)*, humidity measurement height (m)*, neutral drag coefficient (A)*, neutral drag coefficient (B)*, neutral Stanton number*, neutral Dalton number*, wavelength (μm)*, pressure measurement height (m)*, air mass parameter*, and 24hr wind speed*, precipitation rate (mm/hr)*, and precipitation type (0-4)*. * parameter is not required by L(W)WKD - for example 15.0 1010.0 10.0 80.0 500.0 5.0 270 12.0 20.0 1.5 9.0, 0, 0, 0, 0, 0, 0, 0, 10, 3.0 0 0

menu contains two active function keys: F1-Pause/Restart and F5-STOP. Pressing the F1 function key, which initially displays "Pause", causes the data processing to be stopped, changes the F1 function key's display to "Restart", and presents the following message to the user: "Processing Paused". To continue the processing and return the screen to its initial state, the user need only press the F1 function key a second time. The F5-STOP function key can be pushed at any time and presents the user with the following **dialog** window: "Stop processing (Y/N)?". The default response is **No** and returns the user to the previous state of the program, while a **Yes** response, stops all processing, closes all files, and returns the user to the **Wave Selection** window.

As the METDATA file's records are processed, the results are saved to three ASCII files: RFCOND or IRCOND, TDPxxx, MP_H_xxx, and CN2_xxx. The RFCOND or

TABLE VII
General format for the RFCOND or IRCOND output files

Line #	Variables	Comment/Example
1	5 integers (RFCOND) 5 int. and 1 real (IRCOND)	-day, month, hour, minute, measurement interval (min.), and wavelength (micron) -wavelength is only given for the IRCOND file 20 2 8 20 5 - RFCOND example 20 2 8 20 5 0.55 - IRCOND example
The following two lines are output for each weather set.		
2	11 real numbers for each weather condition	-air temperature measurement height (m), atmospheric pressure (mbar), air temperature (° C), relative humidity (%), solar radiation, original wind speed (before any step changes), wind direction, water temperature (° C), wind speed measurement height (m), $H_{1/3}$ wave height (m), and visibility (km). - example 15.0 1010.0 15.0 80.0 500.0 5.0 270 10.0 20.0 1.5 9.0
2	9 real numbers for each weather condition	-stability error code, duct height (m), Monin-Obukhov length (m), the three scaling parameters u_* (m/s), θ_* (°C) and q_* (kg/kg), and the three roughness lengths z_{0u} (m), $z_{0\theta}$ (m) and z_{0q} (m).

IRCOND file is generated depending upon whether the calculation is for the radar domain or the infrared (visible) domain, respectively. The format for either of these two files is given in Table VII. The stability/error code provides the user with an indicator as to the reliability of the results. The format of this code is '*IJ.K*', where *J* can have a value between 0 and 8 depending upon how many of the entered parameters are tested (not all parameters are tested) and found to be outside their respective minimum and maximum bounds (see Table VIII). Thus *J* equal to 5 would indicate that five of the parameters were found to be outside their bounds. Those found to be outside their bounds are set to their respective default values. *I* equal to 2 indicates that a solution was found by incrementing the wind speed in steps of 0.5 m/s, *I* equal to 1 that no solution could be found up to a maximum wind speed of 25 m/s, and I equal to 0 that a solution was found without having to change the wind speed. If a solution is found, *K* equal to 1 indicates that the weather condition was stable, and a value of 2 that the weather condition was unstable.

TABLE VIII
Parameter Bounds and Defaults

Parameter/Units	Minimum Bound	Maximum Bound	Default
Wind Speed (m/s)	0	not tested	1
Sea Temperature (°C)	-10	40	15
Air Temperature (°C)	-40	40	15
Wave Height (m)	0	5	0.5
Wind Speed Measurement Height (m)	0	not tested	10
Temperature Measurement Height (m)	0	not tested	10
Air Pressure (mb)	0	not tested	1010
Relative Humidity (%)	0	100	80

The files TDPxxx, MP_H_xxx, and CN2_xxx are produced for each and every weather condition where xxx is an index referring to the xxxth weather condition in the input METDATA file. The TDPxxx files contain vertical profiles for the air temperature (°C), relative humidity (%), total air pressure (mbar), and wind speed (m/s), the MP_H_xxx files contain vertical profiles of the modified refractivity, and its first and second derivatives, and the CN2_xxx files contain vertical profiles for the refractive index, temperature, water vapour density, and temperature-water vapour density structure parameters. All the profiles go up to **max_height** as given by Table II. The modified refractivity (M) is defined by

$$M(z) = Z(z) + 0.157z \quad (51a)$$
$$M'(z) = Z'(z) + 0.157 \quad (51b)$$
$$M''(z) = Z''(z) \quad (51c)$$

where z is the height in meters and Z is the refractivity. Table IX gives the general format used by these three files.

3.2 BATCH Programs

If either of the two BATCH programs are compiled, the user can run the resultant

TABLE IX

General format for the TDPxxx, MP_H_xxx, or CN2_xxx output files

Line #	Variables	Comment/Example
1	Information lines as column titles	- MP_H_xxx files # h[m], M(h), M'(h), M''(h) - TDPxxx files # HEIGHT TEMPERATURE Rel. Hum. PRESSURE WIND SPEED # [m] [Deg] [%] [mbar] [m/s] # - CN2_xxx files # HEIGHT INDEX TEMP. VAP. DEN. TEMP.-VPDN # [m] [m-2/3] [m-2/3] [m-2/3] [m-2/3] #
2...	real numbers for each weather condition	- MP_H_xxx files height, modified refractivity, 1st and 2nd derivatives - TDPxxx files height, air temperature, relative humidity, total air pressure and wind speed - CN2_xxx files height, refractive index, temperature, water vapour density and temperature-water vapour density structure parameters

programs as DOS command line functions. As mentioned earlier, when it is compiled with the WKDCN2 definition parameter set to 0, the program's principal objective is to produce output files containing vertical profiles of the refractive index and its gradients. Likewise, when it is compiled with the WKDCN2 definition parameter set to 1, the program's principal objective is to produce output files containing vertical profiles of the structure parameters. In fact, the programs obtained by both of these compilation modes follow essentially the same program structure as the INTERACTIVE program (see Fig. 3a) when it is used in BATCH mode. Apart from the fact that the input file must be named "METDATA", and that the file CN2_xxx is not produced when the WKDCN2 definition parameter is set to 0, and that only the CN2_xxx file is produced when the WKDCN2 definition parameter is set to 1, the differences are slight. The remaining differences have to do with the display of Error and Status information, and whether or not this information is sent to the screen, or to one of the two output files "MsgList.txt" or "LogFile.txt". These operational differences are controlled by five programming switches (M, A, L, X, & C) that can be added to the command line. The M switch puts the program into a non-verbose mode (i.e., fewer messages are sent to the

screen or to the files). The A switch tells the program to append all Error & Status information to any previously existing output files instead of creating new output files. The L switch directs the program to redirect all screen output to the file, "LogFile.txt", and to open the file if necessary (dependent upon the A switch). If the program stops prematurely, the X switch directs the program to output any relevant messages to the screen, regardless of the other switches. Finally, the C switch directs the program to check if a previous run of the program exited prematurely. It does this by checking the previous "MsgList.txt" file; consequently, it requires the A switch in order to function. If it finds that it did exit prematurely, the program stops immediately.

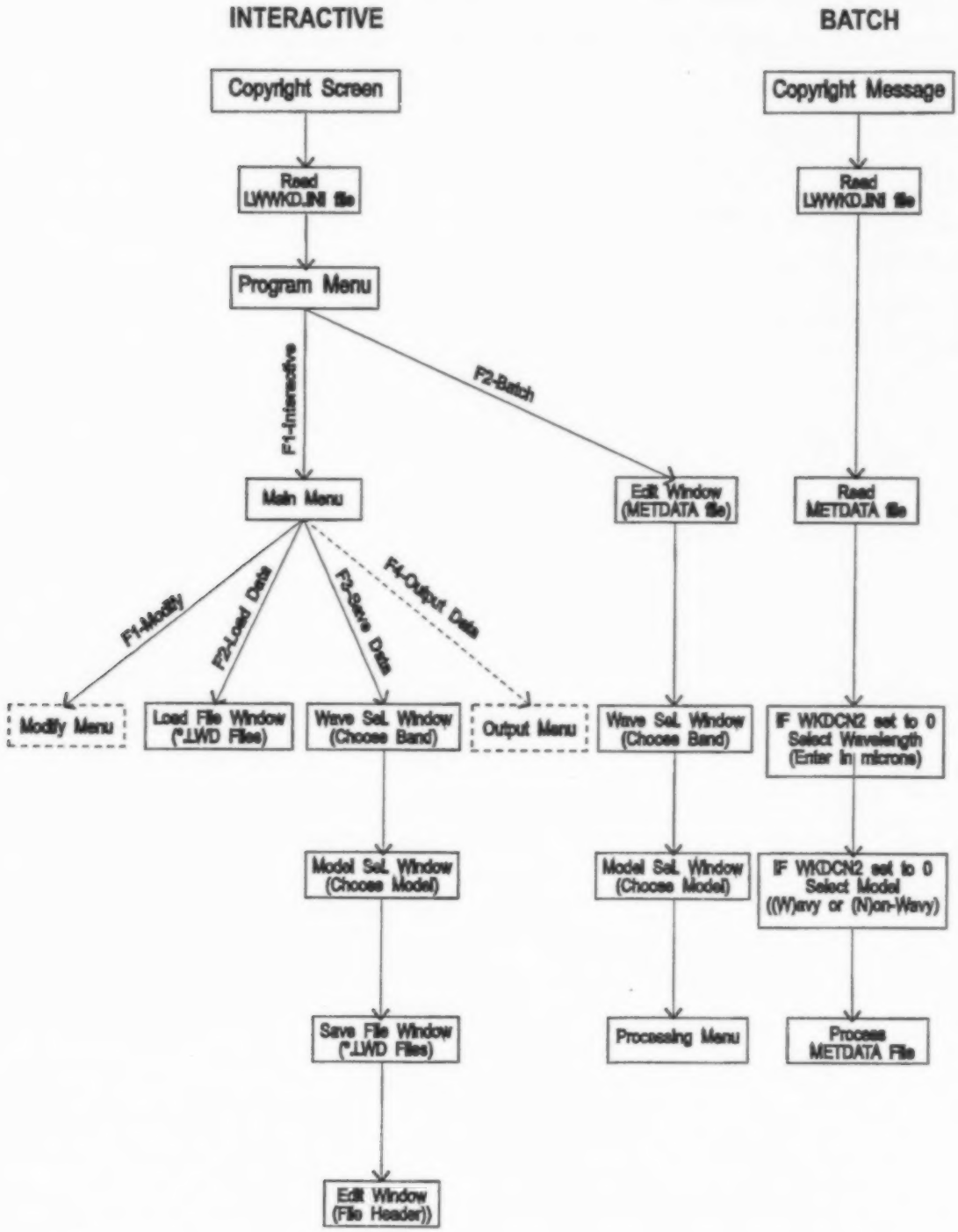

FIGURE 3a - Schematic of the L(W)WKD program's operating structure

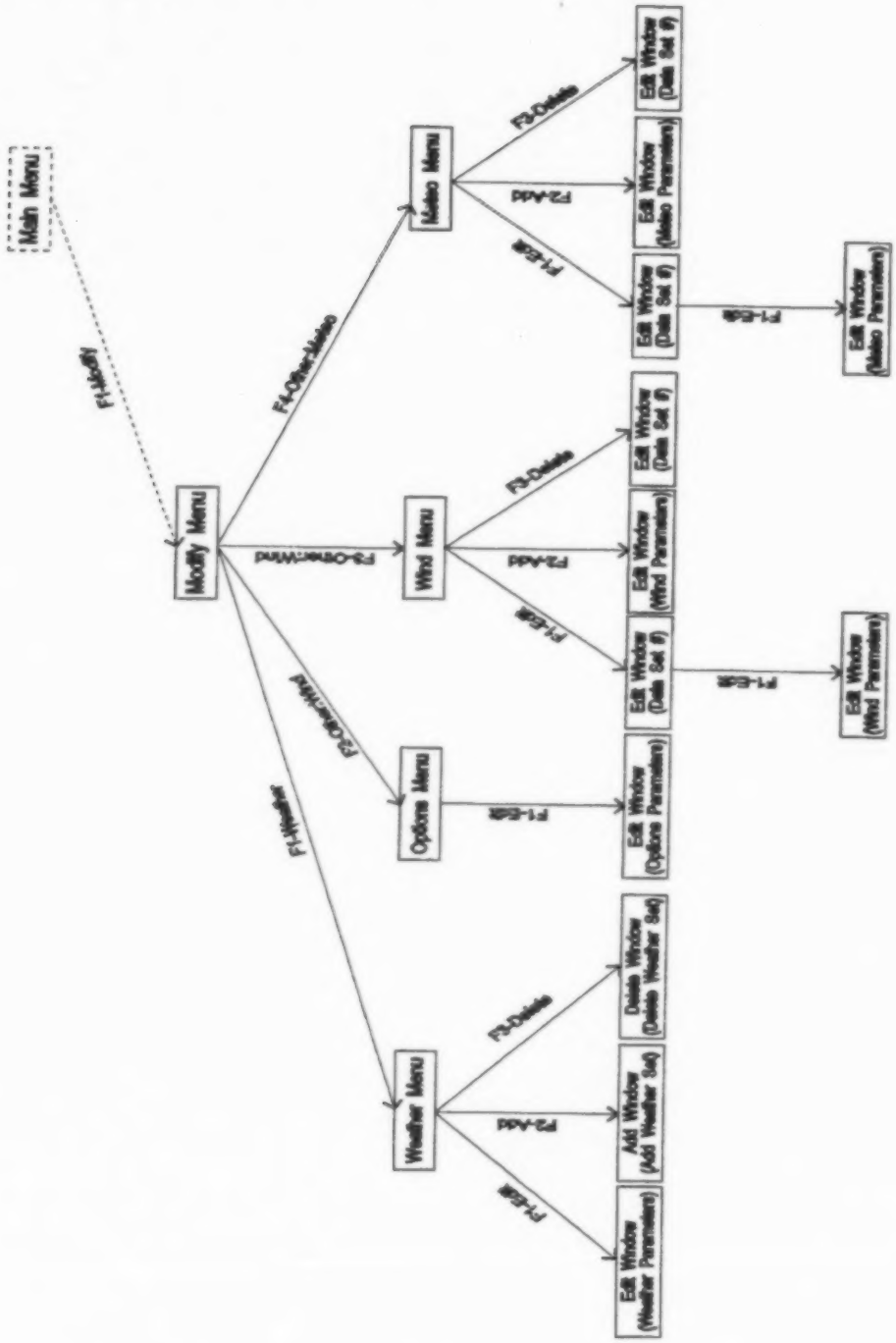

FIGURE 3b - Schematic of the L(W)WKD program's operating structure after selection of the MODIFY menu

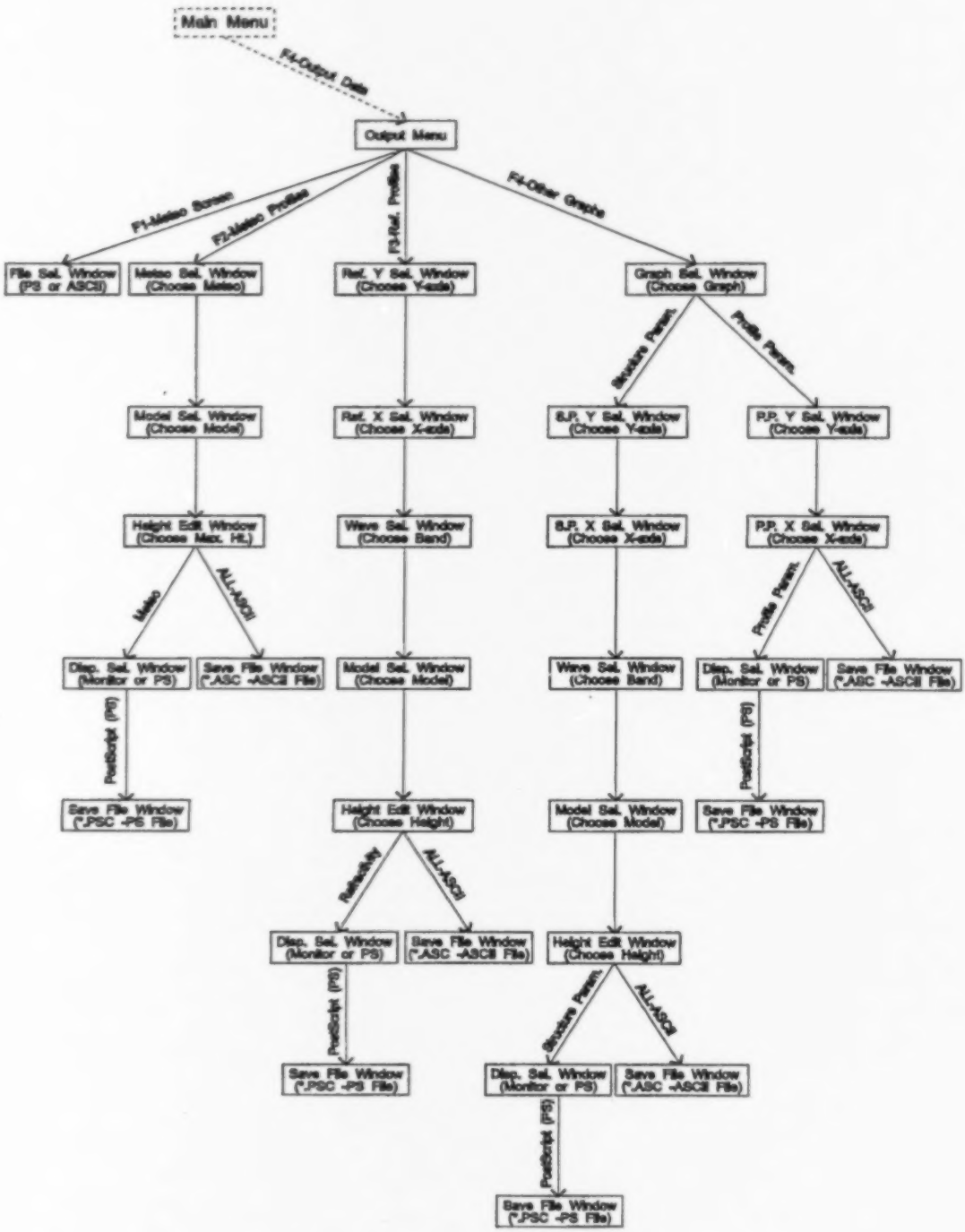
Main Menu
F4-Output Data
Output Menu
F1-Meteo Screen
F2-Meteo Profiles
F3-Ref. Profiles
F4-Other Graphs
File Sel. Window (PS or ASCII)
Meteo Sel. Window (Choose Meteo)
Ref. Y Sel. Window (Choose Y-axis)
Graph Sel. Window (Choose Graph)
Structure Param.
Profile Param.
Model Sel. Window (Choose Model)
Ref. X Sel. Window (Choose X-axis)
S.P. Y Sel. Window (Choose Y-axis)
P.P. Y Sel. Window (Choose Y-axis)
Height Edit Window (Choose Max. Ht.)
Wave Sel. Window (Choose Band)
S.P. X Sel. Window (Choose X-axis)
P.P. X Sel. Window (Choose X-axis)
Meteo
ALL-ASCII
Profile Param.
ALL-ASCII
Disp. Sel. Window (Monitor or PS)
Save File Window (*.ASC -ASCII File)
Model Sel. Window (Choose Model)
Wave Sel. Window (Choose Band)
Disp. Sel. Window (Monitor or PS)
Save File Window (*.ASC -ASCII File)
PostScript (PS)
PostScript (PS)
Save File Window (*.PSC -PS File)
Height Edit Window (Choose Height)
Model Sel. Window (Choose Model)
Save File Window (*.PSC -PS File)
Reflectivity
ALL-ASCII
Disp. Sel. Window (Monitor or PS)
Save File Window (*.ASC -ASCII File)
Height Edit Window (Choose Height)
PostScript (PS)
Structure Param.
ALL-ASCII
Save File Window (*.PSC -PS File)
Disp. Sel. Window (Monitor or PS)
Save File Window (*.ASC -ASCII File)
PostScript (PS)
Save File Window (*.PSC -PS File)

FIGURE 3c - Schematic diagram of the L(W)WKD program's operating structure after selection of the Output Data menu

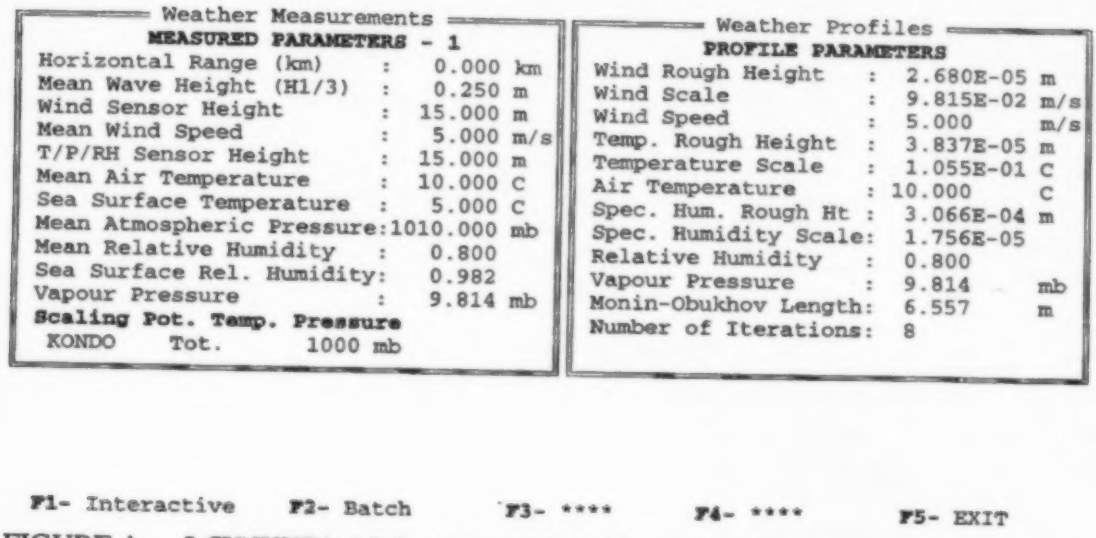
Weather Measurements
MEASURED PARAMETERS - 1
Horizontal Range (km) : 0.000 km
Mean Wave Height (H1/3) : 0.250 m
Wind Sensor Height : 15.000 m
Mean Wind Speed : 5.000 m/s
T/P/RH Sensor Height : 15.000 m
Mean Air Temperature : 10.000 C
Sea Surface Temperature : 5.000 C
Mean Atmospheric Pressure: 1010.000 mb
Mean Relative Humidity : 0.800
Sea Surface Rel. Humidity: 0.982
Vapour Pressure : 9.814 mb
Scaling Pot. Temp. Pressure
KONDO Tot. 1000 mb
Weather Profiles
PROFILE PARAMETERS
Wind Rough Height : 2.680E-05 m
Wind Scale : 9.815E-02 m/s
Wind Speed : 5.000 m/s
Temp. Rough Height : 3.837E-05 m
Temperature Scale : 1.055E-01 C
Air Temperature : 10.000 C
Spec. Hum. Rough Ht : 3.066E-04 m
Spec. Humidity Scale: 1.756E-05
Relative Humidity : 0.800
Vapour Pressure : 9.814 mb
Monin-Obukhov Length: 6.557 m
Number of Iterations: 8
F1- Interactive
F2- Batch
F3- ****
F4- ****
F5- EXIT

FIGURE 4 - L(W)WKD's Main screen with the **Program** menu

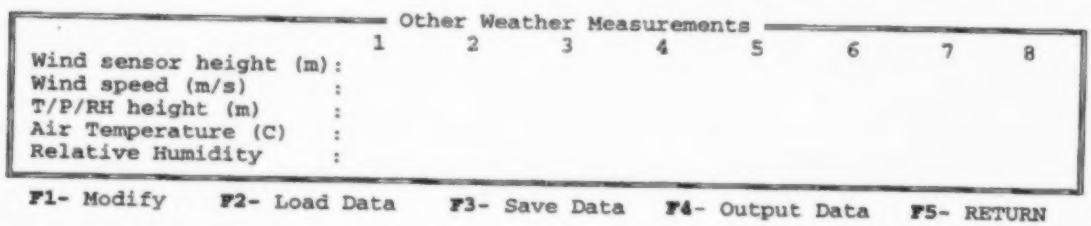

FIGURE 5 - L(W)WKD's "Other Weather Measurements" window with the **Main** menu

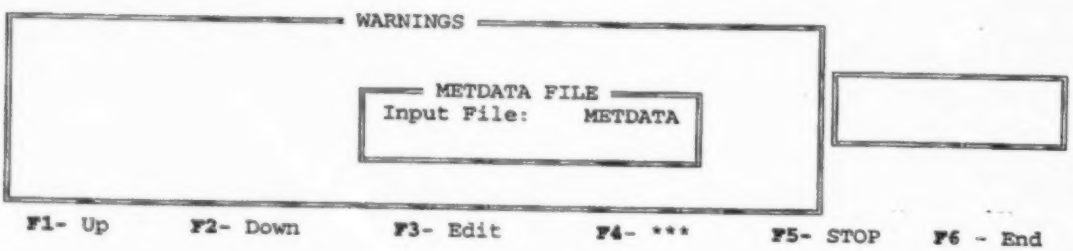

FIGURE 6 - The "Warnings", "Status" and "METDATA File" windows used in "Batch" mode with the **Main** menu

4.0 EXAMPLES

The objectives of this chapter are to illustrate some of L(W)WKD's capabilities when used as an interactive program. Examples of some of the graphics that can be created using L(W)WKD in interactive mode are shown.

Figures 7 to 10 show various graphs of the type of data that can be produced by version 7.09 of the L(W)WKD program (non-wavy model) for visible light (say 550 nm). For each graph, the water temperature is taken to be 12.5 ^{0}C, the wind speed is taken to be 5 m/s at a height of 22.5 m above the water level, the relative humidity is taken to be 65%, and the atmospheric pressure to be 1026 mbar at a height of 12 m above the water level. The $H_{1/3}$ wave height is taken to be 0.18 m, and the air temperature measured at 12 m above the water level is taken to be 8.4 ^{0}C when the ASTD is -4.1 ^{0}C (unstable case), and 16.6 ^{0}C when the ASTD is 4.1 ^{0}C (stable case).

Figure 7 shows a plot of the vertical air temperature (symbols only) and refractivity (solid line with symbols) profiles produced under both of these conditions. Comparing the vertical air temperature profiles for the cases, one notices that the gradient near the water surface (below 1 m) is much stronger in the unstable case than for the stable case and of opposite sign. But at higher elevations, the gradient is stronger in the stable case than in the unstable case and of the same sign. Comparing the vertical refractivity profiles, one notices the same type of behaviour, except that there is actually an inversion in the refractivity for the unstable case. This implies that, for the stable case, light rays are continuously bent towards the surface of the earth with the strongest bending occurring closest to the surface; while in the strongly unstable regime, light rays are bent slightly towards the surface of the earth above ~6 m and away from the surface of the earth below ~6 m. These are the kinds of conditions that can cause ducting of the light, and secondary image formation, respectively.

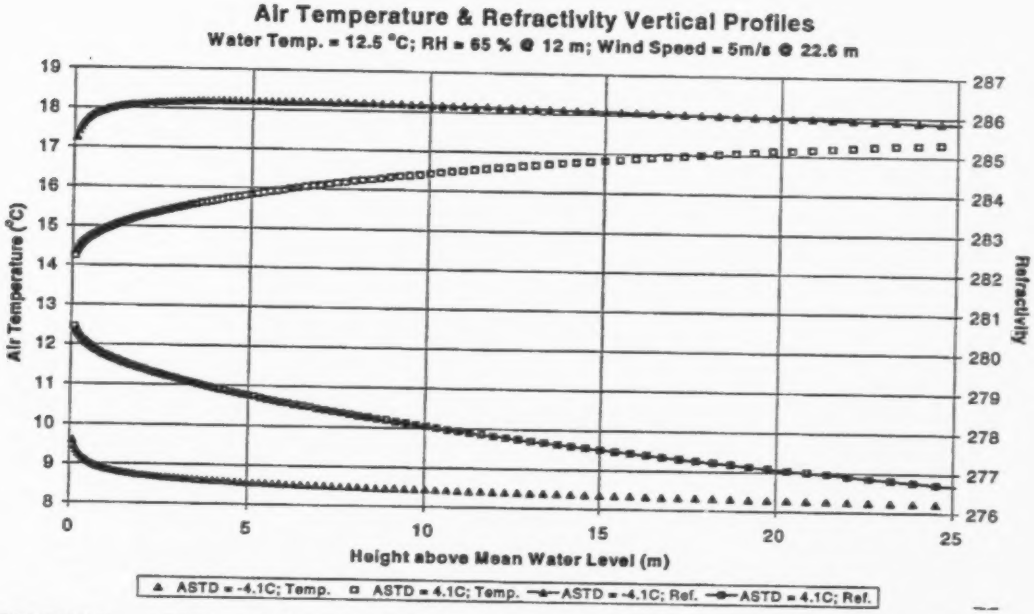
Air Temperature & Refractivity Vertical Profiles
Water Temp. = 12.5 °C; RH = 65 % @ 12 m; Wind Speed = 5m/s @ 22.6 m
Air Temperature (°C)
Refractivity
Height above Mean Water Level (m)
ASTD = -4.1C; Temp.
ASTD = 4.1C; Temp.
ASTD = -4.1C; Ref.
ASTD = 4.1C; Ref.

FIGURE 7 - Plots of the vertical air temperature and visible refractivity profiles for ASTDs of -4.1 °C and 4.1 °C using the L(W)WKD model in non-wavy mode

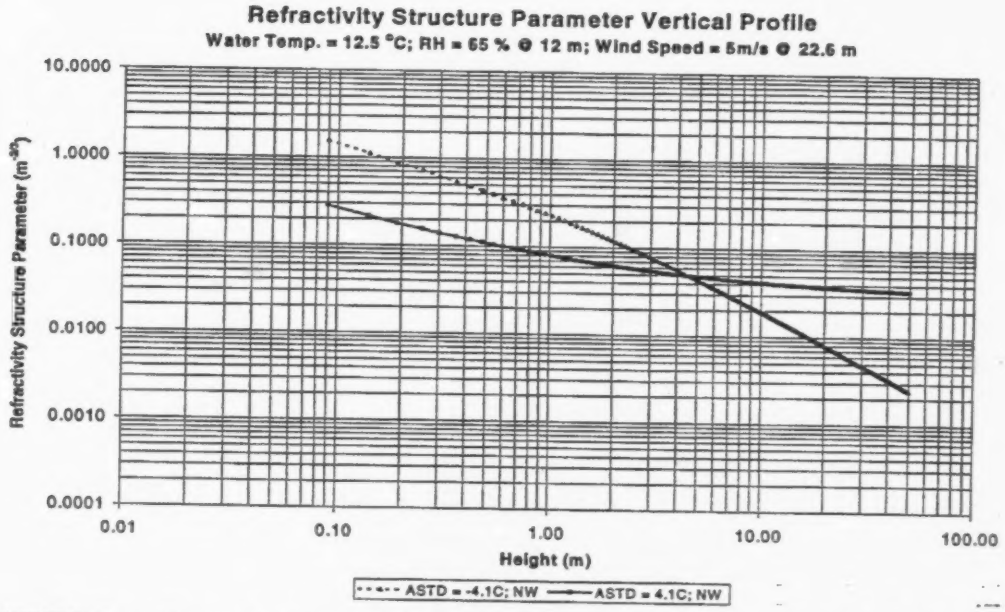
Refractivity Structure Parameter Vertical Profile
Water Temp. = 12.5 °C; RH = 65 % @ 12 m; Wind Speed = 5m/s @ 22.6 m
Refractivity Structure Parameter (m^-2/3)
Height (m)
ASTD = -4.1C; NW
ASTD = 4.1C; NW

FIGURE 8 - Plot of the refractivity structure parameter for ASTDs of -4.1 °C and 4.1 °C using the L(W)WKD model in non-wavy mode

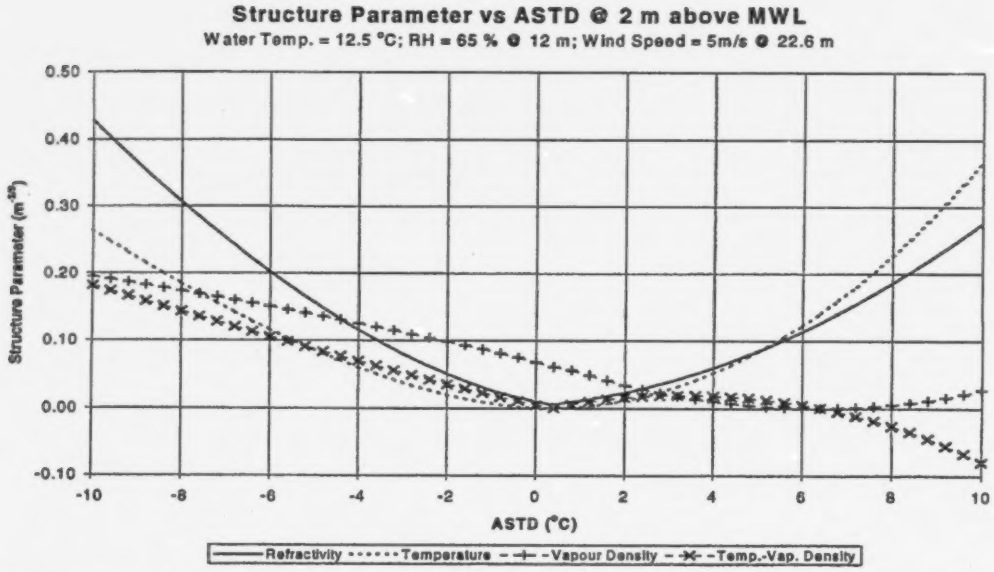

FIGURE 9 - Plot of the refractivity structure parameter and its three components as a function of changing air-sea temperature difference (ASTD) using the L(W)WKD model in non-wavy mode

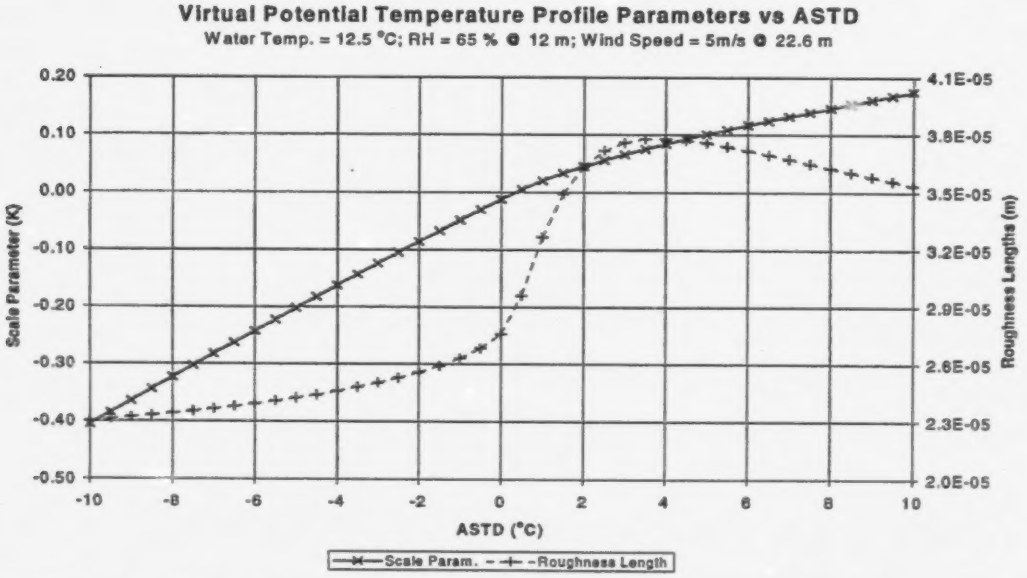

FIGURE 10 - Plot of the scale parameter and roughness height for the virtual potential temperature as a function of air-sea temperature difference (ASTD) using the L(W)WKD model

Figure 8 shows a plot of the calculated vertical refractivity structure parameter profiles for these same unstable and stable cases. As can be seen, the structure parameter for the unstable case is predicted to be as much as 5 times greater than that for the stable case at heights below ~4.5 m, and to become increasingly weaker than the stable case as the height becomes increasingly greater than ~4.5 m. In fact, at a height of ~38 m it is 10 times less. The reason for this is due to the different forms of the structure parameter functions that are used in the unstable and stable regimes (see Eq. 46).

Figure 9 shows a plot of the calculated refractivity structure parameter, and its three components, as a function of the air-sea temperature difference at a height of 2 meters above the mean water level (MWL) for the same conditions. As can be seen, the temperature structure parameter has the form of a parabola with a minimum near an ASTD of zero degrees, and the vapour density structure parameter decreases in a linear manner from about 0.2 for an ASTD of -10 ^{0}C to a minimum close to an ASTD of 6 ^{0}C before increasing slightly to 0.03 at an ASTD of 10 ^{0}C. The temperature-vapour density structure parameter decreases almost linearly from a value of 0.18 at an ASTD of -10 ^{0}C to a value of zero near an ASTD of 0.5 ^{0}C, increases slightly to about 0.02 at an ASTD of 4 ^{0}C, before decreasing to -0.08 for an ASTD of 10 ^{0}C. The appropriate summation of these three structure parameters results in the refractivity structure parameter (solid line). Looking closely at the curve, one notices that it is always greater than the air temperature structure parameter for negative ASTD, and less than the air temperature structure parameter for ASTDs greater then 6 ^{0}C.

Figure 10 shows a plot of the calculated virtual potential temperature scaling parameter (solid line) and roughness height (dashed line) as a function of the ASTD for these same conditions. The scaling parameter is seen to increase linearly from about -0.4 for an ASTD of -10 ^{0}C to zero near an ASTD of 0 ^{0}C, and then to increase almost linearly to about 0.15 for an ASTD of 10 ^{0}C. On the other hand, the roughness height has a shape reminiscent of the arctangent or Heaviside step function, with values from 23 to 26 μm for ASTDs below -1.5 ^{0}C, and from 35 to 38 μm for ASTDs above 1.5 ^{0}C.

5.0 MAPTIP Comparisons

This section shows new calculations of the maximum inter-vision range (MIVR) and minimum mirage range (MMR) using L(W)WKD as a module within IRBLEM compared with earlier results and the measurements made during the 1993 MAPTIP trial (Ref. 2). The Marine Aerosol Properties and Thermal Imager Performance (MAPTIP) trial was held in The Netherlands from Oct. 18 to Nov. 3, 1993, and was sponsored by RSG 8 of NATO's panel 4. The principle goals of the trial were to study the concentrations and properties of marine aerosols, and to study the performance of imaging systems within the marine boundary layer (MBL) (Ref. 15). One of the studies (see Ref. 2), involved measuring the minimum mirage ranges (MMRs) and maximum inter-vision ranges (MIVRs) for a set of halogen lamps installed at various heights aboard the Hr. Ms. Tydeman as it sailed away from a set of visible and infrared cameras placed at the beach station in the town of Katwijk. Under unstable conditions, the MIVR, for an observer (camera) and a source (lamp) at given elevations, is the range at which the source goes beyond the observer's horizon, while the MMR is the range at which a secondary image (or mirage) of the source first appears.

Tables XI to XIV show all the measured MMR and MIVR MAPTIP data for cases A thru M obtained using our Visible 1 and Visible 2 camera systems. They also contain prediction results obtained from calculations using Version 7.09 of the L(W)WKD model, and the earlier version discussed in Ref. 1 (Ver. 6.0). The columns in each of these tables, starting with the first column, show the measurement case (A to M), the name of the light source, the height of the source above the water level and its uncertainty (discussed later), the experimentally measured MMRs or MIVRs and a measure of their uncertainties, the earlier LWKD (non-wavy mode) predicted MMRs or MIVRs and the difference between them and the measured values, the earlier LWWKD (with the wavy mode) predicted MMRs or MIVRs and the difference between them and the measured values, and the LWKD Ver. 7.09 (non-wavy mode) predicted MMRs or MIVRs and the difference between them and the measured values. The average and standard deviation for each of the difference columns

(model prediction - measurement) is given at the bottom of each table along with the number of measurements used in the calculations. Looking at these values, it appears that, on average, the new MMR predictions are at least as good as those obtained using the earlier LWWKD predictions, and that the new MIVR predictions are about 0.3 km less than both the earlier LWKD and LWWKD predictions.

At this point, I would like to come back to the estimation of the uncertainty in the height of each of the light sources. Looking at Tables XI to XIV, one notices that these values vary with respect to both the particular measurement **Case**, and the particular **Object** (light source). This is due to the pitching motion of the Hr. Ms. Tydeman (like a teeter-totter) that is generated by the waves. Assuming that the amplitude of the pitching motion for each of the light sources is only dependent upon the wave height, I have defined the

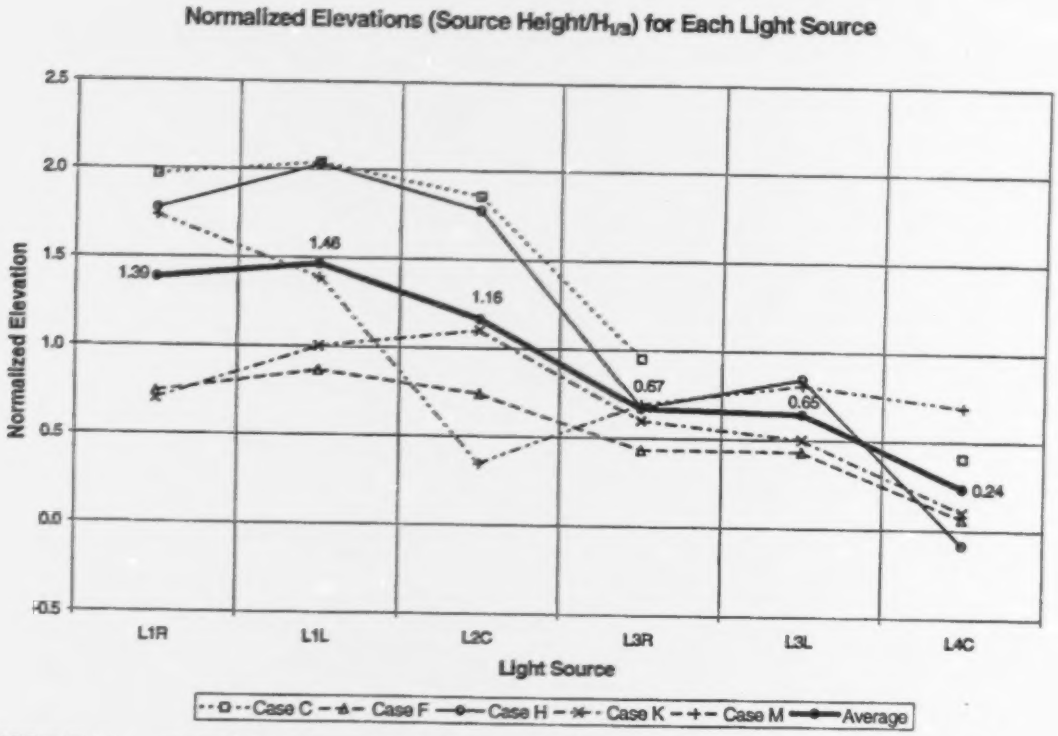

FIGURE 11 - Plot of the normalized elevations for each light source and for MAPTIP cases C, F, H, K, M, and their average

following parameter, which I call the normalized elevation (H^n_{norm}). For each source n, it is defined as:

$$H^n_{norm} = \frac{H^n_{max} - H^n_{min}}{H_{1/3}} , \tag{52}$$

where $H_{1/3}$ is the $H_{1/3}$ wave height, and H^n_{min} and H^n_{max} are the minimum and maximum measured heights of each source above the ships water line. From our video recordings, for several of the MAPTIP cases, it was possible to make a number of measurements of H^n_{min} and H^n_{max}. Figure 11 shows the results for each of the visible lights obtained from an analysis of MAPTIP cases C, F, H, K, and M. The average over all the cases is given by the solid line and the value of each average is located next to each point. Despite the large scatter that can exist between the data for different cases, it is clear that the normalized elevations are larger for the lower elevation lights and much smaller for the higher lights. The reason for this is due to the positioning of the lights on the ship. The lowest lights are positioned at the ship's stern, while the highest light is on its mast near the axis about which the ship pitches, and the other lights are somewhere in between. Thus, using the average values for the normalized elevations, the uncertainties in the source heights given in Tables XI to XIV for each source, δ_n, are obtained using the following relationship;

$$\delta_n = [\langle H^n_{norm} \rangle \; x \; H_{1/3}]/2 , \tag{53}$$

where $\langle Hn_{norm} \rangle$ is the mean value for each source given in Table X. Thus we can define a lower and upper limit for each source height given by;

$$\begin{aligned} H^n_{lower} &= H^n_{mean} - \delta_n \\ H^n_{upper} &= H^n_{mean} + \delta_n , \end{aligned} \tag{54}$$

where Hn_{mean} is the measured height of each source above the ships water line for a flat sea (no waves).

TABLE X

Average Normalized Elevations for each Light Source

Light	1L/1R	2C/2Ca	3L/3R	Chimney	4C
$\langle H^n_{norm} \rangle$	1.43	1.16	0.66	0.24	0.24

Tables XV to XVIII show the results obtained by running L(W)WKD Version 7.09 in the non-wavy mode for three different source heights (mean, lower limit, and upper limit), and two different values for von Karman's constant for each of the MAPTIP cases. The mean source height for each source is that given in Tables XI to XIV, and the lower and upper limits are calculated using Eq. 54. For each table, column one gives the MAPTIP case, column two the light source, and column three the measured MMR or MIVR. The following sets of columns show the results of the model calculations for von Karman constants of 0.40 and 0.41 for the mean, lower limit and upper limit source heights. In addition, Tables XVI and XVIII (contain MIVRs), also give the results for a non-refractive atmosphere (i.e. for free-space propagation). The calculation using a value of 0.41 for von Karman's constant (default value is 0.40) were made due to the results recently reported by Dion and Gardenal (Ref. 26). They found that they obtained a better fit for radio frequency (RF) data to model calculations using refractivity profiles generated by L(W)WKD in non-wavy mode when a value of 0.41 was used instead of 0.40.

Figures 12 to 15 are graphical representation of the data in Tables XVI to XVIII. Figure 12 shows the MMR results obtained using Ver. 7.09 of the model in non-wavy mode (x), and Ver. 6.0 in wavy mode (o) for source heights at their mean heights above the water level versus the experimental data. The dashed line and the solid line give their respective least squares fits and their respective equations are given at the top of the graph. While there is a scatter of about 1 km about the straight lines, and the fits are quite good for both models, our newer model does perform slightly better. The MMRs predicted by the new model are about 1.5% less than the measured values while those predicted by the earlier model are

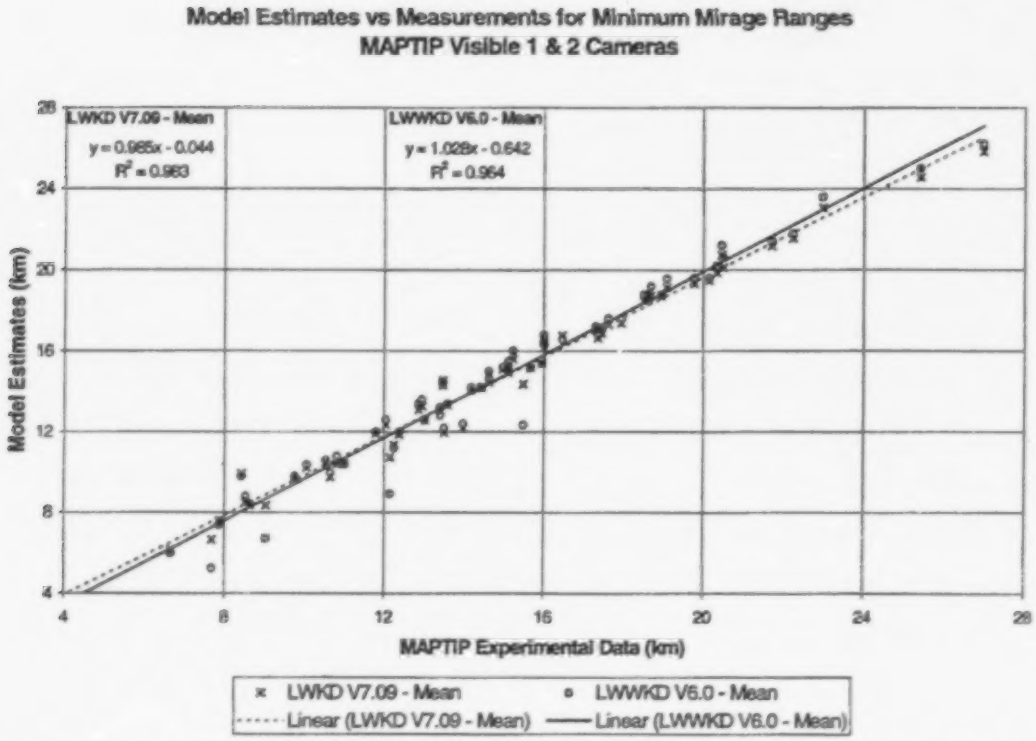
Model Estimates vs Measurements for Minimum Mirage Ranges
MAPTIP Visible 1 & 2 Cameras
LWKD V7.09 - Mean
y = 0.965x - 0.044
R² = 0.983
LWWKD V6.0 - Mean
y = 1.029x - 0.642
R² = 0.964
Model Estimates (km)
MAPTIP Experimental Data (km)
LWKD V7.09 - Mean
LWWKD V6.0 - Mean
Linear (LWKD V7.09 - Mean)
Linear (LWWKD V6.0 - Mean)

FIGURE 12 - Plot of L(W)WKD Ver. 7.09 results using the non-wavy mode (x), and Ver. 6.0 using the wavy mode (o) versus experimental data obtained from our Visible 1 and Visible 2 cameras during the MAPTIP trial. The solid and dashed lines give the respective least squares fits. The mean height for the light sources are used in each case

about 2.8% greater.

Figure 13 shows the MMR results obtained using Ver. 7.09 of the model in non-wavy mode with a von Karman constant of 0.40 (x), and with a von Karman constant of 0.41 (o) for source heights at their lower limits above the water level versus the experimental data. The dashed line and the solid line give their respective least squares fits and their respective equations are given at the top of the graph. Again there is a scatter of about 1 km about the straight lines, and both fits are very good and definitely better than the model calculations given in Fig. 12. Looking at the fits, one notices that the MMRs predicted using both values of von Karman's constant would precisely predict the measured MMRs if it were not for

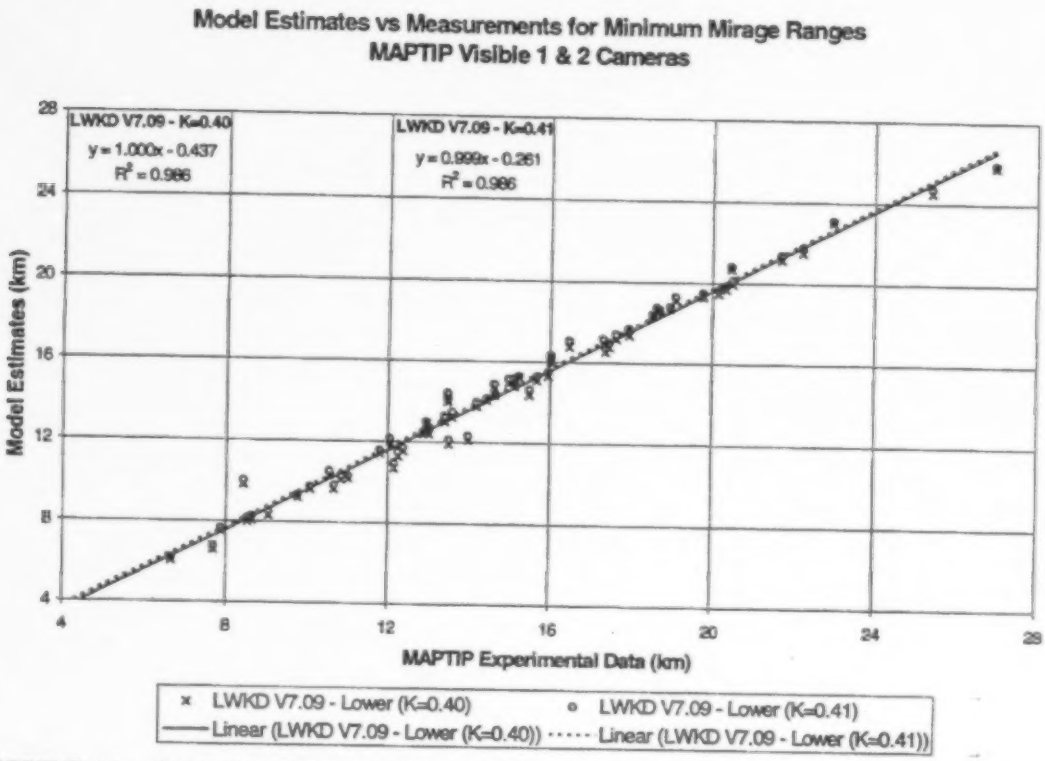
Model Estimates vs Measurements for Minimum Mirage Ranges
MAPTIP Visible 1 & 2 Cameras
LWKD V7.09 - K=0.40
y = 1.000x - 0.437
R² = 0.986
LWKD V7.09 - K=0.41
y = 0.999x - 0.261
R² = 0.986
Model Estimates (km)
MAPTIP Experimental Data (km)
LWKD V7.09 - Lower (K=0.40)
LWKD V7.09 - Lower (K=0.41)
Linear (LWKD V7.09 - Lower (K=0.40))
Linear (LWKD V7.09 - Lower (K=0.41))

FIGURE 13 - Plot of L(W)WKD Ver. 7.09 results using the non-wavy mode for von Karman constants equal to $\kappa = 0.40$ (x) and $\kappa = 0.41$ (o) versus experimental data obtained from our Visible 1 and Visible 2 cameras during the MAPTIP trial. The solid and dashed lines give the respective least squares fits. The lower limits for the heights of each light source is used in each case

constant offsets of 0.44 km and 0.26 km, respectively. In other words, for a von Karman constant of 0.40, the model consistently predicts an MMR that is 0.44 km shorter than the measured value, while for a constant of 0.41 it consistently predicts a value that is 0.26 km shorter than that measured. Consequently, a value of 0.41 for von Karman's constant along with the use of the lower limits for the source heights gives the best fit to the measured MMR data.

Figure 14 shows the MIVR results obtained using Ver. 7.09 of the model in non-wavy mode (x), Ver. 6.0 in wavy mode (o), and for a non-refractive atmosphere (□) for source heights at their mean heights above the water level versus the experimental data. The dashed

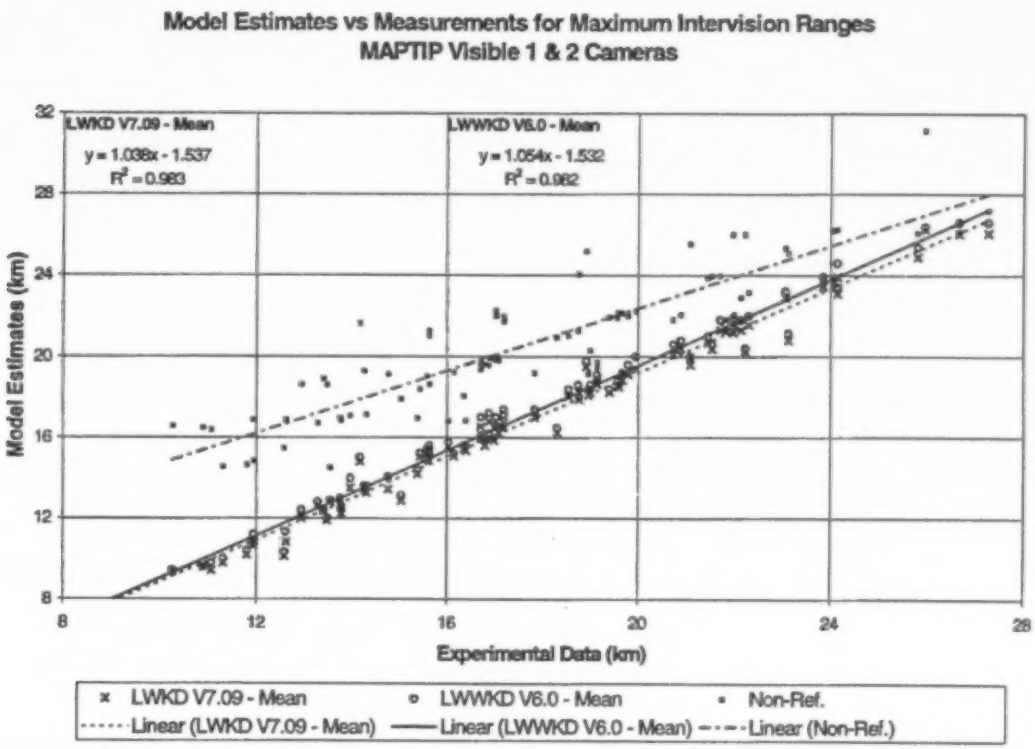

FIGURE 14 - Plot of L(W)WKD Ver. 7.09 results using the non-wavy mode(x), Ver. 6.0 using the wavy mode (o), and free space calculations (□) versus experimental data obtained from our Visible 1 and Visible 2 cameras during the MAPTIP trial. The solid and dashed lines give the respective least squares fits. The mean height for the light sources are used in each case

line and the solid line give the respective least squares fits for the two L(W)WKD model calculations and their respective equations are given at the top of the graph. Again there is a scatter of about 1 km about the straight lines, and while the fits are quite good for both L(W)WKD models, our newer model does perform slightly better, and both perform substantially better than a prediction using a non-refractive atmosphere. The MIVRs predicted by the new model both have offsets of approximately 1.5 km. Thus both models tend to underestimate the measured MIVR data by up to 1.5 km, with the difference diminishing for larger MIVRs.

Figure 15 shows the MIVR results obtained using Ver. 7.09 of the model in non-wavy

mode with a von Karman constant of 0.40 (x), and with a von Karman constant of 0.41 (o) for source heights at their lower limits above the water level versus the experimental data. The dashed line and the solid line give their respective least squares fits and their respective equations are given at the top of the graph. Again there is a scatter of about 1 km about the straight lines, and both fits are very good and definitely better than the model calculations given in Fig. 14. Looking at the fits, one notices that the MIVRs predicted using both values of von Karman's constant would precisely predict the measured MIVRs if it were not for constant offsets of 0.63 km and 0.50 km, respectively. In other words, for a von Karman constant of 0.40, the model consistently predicts an MIVR that is 0.63 km shorter than the

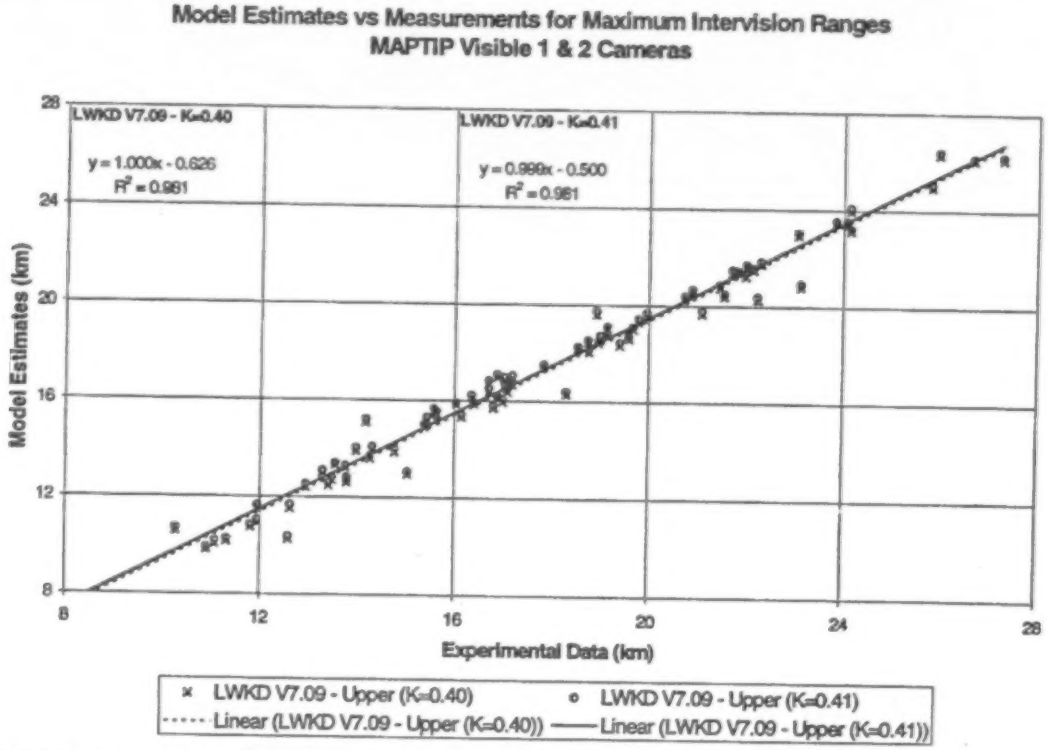

FIGURE 15 - Plot of L(W)WKD Ver. 7.09 results using non-wavy mode for von Karman constants equal to $\kappa = 0.40$ (x) and $\kappa = 0.41$ (o) versus experimental data obtained from our Visible 1 and Visible 2 cameras during the MAPTIP trial. The solid and dashed lines give the respective least squares fits. The upper limits for the heights of each light source is used in each case

measured value, while for a constant of 0.41 it consistently predicts a value that is 0.50 km shorter than that measured. Consequently, a value of 0.41 for von Karman's constant along with the use of the lower limits for the source heights gives the best fit to the measured MMR data.

Thus, for the models studied in this report, Figs. 12 to 15 show that the best fit to the measured MMR and MIVR MAPTIP data is obtained for Ver. 7.09 of the L(W)WKD model in non-wavy mode, when the source heights are corrected for the pitching of the ship, and von Karmen's constant is taken to be 0.41. Breaking this down, we see that correcting for the ships pitching motion resulted in fits of the MMR and MIVR experimental data to the model results that are almost perfectly linear such that only slight y-offsets of approximately 0.5 km remained. This implies that the model, on average, only underestimates the measured values by approximately 0.5 km. Consequent modification of von Karman's constant to 0.41 from 0.40 produced a decrease in the y-offset by about 0.2 km, implying that increasing the values to 0.42 or 0.43 could lead to an even better fit.

6.0 CONCLUSIONS

This report has described, in detail, both the physics, and mathematical structure contained within the most recent version (Version 7.09) of the L(W)WKD model, and how it compares with the previously published version (Ref. 1), and the PIRAM model (Ref. 3). It has also given a complete description of the operational procedures required to operate the associated L(W)WKD computer program. It also presented and discussed a number of results which can be obtained from the model.

A comparison between earlier measurements taken during the MAPTIP trial and the earlier L(W)WKD model calculations shown in Ref. 2 with more recent calculations using Version 7.09 of the L(W)WKD has also been performed. This new analysis also involved a modification to the source heights to account for the pitching of the ship, and a modifica-

tion to von Karman's constant from 0.40 to 0.41. With these two modifications, the least square fits of the MMR and MIVR experimental data to the model results that, on average, only underestimates the measured values by less than 0.5 km.

Future improvements to the model, and to the program include the option of using other functional forms for the gradient functions, and structure parameter functions. This could also involve the possibility of using different values for the various gradient coefficients, and other parameters that are currently fixed by extending the number of variables defined by the initialization file "LWWKD.INI". Additionally, it would be useful to integrate the calculation of aerosol vertical profiles, and to allow files containing this profile to be created by the program when it is being operated in BATCH mode. The production of more meteorological profiles and structure profiles may also be useful. Finally, further study and perhaps modification of the refractivity profile (perhaps by modifying von Karman's constant) may be required in order to better fit the MMR and MIVR predictions given using Ver. 7.09 of L(W)WKD model with measurements obtained during the MAPTIP trial.

TABLE XI

Calculated and Measured Minimum Mirage Ranges (MAPTIP - Visible 1 Camera)

				Visible 1 (Canada)							
				MMR							
				MAPTIP Report (LWWKD Version 6.0)						LWKD	
				Experimental Data		LWKD	Difference	LWWKD	Difference	Ver. 7.09	Difference
	Object	Height	Delta H	Range	Delta R	Range	LWKD - Data	Range	LWWKD - Data	Range	V 7.09 - Data
	(light)	(m)	(m)	(km)	(km)	(km)	(km)	(km)	(km)	(km)	(km)
Case A	1L/1R	3.34	0.22	6.65	0.19	6.60	-0.05	6.00	-0.65	6.15	-0.51
	2Ca	6.08	0.18							7.46	
	2C	6.38	0.18	7.87	0.19	8.20	0.33	7.40	-0.47	7.59	-0.28
	3R	11.00	0.10			10.20		9.20		9.53	
	3L	11.45	0.10			10.40		9.40		9.70	
	Chimney	14.50	0.04							10.86	
	4C	20.69	0.04	13.41	0.19	13.80	0.39	12.80	-0.61	13.01	-0.40
Case B	1L/1R	3.34	0.12							6.98	
	2Ca	6.08	0.10							8.52	
	2C	6.38	0.10							8.67	
	3R	11.00	0.06							10.88	
	3L	11.45	0.06							11.07	
	Chimney	14.50	0.02							12.36	
	4C	20.69	0.02							14.71	
Case C	1L/1R	3.34	1.34							9.32	
	2Ca	6.08	1.08							11.45	
	2C	6.38	1.08					11.60		11.65	
	3R	11.00	0.62	13.49	0.13			14.40	0.91	14.32	0.83
	3L	11.45	0.62	13.49	0.13			14.50	1.01	14.55	1.06
	Chimney	14.50	0.22							16.02	
	4C	20.69	0.22	18.62	0.15			18.80	0.18	18.62	0.00
Case D	1L/1R	3.34	0.70							10.54	
	2Ca	6.08	0.57							12.49	
	2C	6.38	0.57							12.68	
	3R	11.00	0.32							15.23	
	3L	11.45	0.32							15.45	
	Chimney	14.50	0.12							16.88	
	4C	20.69	0.12							19.44	
Case E	1L/1R	3.34	0.65	8.53	0.07	9.40	0.87	8.80	0.27	8.48	-0.05
	2Ca	6.08	0.53							10.22	
	2C	6.38	0.53	10.83	0.08	11.40	0.57	10.80	-0.03	10.39	-0.44
	3R	11.00	0.30			13.80		13.20		12.76	
	3L	11.45	0.30			14.20		13.40		12.96	
	Chimney	14.50	0.11							14.31	
	4C	20.69	0.11			18.00		17.20		16.74	
Case F	1L/1R	3.34	0.66							14.20	
	2Ca	6.08	0.53							16.64	
	2C	6.38	0.53					17.20		16.86	
	3R	11.00	0.30	20.34	0.08			20.20	-0.14	19.87	-0.47
	3L	11.45	0.30	20.50	0.08	20.96	0.46	20.60	0.10	20.12	-0.38
	Chimney	14.50	0.11							21.73	
	4C	20.69	0.11	25.41	0.08	25.58	0.17	25.00	-0.41	24.56	-0.85
Case G	1L/1R	3.34	0.66	12.87	0.09			13.40	0.53	13.08	0.21
	2Ca	6.08	0.54							15.39	
	2C	6.38	0.54	15.24	0.08	16.40	1.16	16.00	0.76	15.60	0.36
	3R	11.00	0.31	18.52	0.09	19.40	0.88	18.80	0.28	18.49	-0.03
	3L	11.45	0.31	18.69	0.09	19.80	1.11	19.20	0.51	18.74	0.05
	Chimney	14.50	0.11							20.30	
	4C	20.69	0.11	22.98	0.08	24.20	1.22	23.60	0.62	23.06	0.08

TABLE XI (continued)

Calculated and Measured Minimum Mirage Ranges (MAPTIP - Visible 1 Camera)

				Visible 1 (Canada)							
				MMR							
				MAPTIP Report (LWWKD Version 6.0)						LWKD	
				Experimental Data		LWKD	Difference	LWWKD	Difference	Ver. 7.09	Difference
	Object	Height	Delta H	Range	Delta R	Range	LWKD - Data	Range	LWWKD - Data	Range	V 7.09 - Data
	(light)	(m)	(m)	(km)	(km)	(km)	(km)	(km)	(km)	(km)	(km)
Case H	1L/1R	3.34	0.49								
	2Ca	6.08	0.39							15.35	
	2C	6.38	0.39							17.86	
	3R	11.00	0.22							18.08	
	3L	11.45	0.22							21.15	
	Chimney	14.50	0.08							21.40	
	4C	20.69	0.08							23.04	
								26.40		25.90	
Case I	1L/1R	3.34	0.55	11.81	0.10			12.00	0.19	11.93	0.12
	2Ca	6.08	0.45	14.20	0.09			14.20	0.00	14.09	-0.11
	2C	6.38	0.45							14.29	
	3R	11.00	0.25	17.31	0.11			17.20	-0.11	17.07	-0.23
	3L	11.45	0.25	17.62	0.11			17.60	-0.02	17.31	-0.31
	Chimney	14.50	0.09							18.84	
	4C	20.69	0.09	22.23	0.09			21.80	-0.43	21.55	-0.68
Case J	1L/1R	3.34	0.50					11.60		11.43	
	2Ca	6.08	0.41							13.62	
	2C	6.38	0.41					14.00		13.83	
	3R	11.00	0.23	17.36	0.07			16.80	-0.56	16.65	-0.71
	3L	11.45	0.23	17.45	0.10			17.00	-0.45	16.89	-0.56
	Chimney	14.50	0.08							18.43	
	4C	20.69	0.08	21.71	0.10			21.40	-0.31	21.17	-0.54
Case K	1L/1R	3.34	0.36	11.03	0.10	11.00	-0.03	10.40	-0.63	10.44	-0.59
	2Ca	6.08	0.30							12.39	
	2C	6.38	0.30	13.03	0.09	13.20	0.17	12.60	-0.43	12.57	-0.45
	3R	11.00	0.17	15.67	0.09	16.00	0.33	15.20	-0.47	15.19	-0.49
	3L	11.45	0.17	15.96	0.09	16.20	0.24	15.40	-0.56	15.41	-0.54
	Chimney	14.50	0.06							16.87	
	4C	20.69	0.06	20.15	0.09	20.40	0.25	19.60	-0.55	19.49	-0.66
Case L	1L/1R	3.34	0.29							9.21	
	2Ca	6.08	0.24							11.08	
	2C	6.38	0.24							11.26	
	3R	11.00	0.14							13.80	
	3L	11.45	0.14							14.02	
	Chimney	14.50	0.05							15.45	
	4C	20.69	0.05							18.02	
Case M	1L/1R	3.34	0.29					8.20		8.03	
	2Ca	6.08	0.23							9.60	
	2C	6.38	0.23	10.67	0.18			10.00	-0.67	9.76	-0.91
	3R	11.00	0.13	13.51	0.19			12.20	-1.31	11.98	-1.54
	3L	11.45	0.13	13.99	0.19			12.40	-1.59	12.18	-1.81
	Chimney	14.50	0.05							13.47	
	4C	20.69	0.05					16.20		15.83	
Number of cases							16		32		32
Average							0.50		-0.16		-0.34
Standard Deviation							0.42		0.59		0.56

TABLE XII

Calculated and Measured Maximum Intervision Ranges (MAPTIP - Visible 1 Camera)

				Visible 1 (Canada)							
				MIVR							
				MAPTIP Report (LWWKD Version 6.0)						LWKD	
				Experimental Data		LWKD	Difference	LWWKD	Difference	Ver. 7.09	Difference
	Object	Height	Delta H	Range	Delta R	Range	LWKD - Data	Range	LWWKD - Data	Range	V 7.09 - Data
	(light)	(m)	(m)	(km)	(km)	(km)	(km)	(km)	(km)	(km)	(km)
Case A	1L/1R	3.34	0.22	10.90	0.19	9.60	-1.30	9.60	-1.30	9.59	-1.31
	2Ca	6.08	0.18							12.10	
	2C	6.38	0.18	13.41	0.19	12.40	-1.01	12.40	-1.01	12.34	-1.08
	3R	11.00	0.10			15.60		15.40		15.44	
	3L	11.45	0.10			15.80		15.80		15.70	
	Chimney	14.50	0.04							17.37	
	4C	20.69	0.04	22.23	0.19	20.40	-1.83	20.40	-1.83	20.25	-1.98
Case B	1L/1R	3.34	0.12							10.58	
	2Ca	6.08	0.10							13.13	
	2C	6.38	0.10							13.37	
	3R	11.00	0.06							16.46	
	3L	11.45	0.06							16.73	
	Chimney	14.50	0.02							18.41	
	4C	20.69	0.02							21.33	
Case C	1L/1R	3.34	1.34	10.27	0.12			9.40	-0.87	9.36	-0.91
	2Ca	6.08	1.08							11.69	
	2C	6.38	1.08	13.49	0.13			12.00	-1.49	11.91	-1.58
	3R	11.00	0.62	15.63	0.15			15.20	-0.43	14.85	-0.77
	3L	11.45	0.62	15.63	0.15			15.40	-0.23	15.10	-0.53
	Chimney	14.50	0.22							16.70	
	4C	20.69	0.22	18.91	0.15			19.80	0.89	19.50	0.58
Case D	1L/1R	3.34	0.70							11.24	
	2Ca	6.08	0.57							13.67	
	2C	6.38	0.57							13.90	
	3R	11.00	0.32							16.93	
	3L	11.45	0.32							17.18	
	Chimney	14.50	0.12							18.80	
	4C	20.69	0.12							21.66	
Case E	1L/1R	3.34	0.65	11.08	0.08	10.00	-1.08	9.80	-1.28	9.42	-1.65
	2Ca	6.08	0.53							11.79	
	2C	6.38	0.53	12.95	0.05	12.40	-0.55	12.40	-0.55	12.01	-0.94
	3R	11.00	0.30			15.40		15.40		14.96	
	3L	11.45	0.30			15.80		15.60		15.21	
	Chimney	14.50	0.11							16.81	
	4C	20.69	0.11	21.08	0.09	20.20	-0.88	20.00	-1.08	19.61	-1.47
Case F	1L/1R	3.34	0.66	15.39	0.08	14.80	-0.59	14.40	-0.99	14.21	-1.18
	2Ca	6.08	0.53							16.78	
	2C	6.38	0.53	17.84	0.08	17.44	-0.40	17.40	-0.44	17.01	-0.83
	3R	11.00	0.30	20.73	0.08	20.52	-0.21	20.60	-0.13	20.12	-0.61
	3L	11.45	0.30	20.89	0.08	20.96	0.07	20.80	-0.09	20.38	-0.51
	Chimney	14.50	0.11							22.03	
	4C	20.69	0.11	25.81	0.08	25.58	-0.23	25.40	-0.41	24.91	-0.91
Case G	1L/1R	3.34	0.66	14.31	0.08	13.80	-0.51	13.60	-0.71	13.28	-1.03
	2Ca	6.08	0.54							15.74	
	2C	6.38	0.54	16.71	0.09	16.60	-0.11	16.40	-0.31	15.97	-0.74
	3R	11.00	0.31	19.79	0.08	19.60	-0.19	19.60	-0.19	19.12	-0.67
	3L	11.45	0.31	19.96	0.08	20.00	0.04	20.00	0.04	19.38	-0.58
	Chimney	14.50	0.11							21.04	
	4C	20.69	0.11	24.14	0.08	24.60	0.46	24.60	0.46	23.92	-0.22

TABLE XII (continued)

Calculated and Measured Maximum Intervision Ranges (MAPTIP - Visible 1 Camera)

				Visible 1 (Canada)							
				MIVR							
				MAPTIP Report (LWWKD Version 6.0)						LWKD	
	Object	Height	Delta H	Experimental Data	Delta R	LWKD	Difference	LWWKD	Difference	Ver. 7.09	Difference
	(light)	(m)	(m)	Range (km)	(km)	Range (km)	LWKD - Data (km)	Range (km)	LWWKD - Data (km)	Range (km)	V 7.09 - Data (km)
Case H	1L/1R	3.34	0.49	16.41	0.09			15.60	-0.81	15.35	-1.05
	2Ca	6.08	0.39							17.88	
	2C	6.38	0.39	18.96	0.09			18.40	-0.56	18.12	-0.84
	3R	11.00	0.22	21.82	0.09			21.60	-0.22	21.24	-0.57
	3L	11.45	0.22	22.00	0.09			21.80	-0.20	21.50	-0.50
	Chimney	14.50	0.08							23.16	
	4C	20.69	0.08	26.67	0.09			26.60	-0.07	26.05	-0.62
Case I	1L/1R	3.34	0.55	13.76	0.08			13.00	-0.76	12.64	-1.13
	2Ca	6.08	0.45	15.59	0.09			15.40	-0.19	15.21	-0.38
	2C	6.38	0.45							15.44	
	3R	11.00	0.25	19.56	0.10			18.80	-0.76	18.59	-0.98
	3L	11.45	0.25	19.67	0.10			19.20	-0.47	18.84	-0.82
	Chimney	14.50	0.09							20.50	
	4C	20.69	0.09	24.07	0.07			23.80	-0.27	23.40	-0.67
Case J	1L/1R	3.34	0.50					12.40		12.14	
	2Ca	6.08	0.41							14.69	
	2C	6.38	0.41					15.20		14.92	
	3R	11.00	0.23	18.55	0.10			18.40	-0.15	18.05	-0.50
	3L	11.45	0.23	18.75	0.10			18.60	-0.15	18.31	-0.44
	Chimney	14.50	0.08							19.99	
	4C	20.69	0.08	23.06	0.10			23.20	0.14	22.91	-0.16
Case K	1L/1R	3.34	0.36	13.79	0.09	12.40	-1.39	12.40	-1.39	12.23	-1.56
	2Ca	6.08	0.30							14.84	
	2C	6.38	0.30	16.15	0.09	15.20	-0.95	15.20	-0.95	15.08	-1.07
	3R	11.00	0.17	19.40	0.10	18.40	-1.00	18.40	-1.00	18.25	-1.15
	3L	11.45	0.17	19.59	0.10	18.80	-0.79	18.60	-0.99	18.51	-1.09
	Chimney	14.50	0.06							20.17	
	4C	20.69	0.06	24.14	0.09	23.40	-0.74	23.40	-0.74	23.11	-1.03
Case L	1L/1R	3.34	0.29							11.10	
	2Ca	6.08	0.24							13.66	
	2C	6.38	0.24							13.89	
	3R	11.00	0.14							16.97	
	3L	11.45	0.14							17.23	
	Chimney	14.50	0.05							18.91	
	4C	20.69	0.05							21.82	
Case M	1L/1R	3.34	0.29	11.95	0.18			10.80	-1.15	10.65	-1.30
	2Ca	6.08	0.23							13.19	
	2C	6.38	0.23	14.27	0.19			13.60	-0.67	13.42	-0.85
	3R	11.00	0.13	17.04	0.19			16.60	-0.44	16.54	-0.50
	3L	11.45	0.13	17.04	0.19			17.00	-0.04	16.80	-0.24
	Chimney	14.50	0.05							18.46	
	4C	20.69	0.05					21.60		21.35	
Number of cases							21		43		43
Average							-0.63		-0.55		-0.84
Standard Deviation							0.55		0.54		0.46

TABLE XIII

Calculated and Measured Minimum Mirage Ranges (MAPTIP - Visible 2 Camera)

				Visible 2 (Canada)							
				MMR							
				MAPTIP Report (LWWKD Version 6.0)						LWKD	
				Experimental Data		LWKD	Difference	LWWKD	Difference	Ver. 7.09	Difference
	Object	Height	Delta H	Range	Delta R	Range	LWKD - Data	Range	LWWKD - Data	Range	V 7.09 - Data
	(light)	(m)	(m)	(km)	(km)	(km)	(km)	(km)	(km)	(km)	(km)
Case A	1L/1R	3.34	0.22	8.44	0.19	10.60	2.16	9.80	1.36	9.93	1.49
	2Ca	6.08	0.18							11.23	
	2C	6.38	0.18	12.25	0.19	12.00	-0.25	11.20	-1.05	11.37	-0.89
	3R	11.00	0.10			14.00		13.00		13.30	
	3L	11.45	0.10			14.20		13.20		13.47	
	Chimney	14.50	0.04							14.62	
	4C	20.69	0.04	16.47	0.19	17.70	1.23	16.60	0.13	16.77	0.30
Case B	1L/1R	3.34	0.12	7.69	0.08	7.13	-0.56	5.24	-2.45	6.66	-1.03
	2Ca	6.08	0.10			8.74		6.59		8.19	
	2C	6.38	0.10	9.05	0.08	8.90	-0.15	6.73	-2.32	8.34	-0.71
	3R	11.00	0.06			11.81		8.73		10.54	
	3L	11.45	0.06	12.16	0.07	11.39	-0.77	8.92	-3.24	10.74	-1.42
	Chimney	14.50	0.02			12.71		10.11		12.02	
	4C	20.69	0.02	15.49	0.08	15.14	-0.35	12.34	-3.15	14.37	-1.12
Case C	1L/1R	3.34	1.34							6.80	
	2Ca	6.08	1.08							8.93	
	2C	6.38	1.08							9.13	
	3R	11.00	0.62							11.80	
	3L	11.45	0.62							12.02	
	Chimney	14.50	0.22							13.49	
	4C	20.69	0.22							16.10	
Case D	1L/1R	3.34	0.70	10.08	0.10	11.04	0.96	10.38	0.30	10.22	0.14
	2Ca	6.08	0.57			13.11		12.40		12.18	
	2C	6.38	0.57	12.05	0.09	13.31	1.26	12.60	0.55	12.37	0.31
	3R	11.00	0.32	15.12	0.09	15.99	0.87	15.25	0.13	14.94	-0.19
	3L	11.45	0.32	15.12	0.09	16.22	1.10	15.48	0.36	15.16	0.03
	Chimney	14.50	0.12			17.71		16.95		16.59	
	4C	20.69	0.12	19.08	0.08	20.36	1.28	19.58	0.50	19.15	0.07
Case E	1L/1R	3.34	0.65							6.53	
	2Ca	6.08	0.53							8.28	
	2C	6.38	0.53							8.45	
	3R	11.00	0.30							10.82	
	3L	11.45	0.30							11.03	
	Chimney	14.50	0.11							12.37	
	4C	20.69	0.11							14.81	
Case F	1L/1R	3.34	0.66							15.41	
	2Ca	6.08	0.53							17.87	
	2C	6.38	0.53			18.76		18.40		18.10	
	3R	11.00	0.30			21.84		21.40		21.12	
	3L	11.45	0.30					21.80		21.37	
	Chimney	14.50	0.11							22.99	
	4C	20.69	0.11	26.97	0.07	26.68	-0.29	26.20	-0.77	25.83	-1.15
Case G	1L/1R	3.34	0.66					11.00		10.75	
	2Ca	6.08	0.54							13.06	
	2C	6.38	0.54	12.96	0.08	14.00	1.04	13.60	0.64	13.27	0.31
	3R	11.00	0.31	16.01	0.09	17.00	0.99	16.40	0.39	16.16	0.14
	3L	11.45	0.31	16.01	0.09	17.40	1.39	16.80	0.79	16.40	0.39
	Chimney	14.50	0.11							17.97	
	4C	20.69	0.11	20.46	0.08	21.80	1.34	21.20	0.74	20.73	0.27

TABLE XIII (continued)
Calculated and Measured Minimum Mirage Ranges (MAPTIP - Visible 2 Camera)

				Visible 2 (Canada)							
				MMR							
				MAPTIP Report (LWWKD Version 6.0)						LWKD	
				Experimental Data		LWKD	Difference	LWWKD	Difference	Ver. 7.09	Difference
	Object	Height	Delta H	Range	Delta R	Range	LWKD - Data	Range	LWWKD - Data	Range	V 7.09 - Data
	(light)	(m)	(m)	(km)	(km)	(km)	(km)	(km)	(km)	(km)	(km)
Case H	1L/1R	3.34	0.49								
	2Ca	6.08	0.39							12.81	
	2C	6.38	0.39							15.32	
	3R	11.00	0.22							15.55	
	3L	11.45	0.22							18.62	
	Chimney	14.50	0.08							18.87	
	4C	20.69	0.08							20.51	
								23.68		23.37	
Case I	1L/1R	3.34	0.55	9.78	0.10			9.80	0.02	9.71	-0.07
	2Ca	6.08	0.45	12.38	0.10			12.00	-0.38	11.87	-0.51
	2C	6.38	0.45							12.07	
	3R	11.00	0.25	14.63	0.09			15.00	0.37	14.86	0.22
	3L	11.45	0.25	14.98	0.09			15.20	0.22	15.09	0.11
	Chimney	14.50	0.09							16.62	
	4C	20.69	0.09	19.77	0.10			19.60	-0.17	19.33	-0.44
Case J	1L/1R	3.34	0.50					9.00		8.97	
	2Ca	6.08	0.41							11.18	
	2C	6.38	0.41					11.40		11.38	
	3R	11.00	0.23	14.44	0.10			14.20	-0.24	14.21	-0.23
	3L	11.45	0.23	14.64	0.10			14.60	-0.04	14.45	-0.19
	Chimney	14.50	0.08							16.00	
	4C	20.69	0.08	18.95	0.10			18.80	-0.15	18.74	-0.21
Case K	1L/1R	3.34	0.36	8.65	0.10	9.00	0.35	8.40	-0.25	8.35	-0.30
	2Ca	6.08	0.30							10.29	
	2C	6.38	0.30	10.55	0.10	11.20	0.65	10.60	0.05	10.48	-0.07
	3R	11.00	0.17	13.41	0.09	13.80	0.39	13.20	-0.21	13.08	-0.32
	3L	11.45	0.17	13.60	0.09	14.00	0.40	13.40	-0.20	13.31	-0.29
	Chimney	14.50	0.06							14.77	
	4C	20.69	0.06	17.94	0.10	18.20	0.26	17.60	-0.34	17.38	-0.56
Case L	1L/1R	3.34	0.29							7.10	
	2Ca	6.08	0.24							8.97	
	2C	6.38	0.24							9.15	
	3R	11.00	0.14							11.69	
	3L	11.45	0.14							11.91	
	Chimney	14.50	0.05							13.34	
	4C	20.69	0.05							15.91	
Case M	1L/1R	3.34	0.29							6.32	
	2Ca	6.08	0.23							7.88	
	2C	6.38	0.23							8.04	
	3R	11.00	0.13							10.25	
	3L	11.45	0.13							10.45	
	Chimney	14.50	0.05							11.73	
	4C	20.69	0.05							14.09	
Number of cases							22		30		30
Average							0.60		-0.28		-0.20
Standard Deviation							0.76		1.12		0.58

TABLE XIV

Calculated and Measured Maximum Intervision Ranges (MAPTIP - Visible 2 Camera)

				Visible 2 (Canada)							
				MIVR							
				MAPTIP Report (LWWKD Version 6.0)						LWKD	
				Experimental Data		LWKD	Difference	LWWKD	Difference	Ver. 7.08	Difference
	Object	Height	Delta H	Range	Delta R	Range	LWKD - Data	Range	LWWKD - Data	Range	V 7.08 - Data
	(light)	(m)	(m)	(km)	(km)	(km)	(km)	(km)	(km)	(km)	(km)
Case A	1L/1R	3.34	0.22	14.18	0.19	15.00	0.82	15.00	0.82	14.83	0.65
	2Ca	6.08	0.18							17.65	
	2C	6.38	0.18	18.77	0.19	18.00	-0.77	18.00	-0.77	17.89	-0.87
	3R	11.00	0.10			21.40		21.40		21.25	
	3L	11.45	0.10			21.60		21.60		21.53	
	Chimney	14.50	0.04							23.26	
	4C	20.69	0.04	25.97	0.09	26.60	0.63	26.40	0.43	26.28	0.32
Case B	1L/1R	3.34	0.12	12.59	0.07	10.36	-2.23	10.33	-2.26	10.13	-2.46
	2Ca	6.08	0.10			12.89		12.91		12.65	
	2C	6.38	0.10	15.04	0.07	13.12	-1.92	13.14	-1.90	12.88	-2.16
	3R	11.00	0.06			16.27		16.23		16.01	
	3L	11.45	0.06	18.31	0.09	16.53	-1.78	16.49	-1.82	16.26	-2.05
	Chimney	14.50	0.02			18.21		18.16		17.90	
	4C	20.69	0.02	23.12	0.09	21.13	-1.99	21.13	-1.99	20.81	-2.31
Case C	1L/1R	3.34	1.34							6.80	
	2Ca	6.08	1.08							8.95	
	2C	6.38	1.08							9.15	
	3R	11.00	0.62							11.91	
	3L	11.45	0.62							12.14	
	Chimney	14.50	0.22							13.66	
	4C	20.69	0.22							16.34	
Case D	1L/1R	3.34	0.70	12.62	0.09	11.48	-1.14	11.32	-1.30	10.82	-1.81
	2Ca	6.08	0.57			13.92		13.83		13.24	
	2C	6.38	0.57	14.77	0.09	14.15	-0.62	14.06	-0.71	13.46	-1.31
	3R	11.00	0.32	17.20	0.09	17.18	-0.02	17.12	-0.08	16.49	-0.71
	3L	11.45	0.32	17.20	0.09	17.45	0.25	17.38	0.18	16.74	-0.46
	Chimney	14.50	0.12			19.09		19.03		18.35	
	4C	20.69	0.12	21.97	0.09	21.95	-0.02	21.89	-0.08	21.18	-0.79
Case E	1L/1R	3.34	0.65							7.04	
	2Ca	6.08	0.53							9.21	
	2C	6.38	0.53							9.41	
	3R	11.00	0.30							12.19	
	3L	11.45	0.30							12.42	
	Chimney	14.50	0.11							13.95	
	4C	20.69	0.11							16.65	
Case F	1L/1R	3.34	0.66	16.38	0.08	15.90	-0.48	15.60	-0.76	15.42	-0.94
	2Ca	6.08	0.53							17.99	
	2C	6.38	0.53	19.00	0.08	18.76	-0.24	18.60	-0.40	18.22	-0.78
	3R	11.00	0.30	22.14	0.08	21.84	-0.30	21.80	-0.34	21.31	-0.83
	3L	11.45	0.30	22.30	0.08	22.06	-0.24	22.00	-0.30	21.57	-0.73
	Chimney	14.50	0.11							23.21	
	4C	20.69	0.11	27.27	0.07	26.68	-0.59	26.60	-0.67	26.08	-1.19
Case G	1L/1R	3.34	0.66	11.96	0.08	11.40	-0.56	11.20	-0.76	10.85	-1.11
	2Ca	6.08	0.54							13.29	
	2C	6.38	0.54	13.98	0.08	14.00	0.02	14.00	0.02	13.51	-0.46
	3R	11.00	0.31	16.71	0.09	17.20	0.49	17.00	0.29	16.55	-0.17
	3L	11.45	0.31	16.89	0.09	17.40	0.51	17.20	0.31	16.81	-0.08
	Chimney	14.50	0.11							18.45	
	4C	20.69	0.11	21.70	0.08	22.00	0.30	21.80	0.10	21.31	-0.40

TABLE XIV (continued)

Calculated and Measured Maximum Intervision Ranges (MAPTIP - Visible 2 Camera)

				Visible 2 (Canada)							
				MIVR							
				MAPTIP Report (LWWKD Version 6.0)						LWKD	
				Experimental Data		LWKD	Difference	LWWKD	Difference	Ver. 7.08	Difference
	Object	Height	Delta H	Range	Delta R	Range	LWKD - Data	Range	LWWKD - Data	Range	V 7.08 - Data
	(light)	(m)	(m)	(km)	(km)	(km)	(km)	(km)	(km)	(km)	(km)
Case H	1L/1R	3.34	0.49	13.55	0.09			12.88	-0.67	12.81	-0.74
	2Ca	6.08	0.39							15.32	
	2C	6.38	0.39	16.04	0.10			15.76	-0.28	15.55	-0.49
	3R	11.00	0.22	19.14	0.09			18.88	-0.26	18.64	-0.50
	3L	11.45	0.22	19.14	0.09			19.12	-0.02	18.90	-0.24
	Chimney	14.50	0.08							20.56	
	4C	20.69	0.08	23.84	0.09			23.92	0.08	23.44	-0.40
Case I	1L/1R	3.34	0.55	11.81	0.10			10.40	-1.41	10.20	-1.61
	2Ca	6.08	0.45	13.30	0.08			12.80	-0.50	12.64	-0.65
	2C	6.38	0.45							12.88	
	3R	11.00	0.25	16.88	0.11			16.20	-0.68	15.96	-0.92
	3L	11.45	0.25	17.10	0.11			16.40	-0.70	16.22	-0.88
	Chimney	14.50	0.09							17.86	
	4C	20.69	0.09	21.44	0.10			21.00	-0.44	20.71	-0.74
Case J	1L/1R	3.34	0.50					9.60		9.34	
	2Ca	6.08	0.41							11.78	
	2C	6.38	0.41					12.20		12.01	
	3R	11.00	0.23	15.44	0.10			15.20	-0.24	15.06	-0.38
	3L	11.45	0.23	15.64	0.10			15.60	-0.04	15.32	-0.32
	Chimney	14.50	0.08							16.95	
	4C	20.69	0.08					20.00		19.79	
Case K	1L/1R	3.34	0.36	11.31	0.10	10.00	-1.31	10.00	-1.31	9.79	-1.52
	2Ca	6.08	0.30							12.27	
	2C	6.38	0.30	13.79	0.09	12.60	-1.19	12.60	-1.19	12.51	-1.28
	3R	11.00	0.17	16.80	0.09	15.80	-1.00	15.80	-1.00	15.61	-1.20
	3L	11.45	0.17	16.99	0.09	16.00	-0.99	16.00	-0.99	15.87	-1.13
	Chimney	14.50	0.06							17.51	
	4C	20.69	0.06	21.54	0.09	20.60	-0.94	20.60	-0.94	20.38	-1.16
Case L	1L/1R	3.34	0.29							8.41	
	2Ca	6.08	0.24							10.80	
	2C	6.38	0.24							11.02	
	3R	11.00	0.14							14.03	
	3L	11.45	0.14							15.99	
	Chimney	14.50	0.05							15.89	
	4C	20.69	0.05							18.71	
Case M	1L/1R	3.34	0.29							8.37	
	2Ca	6.08	0.23							10.76	
	2C	6.38	0.23							10.98	
	3R	11.00	0.13							13.96	
	3L	11.45	0.13							14.21	
	Chimney	14.50	0.05							15.83	
	4C	20.69	0.05							18.64	
Number of cases							27		39		39
Average							-0.57		-0.58		-0.89
Standard Deviation							0.84		0.70		0.67

TABLE XV

Calculate and Measured MMRs for Different Source Heights (MAPTIP Visible 1)

Visible 1 Camera											
MMR (km)											
			MEAN			LOWER LIMIT			UPPER LIMIT		
		MAPTIP		LWKD 7.09			LWKD 7.09			LWKD 7.09	
Case	Light	Experiment	Height	K = 0.40	K = 0.41	Height	K = 0.40	K = 0.41	Height	K = 0.40	K = 0.41
		(km)	(m)	(km)	(km)	(m)	(km)	(km)	(m)	(km)	(km)
A	1L/1R	6.65	3.34	6.15	6.27	3.12	6.03	6.15	3.56	6.26	6.38
A	2C	7.87	6.38	7.59	7.74	6.20	7.51	7.66	6.56	7.67	7.82
A	4C	13.41	20.69	13.01	13.22	20.65	13.00	13.21	20.73	13.02	13.23
C	3R	13.49	11.00	14.32	14.49	10.38	14.00	14.16	11.62	14.63	14.80
C	3L	13.49	11.45	14.55	14.72	10.83	14.23	14.40	12.07	14.86	15.03
C	4C	18.62	20.69	18.62	18.81	20.47	18.54	18.72	20.91	18.71	18.90
E	1L/1R	8.53	3.34	8.48	8.64	2.69	7.99	8.14	3.99	8.94	9.10
E	2C	10.83	6.38	10.39	10.58	5.85	10.09	10.27	6.91	10.69	10.88
F	3R	20.34	11.00	19.87	20.05	10.70	19.69	19.87	11.30	20.04	20.22
F	3L	20.50	11.45	20.12	20.30	11.15	19.95	20.13	11.75	20.29	20.47
F	4C	25.41	20.69	24.56	24.76	20.58	24.51	24.71	20.80	24.61	24.81
G	1L/1R	12.87	3.34	13.08	13.17	2.68	12.38	12.47	4.00	13.72	13.80
G	2C	15.24	6.38	15.60	15.68	5.84	15.21	15.29	6.92	15.99	16.06
G	3R	18.52	11.00	18.49	18.57	10.69	18.32	18.40	11.31	18.66	18.74
G	3L	18.69	11.45	18.74	18.82	11.14	18.57	18.65	11.76	18.90	18.98
G	4C	22.98	20.69	23.06	23.15	20.58	23.02	23.10	20.80	23.11	23.19
I	1L/1R	11.81	3.34	11.93	12.10	2.79	11.41	11.57	3.89	12.42	12.59
I	2Ca	14.20	6.08	14.09	14.28	5.63	13.77	13.96	6.53	14.39	14.58
I	3R	17.31	11.00	17.07	17.28	10.75	16.93	17.14	11.25	17.21	17.42
I	3L	17.62	11.45	17.31	17.52	11.20	17.18	17.39	11.70	17.44	17.66
I	4C	22.23	20.69	21.55	21.78	20.60	21.51	21.74	20.78	21.59	21.82
J	3R	17.36	11.00	16.65	16.86	10.77	16.52	16.73	11.23	16.77	16.98
J	3L	17.45	11.45	16.89	17.10	11.22	16.77	16.98	11.68	17.01	17.22
J	4C	21.71	20.69	21.17	21.39	20.61	21.13	21.36	20.77	21.20	21.43
K	1L/1R	11.03	3.34	10.44	10.57	2.98	10.15	10.28	3.70	10.72	10.86
K	2C	13.03	6.38	12.57	12.73	6.08	12.39	12.54	6.68	12.76	12.92
K	3R	15.67	11.00	15.19	15.36	10.83	15.10	15.27	11.17	15.27	15.44
K	3L	15.96	11.45	15.41	15.59	11.28	15.33	15.50	11.62	15.50	15.67
K	4C	20.15	20.69	19.49	19.68	20.63	19.47	19.66	20.75	19.52	19.71
M	2C	10.67	6.38	9.76	9.92	6.15	9.64	9.79	6.61	9.88	10.04
M	3R	13.51	11.00	11.98	12.16	10.87	11.92	12.10	11.13	12.04	12.22
M	3L	13.99	11.45	12.18	12.36	11.32	12.12	12.30	11.58	12.23	12.42

TABLE XVI

Calculated and Measured MIVRs for Different Source Heights (MAPTIP - Visible 1)

Visible 1 Camera															
			MIVR (km)												
			MEAN				LOWER LIMIT				UPPER LIMIT				
		MAPTIP	LWKD 7.09				LWKD 7.09				LWKD 7.09				
Case	Light	Experiment	Height	K = 0.40	K = 0.41	Non-Ref.	Height	K = 0.40	K = 0.41	Non-Ref.	Height	K = 0.40	K = 0.41	Non-Ref.	
		(km)	(m)	(km)	(km)	(km)	(m)	(km)	(km)	(km)	(m)	(km)	(km)	(km)	
A	1L/1R	10.90	3.34	9.59	9.69	16.26	3.12	9.36	9.45	16.05	3.56	9.83	9.93	16.47	
A	2C	13.41	6.38	12.34	12.45	18.76	6.20	12.20	12.31	18.64	6.56	12.48	12.59	18.89	
A	4C	22.23	20.69	20.25	20.37	25.99	20.65	20.23	20.35	25.98	20.73	20.27	20.38	26.00	
C	1L/1R	10.27	3.34	9.36	9.49	15.36	2.00	7.89	8.01	13.90	4.68	10.59	10.72	16.56	
C	2C	13.49	6.38	11.91	12.05	17.86	5.30	11.09	11.22	17.06	7.46	12.68	12.82	18.60	
C	3R	15.63	11.00	14.85	15.00	20.69	10.38	14.50	14.64	20.35	11.62	15.19	15.33	21.01	
C	3L	15.63	11.45	15.10	15.24	20.93	10.83	14.76	14.90	20.60	12.07	15.43	15.58	21.25	
C	4C	18.91	20.69	19.50	19.65	25.09	20.47	19.40	19.56	25.00	20.91	19.59	19.74	25.17	
E	1L/1R	11.08	3.34	9.42	9.55	15.76	2.69	8.73	8.86	15.08	3.99	10.07	10.20	16.38	
E	2C	12.95	6.38	12.01	12.15	18.26	5.85	11.61	11.75	17.88	6.91	12.40	12.53	18.63	
E	4C	21.08	20.69	19.61	19.75	25.49	20.58	19.56	19.71	25.44	20.80	19.66	19.80	25.53	
F	1L/1R	15.39	3.34	14.21	14.33	16.32	2.68	13.46	13.57	15.63	4.00	14.90	15.01	16.94	
F	2C	17.84	6.38	17.01	17.11	18.82	5.85	16.59	16.68	18.43	6.91	17.43	17.52	19.19	
F	3R	20.73	11.00	20.12	20.22	21.65	10.70	19.94	20.03	21.48	11.30	20.30	20.39	21.81	
F	3L	20.89	11.45	20.38	20.48	21.88	11.15	20.21	20.30	21.72	11.75	20.55	20.65	22.04	
F	4C	25.81	20.69	24.91	25.00	26.04	20.58	24.86	24.95	26.00	20.80	24.95	25.05	26.09	
G	1L/1R	14.31	3.34	13.28	13.39	16.49	2.68	12.50	12.62	15.80	4.00	13.97	14.08	17.12	
G	2C	16.71	6.38	15.97	16.08	18.99	5.84	15.55	15.66	18.60	6.92	16.39	16.50	19.37	
G	3R	19.79	11.00	19.12	19.24	21.82	10.69	18.93	19.05	21.65	11.31	19.30	19.41	21.98	
G	3L	19.96	11.45	19.38	19.50	22.06	11.14	19.20	19.32	21.89	11.76	19.56	19.68	22.22	
G	4C	24.14	20.69	23.92	24.04	26.22	20.58	23.88	24.00	26.17	20.80	23.97	24.09	26.26	
H	1L/1R	16.41	3.34	15.35	15.42	16.37	2.85	14.81	14.88	15.88	3.83	15.86	15.93	16.83	
H	2C	18.96	6.38	18.12	18.19	18.87	5.99	17.81	17.88	18.59	6.77	18.42	18.49	19.14	
H	3R	21.82	11.00	21.24	21.32	21.70	10.78	21.11	21.18	21.57	11.22	21.37	21.44	21.82	
H	3L	22.00	11.45	21.50	21.58	21.93	11.23	21.37	21.45	21.82	11.67	21.63	21.70	22.05	
H	4C	26.67	20.69	26.05	26.13	26.09	20.61	26.02	26.09	26.06	20.77	26.09	26.16	26.13	
I	1L/1R	13.76	3.34	12.64	12.74	16.43	2.79	12.01	12.12	15.86	3.89	13.21	13.30	16.95	
I	2Ca	15.59	6.08	15.21	15.31	18.72	5.63	14.82	14.92	18.38	6.53	15.56	15.66	19.03	
I	3R	19.56	11.00	18.59	18.69	21.76	10.75	18.43	18.53	21.61	11.25	18.73	18.83	21.89	
I	3L	19.67	11.45	18.84	18.95	21.99	11.20	18.70	18.80	21.86	11.70	18.99	19.09	22.13	
I	4C	24.07	20.69	23.40	23.49	26.15	20.60	23.36	23.45	26.12	20.78	23.44	23.53	26.19	
J	3R	18.55	11.00	18.05	18.14	20.89	10.77	17.90	17.99	20.76	11.23	18.18	18.27	21.01	
J	3L	18.75	11.45	18.31	18.40	21.13	11.22	18.18	18.26	21.00	11.68	18.45	18.54	21.25	
J	4C	23.06	20.69	22.91	23.00	25.29	20.61	22.87	22.96	25.25	20.77	22.94	23.04	25.32	
K	1L/1R	13.79	3.34	12.23	12.32	16.50	2.98	11.84	11.93	16.14	3.70	12.62	12.71	16.84	
K	2C	16.15	6.38	15.08	15.17	19.00	6.08	14.84	14.93	18.79	6.68	15.32	15.41	19.20	
K	3R	19.40	11.00	18.25	18.34	21.83	10.83	18.14	18.24	21.73	11.17	18.34	18.44	21.91	
K	3L	19.59	11.45	18.51	18.60	22.06	11.28	18.41	18.50	21.97	11.62	18.60	18.70	22.15	
K	4C	24.14	20.69	23.11	23.20	26.22	20.63	23.09	23.18	26.20	20.75	23.14	23.23	26.25	
M	1L/1R	11.95	3.34	10.65	10.75	16.61	3.05	10.35	10.46	16.34	3.63	10.94	11.05	16.88	
M	2C	14.27	6.38	13.42	13.53	19.11	6.15	13.25	13.35	18.95	6.61	13.60	13.71	19.27	
M	3R	17.04	11.00	16.54	16.65	21.94	10.87	16.46	16.57	21.87	11.13	16.61	16.73	22.01	
M	3L	17.04	11.45	16.80	16.91	22.18	11.32	16.72	16.83	22.11	11.58	16.87	16.99	22.25	

TABLE XVII

Calculated and Measured MMRs for Different Source Heights (MAPTIP - Visible 2)

Visible 2 Camera											
MMR (km)											
				MEAN			LOWER LIMIT			UPPER LIMIT	
		MAPTIP		LWKD 7.09			LWKD 7.09			LWKD 7.09	
Case	Light	Experiment	Height	K = 0.40	K = 0.41	Height	K = 0.40	K = 0.41	Height	K = 0.40	K = 0.41
		(km)	(m)	(km)	(km)	(m)	(km)	(km)	(m)	(km)	(km)
A	1L/1R	8.44	3.34	9.93	10.13	3.12	9.82	10.01	3.56	10.04	10.24
A	2C	12.25	6.38	11.37	11.59	6.20	11.29	11.51	6.56	11.45	11.67
A	4C	16.47	20.69	16.77	17.07	20.65	16.76	17.06	20.73	16.78	17.08
B	1L/1R	7.69	3.34	6.66	6.83	3.22	6.58	6.76	3.46	6.73	6.91
B	2C	9.05	6.38	8.34	8.55	6.28	8.29	8.50	6.48	8.39	8.60
B	3L	12.16	11.45	10.74	10.98	11.39	10.71	10.96	11.51	10.76	11.01
B	4C	15.49	20.69	14.37	14.66	20.67	14.37	14.65	20.71	14.38	14.66
D	1L/1R	10.08	3.34	10.22	10.35	2.64	9.61	9.74	4.04	10.78	10.91
D	2C	12.05	6.38	12.37	12.51	5.81	12.01	12.15	6.95	12.72	12.87
D	3R	15.12	11.00	14.94	15.10	10.68	14.77	14.93	11.32	15.09	15.26
D	3L	15.12	11.45	15.16	15.32	11.13	15.00	15.16	11.77	15.32	15.48
D	4C	19.08	20.69	19.15	19.33	20.57	19.11	19.29	20.81	19.20	19.38
F	4C	26.97	20.69	25.83	25.91	20.58	25.78	25.87	20.80	25.87	25.96
G	2C	12.96	6.38	13.27	13.36	5.84	12.88	12.97	6.92	13.65	13.74
G	3R	16.01	11.00	16.16	16.25	10.69	15.98	16.08	11.31	16.32	16.42
G	3L	16.01	11.45	16.40	16.50	11.14	16.24	16.33	11.76	16.57	16.66
G	4C	20.46	20.69	20.73	20.83	20.58	20.68	20.78	20.80	20.78	20.87
I	1L/1R	9.78	3.34	9.71	9.85	2.79	9.19	9.32	3.89	10.20	10.34
I	2Ca	12.38	6.08	11.87	12.03	5.63	11.55	11.70	6.53	12.17	12.33
I	3R	14.63	11.00	14.86	15.03	10.75	14.72	14.89	11.25	14.99	15.17
I	3L	14.98	11.45	15.09	15.27	11.20	14.96	15.14	11.70	15.23	15.40
I	4C	19.77	20.69	19.33	19.52	20.60	19.30	19.49	20.78	19.37	19.56
J	3R	14.44	11.00	14.21	14.28	10.77	14.08	14.15	11.23	14.34	14.40
J	3L	14.64	11.45	14.45	14.52	11.22	14.33	14.39	11.68	14.58	14.64
J	4C	18.95	20.69	18.74	18.81	20.61	18.70	18.77	20.77	18.77	18.84
K	1L/1R	8.65	3.34	8.35	8.55	2.98	8.06	8.26	3.70	8.63	8.84
K	2C	10.55	6.38	10.48	10.71	6.08	10.29	10.53	6.68	10.66	10.90
K	3R	13.41	11.00	13.08	13.35	10.83	13.00	13.26	11.17	13.17	13.43
K	3L	13.60	11.45	13.31	13.57	11.28	13.22	13.49	11.62	13.39	13.66
K	4C	17.94	20.69	17.38	17.68	20.63	17.36	17.65	20.75	17.41	17.70

TABLE XVIII

Calculated and Measured MIVRs for Different Source Height (MAPTIP - Visible 2)

Visible 2 Camera MIVR (km)														
			MEAN				LOWER LIMIT				UPPER LIMIT			
		MAPTIP		LWKD 7.09				LWKD 7.09				LWKD 7.09		
Case	Light	Experiment	Height	K = 0.40	K = 0.41	Non-Ref.	Height	K = 0.40	K = 0.41	Non-Ref.	Height	K = 0.40	K = 0.41	Non-Ref.
		(km)	(m)	(km)	(km)	(km)	(m)	(km)	(km)	(km)	(m)	(km)	(km)	(km)
A	1L/1R	14.18	3.34	14.83	14.95	21.41	3.12	14.58	14.70	21.20	3.56	15.08	15.20	21.62
A	2C	18.77	6.38	17.89	18.01	23.91	6.20	17.75	17.86	23.79	6.56	18.04	18.15	24.04
A	4C	25.97	20.69	26.28	26.40	31.14	20.65	26.27	26.38	31.12	20.73	26.30	26.41	31.15
B	1L/1R	12.59	3.34	10.13	10.23	15.33	3.22	10.00	10.10	15.21	3.46	10.26	10.36	15.45
B	2C	15.04	6.38	12.88	12.98	17.83	6.28	12.80	12.90	17.76	6.48	12.96	13.06	17.90
B	3L	18.31	11.45	16.26	16.36	20.90	11.39	16.23	16.33	20.87	11.51	16.29	16.39	20.93
B	4C	23.12	20.69	20.81	20.92	25.06	20.67	20.81	20.91	25.05	20.71	20.82	20.93	25.06
D	1L/1R	12.62	3.34	10.82	10.95	16.22	2.64	10.04	10.17	15.49	4.04	11.53	11.67	16.89
D	2C	14.77	6.38	13.46	13.60	18.73	5.81	13.03	13.17	18.32	6.95	13.87	14.01	19.12
D	3R	17.20	11.00	16.49	16.64	21.55	10.68	16.30	16.44	21.38	11.32	16.67	16.82	21.72
D	3L	17.20	11.45	16.74	16.89	21.79	11.13	16.56	16.71	21.62	11.77	16.92	17.07	21.96
D	4C	21.97	20.69	21.18	21.33	25.95	20.57	21.13	21.28	25.90	20.81	21.23	21.38	26.00
F	1L/1R	16.36	3.34	15.42	15.51	17.42	2.68	14.65	14.74	16.73	4.00	16.13	16.23	18.04
F	2C	19.00	6.38	18.22	18.31	19.92	5.85	17.80	17.89	19.53	6.91	18.63	18.72	20.29
F	3R	22.14	11.00	21.31	21.41	22.75	10.70	21.13	21.22	22.58	11.30	21.49	21.58	22.91
F	3L	22.30	11.45	21.57	21.66	22.98	11.15	21.40	21.49	22.82	11.75	21.74	21.84	23.14
F	4C	27.27	20.69	26.08	26.18	27.14	20.58	26.03	26.13	27.10	20.80	26.12	26.22	27.19
G	1L/1R	11.96	3.34	10.85	10.96	14.19	2.68	10.10	10.20	13.49	4.00	11.53	11.64	14.82
G	2C	13.98	6.38	13.51	13.62	16.69	5.84	13.10	13.22	16.30	6.92	13.91	14.02	17.07
G	3R	16.71	11.00	16.55	16.67	19.52	10.69	16.36	16.48	19.35	11.31	16.72	16.84	19.68
G	3L	16.89	11.45	16.81	16.92	19.76	11.14	16.63	16.75	19.59	11.76	16.98	17.10	19.92
G	4C	21.70	20.69	21.31	21.43	23.91	20.58	21.26	21.38	23.87	20.80	21.35	21.48	23.96
H	1L/1R	13.55	3.34	12.81	12.88	14.03	2.85	12.27	12.34	13.54	3.83	13.33	13.40	14.49
H	2C	16.04	6.38	15.55	15.62	16.53	5.99	15.25	15.32	16.25	6.77	15.85	15.92	16.81
H	3R	19.14	11.00	18.64	18.71	19.36	10.78	18.51	18.58	19.24	11.22	18.77	18.84	19.48
H	3L	19.14	11.45	18.90	18.97	19.60	11.23	18.77	18.84	19.48	11.67	19.03	19.10	19.71
H	4C	23.84	20.69	23.44	23.51	23.76	20.61	23.41	23.48	23.72	20.77	23.48	23.55	23.79
I	1L/1R	11.81	3.34	10.20	10.29	14.10	2.79	9.58	9.68	13.54	3.89	10.76	10.86	14.63
I	2Ca	13.30	6.08	12.64	12.75	16.40	5.63	12.28	12.38	16.06	6.53	12.99	13.09	16.71
I	3R	16.88	11.00	15.96	16.07	19.44	10.75	15.81	15.91	19.29	11.25	16.11	16.21	19.57
I	3L	17.10	11.45	16.22	16.32	19.67	11.20	16.07	16.18	19.54	11.70	16.36	16.47	19.81
I	4C	21.44	20.69	20.71	20.82	23.83	20.60	20.67	20.78	23.80	20.78	20.74	20.86	23.87
J	3R	15.44	11.00	15.06	15.16	18.26	10.77	14.93	15.02	18.14	11.23	15.19	15.29	18.38
J	3L	15.64	11.45	15.32	15.42	18.50	11.22	15.19	15.28	18.38	11.68	15.45	15.55	18.62
K	1L/1R	11.31	3.34	9.79	9.88	14.20	2.98	9.41	9.50	13.84	3.70	10.17	10.26	14.54
K	2C	13.79	6.38	12.51	12.60	16.70	6.08	12.28	12.37	16.49	6.68	12.74	12.83	16.91
K	3R	16.80	11.00	15.61	15.71	19.53	10.83	15.51	15.60	19.43	11.17	15.71	15.80	19.62
K	3L	16.99	11.45	15.87	15.96	19.76	11.28	15.77	15.87	19.68	11.62	15.96	16.06	19.85
K	4C	21.54	20.69	20.38	20.47	23.92	20.63	20.35	20.45	23.90	20.75	20.41	20.50	23.95

7.0 ACKNOWLEDGEMENTS

I would like to thank the efforts of Jacques Claverie of France and Yvonnick Hurtaud of CELAR in France for their many useful discussions while we worked towards a common vision, and even more concretely, towards common physical equations for use in current and future maritime boundary layer models. I would also like to thank Denis Dion of DREV and Lionel Gardenal of Informission for their help and advice during the various stages of this project.

8.0 REFERENCES

1. Forand, J.L., "The L(W)WKD Marine Boundary Layer Model", DREV-R-9618, March 1997, UNCLASSIFIED

2. Forand, J.L., Dion, D., Hurtaud, Y., and Stein, K., "MAPTIP Work Group Report: Refractive Effects in the Visible and the Infrared", DREV R-9621, June 1997, UNCLASSIFIED

3. Claverie, J., Hurtaud, Y., de Fromont, Y. and Junchat, A., "Modelisation des Profils Verticaux d'Indice de Réfraction et de C^2_n en Atmosphère Marine", Propagation Assessment in Coastal Environments, AGARD Conference Proceedings 567, p. 29-1, 1994.

4. Monin, A.S. and Obukhov, A.M., "Basic Regularity in Turbulent Mixing in the Surface Layer of the Atmosphere", Trad. Geophys. Inst. ANSSSR, No. 24, p. 163, 1954.

5. Lumley, J.L. and Panofsky, H.A., "The Structure of Atmospheric Turbulence", Interscience Monographs and Texts in Physics and Astronomy, Vol. XII, p. 99, Edited by R.E. Marshak, University of Rochester, Rochester, New York, 1964.

6. Hill, R.J., Clifford, S.F. and Lawrence, R.S., "Refractive-Index and Absorption Fluctuations in the Infrared caused by Temperature, Humidity and Pressure Fluctuations", J. Opt. Soc. Am., Vol. 70, No. 10, pp. 1192-1205, 1980.

7. Hill, R.J. and Lawrence, R.S., "Refractive Index of Water Vapor in Infrared Windows", Infrared Phys., Vol. 26, No. 6, pp. 371-376, 1986.

8. Dion, D. and Schwering, P., "On the Analysis of Atmospheric Effects on Electro-Optical Sensors in the Marine Surface Layer", IRIS Conference, UK, June 1996

9. Low, T.B. and Hudak, D.R., "Final Report on the Development and Testing of a Marine Boundary Layer Model", KelResearch Corp. Report under DSS contract #W7701-8-2419/01-XSK, September 1990

10. Beaulieu, A.J., "Atmospheric Refraction Model and the Effects of Surface Waves", DREV R-4661/92, May 1992, UNCLASSIFIED

11. Walmsley, J.L., "On Theoretical Wind Speed and Temperature Profiles over the Sea with Applications to Data from Sable Island, Nova Scotia", Atmosphere Ocean, Vol. 26, pp. 203-233, 1988.

12. Kondo, J., "Air-Sea Bulk Transfer Coefficients in Diabetic Conditions", Bound. Layer Meteo., 9, 1975, pp 91-112.

13. Claverie, J., "Private communication", July 1998.

14. Businger, J.A., Wyngaard, J.C., Isumi, Y. and Bradley, E.F., "Flux-Profile Relationships in the Atmospheric Surface Layer", J. Atmos. Sci., 28, pp. 181-189, March 1971.

15. Smith, S.D., "Water Vapour Flux at the Sea Surface", Boundary-Layer Meteorology, 47, pp. 277-293, 1989.

16. Garratt, J.R., "The Atmospheric Boundary Layer", Cambridge University Press, Cambridge, p. 286, 1992.

17. Born, M., and Wolf, E., "Principles of Optics", 6th (Corrected) Ed., Pergamon Press, Toronto, pp. 87-98, 1980.

18. Edlén, B., "The Dispersion of Standard Air", J. Opt. Soc. Am., 43, pp. 339-344, 1953.

19. Erickson, K.E., "Investigation of the Invariance of Atmospheric Dispersion with a Long-Path Refractometer", J. Opt. Soc. Am., 52, pp. 777-780, 1962.

20. Bean, B.R. and Dutton, E.J., "Radio Meteorology", National Bureau of Standards Monograph 92, p. 1-22, 1966.

21. Edson, J.B., Fairall, C.W., Mestayer, P.G. and Larsen, S.E., "A Study of the Inertial-Dissipation Method for Computing Air-Sea Fluxes", J. of Geoph. Res., 96, pp.

10689-10711, 1991.

22. Wyngaard, J.C., Izumi, Y. and Stuart Jr., A.S., "Behavior of the Refractive-Index-Structure Parameter Near the Ground", J. Opt. Soc. Am., 61, pp. 1646-1650, 1971.

23. Bataille, P., "Analyse du comportement d'un système de télécommunication optique fonctionnant à 0.83 µm dans la basse troposphère", thèse de doctorat de l'Université de Rennes, Nov. 1, 1992.

24. Davidson, K.L., Schacher, G.E., Fairall, C.W., and Goroch, A.K., "Verification of the Bulk Method of Calculating Overwater Optical Turbulence", Applied Optics, 20, pp. 2919-2924, 1981.

25. Forand, J.L., "Horizontal Non-homogeneous Effects in the Marine Boundary Layer", Propagation and Imaging through the Atmosphere, SPIE Meeting, Denver CO, pp. 180-191, 1997.

26. Dion, D. and Gardenal, L., "On the accuracy of bulk methods for predicting path losses in the marine surface layer", 1999 IEEE AP-S/URSI International Symposium, Orlando, USA, July 11-16, 1999.

27. Hurtaud, Y., Dion, D., Claverie, J. and Forand, L., "Coopérations Franco-canadienne: Arrangement Spécifiques n°7 sur la propagation électromagnétique au-dessus de la mer, Rapport Final", DGA GEOS/99.49/SOP/80832, le 13 avril 1999.

APPENDIX A

PHYSICAL CONSTANTS AND VARIABLES

Quantity	Symbol	Value	Units
Height above mean water level (m)	z		m
Wind speed measurement height	z_0		m
Temp., pressure, rel. humidity measurement height	z_1		m
Wind speed	u		m/s
Wind speed constant of integration	u_0		m/s
Wind speed roughness length	z_{0u}		m
Wind speed scaling constant	u_*		m/s
Wind speed gradient function	φ_u		
Integrated wind speed gradient function	Ψ_u		
Sea temperature	T_s		K
Virtual sea temperature	T_{vs}		K
Virtual potential sea temperature	θ_{vs}		K
Air temperature	T		K
Mean virtual temperature in MBL	T_{vm}		K
Virtual temperature	T_v		K
Virtual potential temperature	θ_v		K
Mean virtual potential temperature in MBL	θ_{vm}		K
Virt. pot. air-sea temperature difference (VPASTD)	$\Delta\theta_v(z_1)$		K
Virt. pot. temperature constant of integration	θ_{vo}		K
Virt. potential temperature roughness length	$z_{0\theta_v}$		m
Virtual potential temperature scaling constant	θ_{v*}		K
Virtual potential temperature gradient function	φ_{θ_v}		
Integrated virt. pot. temperature gradient function	Ψ_{θ_v}		
Specific humidity	q		g/g
Air-sea specific humidity diference (ASSH)	$\Delta q(z_1)$		g/g

Specific humidity constant of integration	q_0		g/g
Specific humidity roughness length	z_{0q}		m
Specific humidity scaling constant	q_*		g/g
Specific humidity gradient function	φ_q		
Integrated specific humidity gradient function	Ψ_q		
Acceleration of gravity	g	9.81	m/s^2
Von Karman's constant	κ	0.4	
Monin-Obukhov length	L		m
Normalized height (= z/L)	ζ		
WKD stable gradient function coefficient ($\zeta \geq 0$)	α	5	
WKD stable wind speed gradient function coefficient	α_1	5	
WKD stable virt. pot. temp. gradient function coef.	α_2	5	
WKD stable specific humidity gradient function coef.	α_3	5	
Unstable gradient function coefficient ($\zeta < 0$)	β	16	
Unstable wind speed gradient function coefficient	β_1	16	
Unstable virt. pot. temp. gradient function coef.	β_2	16	
Unstable specific humidity gradient function coef.	β_3	16	
Kondo gradient function coefficient ($\zeta \geq 0$)	γ	6	
Kondo stable wind speed gradient function coefficient	γ_1	6	
Kondo stable virt. pot. temp. gradient function coef.	γ_2	6	
Kondo stable specific humidity gradient function coef.	γ_3	6	
Molecular mass of dry air	M_a	28.9	g
Molecular mass of water	M_w	18.0	g
Ratio of mol. masses of water and dry air (= M_w/M_a)	μ	0.622	
Boltzmann's constant	k	1.381×10^{-23}	J/K
Universal gas constant	R	8.31	J/mol/K
Dry air gas constant (= R/M_a)	R_a	0.288	J/g/K
Water vapour gas constant (=R_w/M_w)	R_w	0.462	J/g/K

Moist air gas constant	R_m		J/g/K
Total atmospheric pressure	P		mbar
Total atmospheric reference pressure	P_{ref}	1000	mbar
Dry air atmospheric pressure	P_a		mbar
Water vapour pressure	P_w		mbar
Total air density	ρ		g/m^3
Dry air density	ρ_a		g/m^3
Water vapour density	ρ_w		g/m^3
Mixing ratio	w		g/g
Spec. heat capacity of dry air at constant pressure	c_p	1.004	J/g/K
Spec. heat capacity of dry air at constant volume	c_v	0.717	J/g/K
Ratio of heat capacities for dry air ($=c_p/c_v$)	γ	1.40	
Saturated water vapour pressure over water	P_w^s		mbar
Saturated water vapour pressure over salt water	P_{sw}^s		mbar
Relative humidity	H_r		
Dew-point temperature	T_d		K
Salinity	S		g/kg
Salinity coefficient	ε	5.37×10^{-3}	
10-m neutral heat flux coefficient	C_{TN}	1.0×10^{-3}	
10-m neutral moisture flux coefficient	C_{EN}	1.2×10^{-3}	
Charnock's constant	α_c	0.011	
Dynamic viscosity	ν_d		m^2/s
'a_d' coefficient in wind dependent relation	a_d	9.267x10-8	$m^2/s/^oC$
'b_d' coefficient in wind dependent relation	b_d	1.346x10-5	m^2/s
'C' coefficient in wind dependent relation	C	-5.5	
Average of the 1/3 highest wave heights	$H_{1/3}$		m
Water wave height	H_w		m
Water wavelength	λ_w		m

Molecular refractivity for dry air	D_a		
Molecular refractivity for water vapour	D_w		
Refractivity coefficient for dry-air	A		K/mbar
Refractivity coefficient for water vapour	B		K/mbar
i^{th} Line strength	S_i		
Wavelength	λ		μm
i^{th} wavelength resonance	λ_i		μm
Refractive index	n		
Refractivity [= (n - 1) x 10^{-6}]	Z		
Refractivity for dry air	Z_a		
Refractivity for water vapour	Z_w		
Refractive index structure parameter	C_{n^2}		$m^{-2/3}$
Refractivity index structure parameter	C_{Z^2}		$m^{-2/3}$
Temperature structure parameter	C_{T^2}		$m^{-2/3}$
Temp.-specific humidity structure parameter	C_{Tq}		$m^{-2/3}$
Specific humidity structure parameter	C_{q^2}		$m^{-2/3}$
Virtual temperature structure parameter	$C_{T_v^2}$		$m^{-2/3}$
Virtual temp.-spec. humidity structure parameter	$C_{T_v q}$		$m^{-2/3}$
Virt. potential temperature structure parameter	$C_{\theta_v^2}$		$m^{-2/3}$
Virt. pot. temp.-specific humidity structure parameter	$C_{\theta_v q}$		$m^{-2/3}$
Virt. pot. temp.-water vap. density structure parameter	$C_{\theta_v \rho_w}$		$m^{-2/3}$
Water vapour density structure parameter	$C_{\rho_w^2}$		$m^{-2/3}$
i^{th} structure parameter function	f_i		
Structure parameter function ratio (=f_2/f_1)	A_{21}	1	
Virt. pot. temp.-spec. humidity correlation coefficient	$r_{\theta_v q}$	± 0.8	

APPENDIX B

LISTING OF MODIFICATIONS

```
// Mar. 1995
// Ver. 5.0   Oldest version.
// Sept. 1995
// Ver. 6.0   1) Modified to include batch file option (Sept. 95) by
//            Lionel Gardenal - Informission Inc.
//             2) Added copyright screen.
// June 1996
// Ver. 6.01  1) Modified to use the hydrostatic equation to calculate the total
//           pressure instead of the dry-air pressure.
// Nov. 1996
// Ver. 6.11  1) use dry-air or total air pressure for potential temp. calculation
//            2) enter desired adiabatic pressure for potential temp. calculation
//            3) can now choose between LWWKD or Kondo profile for stable case
//            The defaults are LWWKD, Dry-Air and 1000 mb.
//            Note: while these options can not be directly chosen in the "batch"
//            mode, if the user goes into the "interactive" mode, modifies them and
//            then returns and runs the "batch" mode, the batch mode will use these
//            modified options until they are again changed in "interactive" mode.
//            4) the saved binary file is slightly different as it saves the options;
//            thus, the file ID is now 1.
// Nov. 1996
// Ver. 6.2   Modified to include multiple weather parameter sets where each one is
//            distinquished by a horizontal range.
//            1) the horizontal range is a new parameter which has been added to the
//            PARAM structure.
//            2) there are two new options (Add & Delete) in the modify weather menu.
//            The 'Add' key adds a new weather set which can subsequently be edited,
//            and the 'Delete' key removes the currently displayed weather set.
//            3) the user can add up to 10 weather sets and can cycle between them using
//            the LEFT and RIGHT arrows.  These keys can also be used in other windows.
//            For example, if you are in the graphics menu, change the weather set which
//            is displayed to get graphs pertaining to it.
//            4) the weather sets are always arranged in order of increasing range.
//            5) the saved binary file is again different (file ID = 2) as it saves
//            information for all the weather sets.  The file saves all the weather
//            set data as well as the refraction data for a chosen wavelength and
//            model as before, except that now it has it for all the weather sets.
//            This means that the file can now have range-dependent refractivity data.
//            6) Note: the options are the same for all weather sets and the wave height
//            for all the sets are always the same.  This makes the file easier to use
//            in ray tracing.
//            7) Added extra plot so that different profile parameters can be plotted
//            against the adiabatic pressure (900 - 1200 mb).
// April 17, 1997
// Ver 6.21   1) Corrected problem with structure parameter calculations.  The calculation
//            of pow(x,2/3), etc. were giving 1.  Now changed to pow(x,2.0/3.0).
// May 20,1997
// Ver 6.22   1) Corrected problem in the subroutines wvap_struct & vptemp_wvap_struct
//            of the module profile.c.  The problem was that the temperature was being
//            converted to Kelvin when it shouldn't have been.  This caused there to be
//            two conversions from Celsius to Kelvin; one in the above functions and
//            a second in the subroutines vapour_density and air_density of the module
//            weather.c.  These corrections only affect the structure parameter calcu-
//            lations.
//            2) A second problem was noticed with respect to the calculation of the
//            virtual potential temperature structure parameter, specific humidity
//            structure parameter, and the virtual potential temperature-specific humidity
//            structure parameter.  A factor of K^2 (von Karmen's constant) must be added
//            to each of the subroutines virt_pot_temp_struct, spec_humid_struct, and
```

```
//            vptemp_shum_struct of the module profile.c.  This is due to an error in my
//            LWWKD report.
//            3) Noticed a problem with the calculate_weather(mode) subroutine in the
//            graphics modules.  The problem was that they were not using the proper
//            value for mode.  The calls to calculate_weather were changed from
//            calculate_weather(mode) to calculate_weather(pot_mode).  'pot_mode' is a
//            global constant.
// Dec. 19, 1997
// Ver. 6.3   1) Allows the possibility that the surface relative humidity can be
//            something other than 100%
//            2) Corrected error in the Kondo formula (5.0 to 6.0)
// Apr. 02, 1998
// Ver. 6.31  1) Correct calculation of duct height in batch section of the
//            program.
//            2) Correct problem where an IRCOND file was created for the radar
//            case instead of the desired file RFCOND
// July 16, 1998
// Ver. 6.40  1) Modify certain modules so that most input/output functions
//            are separate from any calculation functions.  This will make it
//            easier to incorporate the core LWWKD routines into other
//            operating systems.
// Sept. 28, 1998
// Ver. 7.00  1) Modifications are made to a number of routines in order to
//            comply with common options (options commune) agreed upon by
//            Canada & France.
//            a) The vertical pressure profile is calculated using the same
//            earlier equation except that the virtual temperature is used.
//            b) In the equation that relates the wind speed roughness length
//            to the wind speed scaling constant, the v term (dynamic viscosity)
//            is now a function of the virtual potential temperature.
//            c) The relative humidity at the surface has a default value of
//            98.2%.  This is good for salt water with a salinity of 34g/kg
//            (RHsea = 1 - 5.37e-3 x S).
//            d) The Kondo function is now the default mode.  This means that
//            the Kondo function is used for the stable case (VPASTD > 0).
//            e) The Monin-Obukhov length is now calculated using the average
//            of the virtual temperature instead of the average temperature.
//            f) The scaling parameters have been modified so that they agree
//            with the definitions used by the French.  In other words, our
//            scaling equations have been multiplied by von Karman's to give
//            those used by the French.
//            2) In order to make these changes, a number of changes were also
//            made to many of the subroutines, including changing their names,
//            moving them to a different or newly created module, and rewriting
//            their codes.
//            3) Made slight changes to ASCII & Postscript files containing the
//            Met & Profile data.
//            4) The program can be compiled in either batch or interactive
//            by setting the INTERACT definition to (0) or (1) respectively.  In
//            batch mode the program can easily be interfaced with any other
//            set of programs that are able to provide it with a 'metdata' file.
//            5) The batch part of the program, the LWWKD.C & LWWKDBAT.C modules,
//            owes many of its modifications to the work of Lionel Gardenal of
//            Le Groupe Informission Inc.  The two modules have been changed so
//            that they produce a file containing the vertical refractive index
//            profiles (MP_R_xxx) for wavelengths in visible, infrared or radar
//            bands under given weather meteorological conditions and sea state.
//            It also produces a file containing vertical profiles of main
//            meteorological parameters (TDPxxx).  Finally, it creates a file
//            (RFCOND or IRCOND) containing values of the internal parameters of
//            the used model. This latter is the Wavy WKD boundary layer model
//            developed at DREV.  Evaluation of atmospheric stability is based
//            the value of the Monin-Obukhov length.
//             a) The following run-time arguments have been added to LWWKD.C
//                -A : Append; The log file information will also be appended
```

```
//                    if in Log mode (see -L). If A is not specified,
//                    1.the previous output messages file will be erased.
//                    2.Log file will be first reseted.
//                -C : Conditional; If in Append mode and if a previous program
//                    has already been exited this one will also be stopped.
//                    No effect if not in Append mode since the message file
//                    will first be erased.
//                -L : Log; Information normally sent to the output screen will
//                    be sent to a log file instead. No interaction with user.
//                    Abnormal execution messages will be sent to the output
//                    message file and log file. (see also -A arg.)
//             b) Modifications of 1997-04-03 (Lionel Gardenal, Informission)
//                Profile of water vapour density is replaced by the profile of
//               relative humidity in TDPxxx output file.
//             c) Modifications du 1997-07-11 (Lionel Gardenal, Informission)
//                When the input values are outside valid range, LWWKD displays
//                a Monin-Obukhov length equal to 9999.99; furthermore, the
//                TDPxxx file contains constant values for the meteorological
//                profiles. These values are equals to measured data as read
//                by LWWKD from the METDATA file.
//             d) Modifications du 1997-07-22 : (Lionel Gardenal, Informission)
//                TDPxxx files contains scalar values of measured wind speed
//                (instantaneous and mean value on 24h), visibility and air
//                mass parameter.  These parameters are used by MERGPROP.
//             e) Modifications du 1997-07-30 : (Jean Gilbert, Informission)
//                Adding of running options to the program permetting to redirect
//                output to a log file and to send copy abnormal messages to a
//                message file.
//             f) Modifications du 1998-08-19 : (Lionel Gardenal, Informission)
//                A new process has been integrated. It is called when the WKD
//                model doesn't converge. It consists of increasing the wind
//                speed until a solution is obtained (convergence).
// Sept. 29, 1998
// Ver. 7.01  1) Added a new graph type so that one can now plot the dependence
//            of the fit parameters against changes in von Karmen's constant.
//            2) Added a new parameter to the PARAM structure.  The new parameter
//            is the wind speed at the surface.  For the moment it is set to zero
//            and can not be changed from within the program.  The only way to
//            change it is by recompiling the program.
// Oct. 9, 1998
// Ver. 7.02  1) Changed B coefficient for radar to 373256/T.
//            2) Corrected A coefficients used with the refractivity structure parameter.
//            Previous values were 77.7, 77.5, 77.5 & 78.5 instead of 78.5, 77.7, 77.5 &
//            77.5 for the VIS, NIR, MIR & FIR respectively.
//            3) Modified calculation of duct height used in batch mode.  Added
//            a new routine "duct_height" and modified "save_mp_h".
// Oct. 16, 1998
// Ver. 7.03  1) Corrected stability/error output in batch mode when a fit is found
//            by modifying the wind speed.
// Oct. 27, 1998
// Ver. 7.04  1) Modified the RF refractivity's B coefficient to agree with Bean & Dutton.
//            Thus the B coefficient is now '72 + 3.75E5/T'.
// Nov. 13, 1998
// Ver. 7.05  1) Corrected error in loading a previous created "lwwkd" saved file.
// Mar. 3, 1999
// Ver. 7.06  1) Corrected error noticed by Espen Lippert, of Norway, pertaining to our
//             B coefficients.  As a result we have changed the values in this version.
//             The change is less than 1% in the visible, near and mid IR and about 20%
//             in the far IR.
// May 4, 1999
// Ver. 7.07  1) Add output of a file containing structure parameter profiles (C2N, etc.).
//            2) Change structure parameter graphs so that they allow the user to choose
//            the x-axis range and the number of data points. */
//            3) Corrected values of coindex output by "save_mp_h" when their is no fit.
//            4) A second compiling option has been added to the program for operation in
```

```
//            batch mode.  By setting the WKDCN2 definition to (1), the program is
//            compiled so that it functions like the WKDCN2 routine in IRBLEM.  If set to
//            (0) it is compiled so that it functions like the LWWKD routine in IRBLEM.
//            Note: this compiling option is only valid when it's compiled in BATCH mode.
//            Note: can not use the wavy model.
//            5) For INTERACTIVE compilation the BATCH mode also produces profiles of the
//            the structure parameters.
// June 10, 1999
// Ver. 7.08  1) Corrected error in Cn2 calculation.  The program was subtracting the
//            the cross-term Ctq instead of adding it.  I.E. the -2 was changed to +2.
//            2) Also changed all C++ style comments to C style comments.
// June 15, 1999
// Ver. 7.09  1) Mike Duffy added a user-configurable parameter file (LWWKD.INI).  It
//            allows the modification of Kel_cel, Mair, Mwater, R, g  gamm, cp, Kconst,
//            p_adiab, max_height, pot_mode, and scale_mode.  More will be added at a
//            later date.
//            2) The routine Runmode was moved from LWWKDBAT.C to LIBERROR.C.  Other minor
//            changes were also made to Mike's original code.
```

UNCLASSIFIED

INTERNAL DISTRIBUTION

DREV - TR - 1999-099

1 - Director General

1 - Deputy Director General

1 - Chief Scientist

6 - Document Library

2 - J.L. Forand (author)

1 - C/SASAC

1 - D. Dion

1 - Guy Boivin

1 - J-M. Thériault

1 - L. Bissonnette

1 - V. Larochelle

1 - G. Fournier

1 - M. Duffy

1 - Luc Gauthier

1 - Lionel Gardenal

EXTERNAL DISTRIBUTION

DREV - TR - 1999-099

2 - DRDIM

1 - DRDB

1 - ICIST

1 - DTIC

1 - DREO

1 - DREA

1 - Dr. Doug Jensen
SPAWARSYSCEN San Diego D883
49170 Propagation Path
San Diego, CA
U.S.A 92152-7385

1 - Dr. Karin Stein
Forschungsinstitut fuer Optik
Schloss Kressbach
D-7400 Tübingen 1
Germany

1 - Dr. Yvonnick Hurtaud
Centre d'électronique de l'armement
Division ASRE
35170 Bruz
France

1 - Dr. Jacques Claverie
Centre de recherche des écoles de Coétquidan
56381 Guer Cedex
France

1 - Dr. Arie de Jong
Physics and Electronics Laboratory TNO
P.O. Box 96864
2509 JG The Hague

9a. PROJECT OR GRANT NO. (Please specify whether project or grant) 1ab11	9b. CONTRACT NO.
10a. ORIGINATOR'S DOCUMENT NUMBER	10b. OTHER DOCUMENT NOS N/A
11. DOCUMENT AVAILABILITY (any limitations on further dissemination of the document, other than those imposed by security classification)	

The Netherlands

1 - Dr. K.L. Davidson, Code MR/Ds
Meteorology Department
Naval Postgraduate School
589 Dyer Road RM254
Monterey, CA 93493-5114

1 - Dr. Tom Low
KelResearch Corporation
850-A Alness Street, Suite 9
Downsview, Ontario
Canada M3J 2H5

1 - Espen Lippert
Norwegian Defence Research Establishment
Division for Electronics
PO Box 25
N-2007 Kjeller
Norway

DOCUMENT CONTROL DATA

1. ORIGINATOR (name and address)	2. SECURITY CLASSIFICATION (Including special warning terms if applicable)
Luc Forand SASAC DREV	UNCLASSIFIED

3. TITLE (Its classification should be indicated by the appropriate abbreviation (S, C, R or U)
The L(W)WKD Boundary Layer Model: Version 7.09

4. AUTHORS (Last name, first name, middle initial. If military, show rank, e.g. Doe, Maj. John E.)
J. L. Forand

5. DATE OF PUBLICATION (month and year)	6a. NO. OF PAGES	6b. NO. OF REFERENCES
March 1999	81	25

7. DESCRIPTIVE NOTES (the category of the document, e.g. technical report, technical note or memorandum. Give the inclusive dates when a specific reporting period is covered.)
Report

8. SPONSORING ACTIVITY (name and address)

9a. PROJECT OR GRANT NO. (Please specify whether project or grant)	9b. CONTRACT NO.
1ab11	

10a. ORIGINATOR'S DOCUMENT NUMBER	10b. OTHER DOCUMENT NOS
	N/A

11. DOCUMENT AVAILABILITY (any limitations on further dissemination of the document, other than those imposed by security classification)

- ☒ Unlimited distribution
- ☐ Contractors in approved countries (specify)
- ☐ Canadian contractors (with need-to-know)
- ☐ Government (with need-to-know)
- ☐ Defense departments

12. DOCUMENT ANNOUNCEMENT (any limitation to the bibliographic announcement of this document. This will normally correspond to the Document Availability (11). However, where further distribution (beyond the audience specified in 11) is possible, a wider announcement audience may be selected.)

13. ABSTRACT (a brief and factual summary of the document. It may also appear elsewhere in the body of the document itself. It is highly desirable that the abstract of classified documents be unclassified. Each paragraph of the abstract shall begin with an indication of the security classification of the information in the paragraph (unless the document itself is unclassified) represented as (S), (C), (R), or (U). It is not necessary to include here abstracts in both official languages unless the text is bilingual).

The objective of this report is to bring up to date the present state of DREV's L(W)WKD program. Important changes to the L(W)WKD program have recently been made as a result of exchanges of both models and experimental data between Canada and France during the last few years. This has led to an agreement on a common set of equations and options that are somewhat different from those used in earlier versions of L(W)WKD and in earlier versions of the French model, PIRAM.

The first part of the report discusses changes to the basic scaling equations that are used in the L(W)WKD model, and the iterative method used by DREV. It also discusses changes to the equations that relate the parameters produced by the basic scaling equations to meteorologi-cally important parameters, and to the model used to calculate the refractive index profiles from the visible to the far infrared. The second part describes the additions and changes to the program's modes of operation-, its new options, outputs, and compilation modes. The third part of the report presents some typical examples of the results obtainable using the program. Finally, some conclusions and future improve-ments to the program are discussed.

#511546

14. KEYWORDS, DESCRIPTORS or IDENTIFIERS (technically meaningful terms or short phrases that characterize a document and could be helpful in cataloguing the document. They should be selected so that no security classification is required. Identifiers, such as equipment model designation, trade name, military project code name, geographic location may also be included. If possible keywords should be selected from a published thesaurus, e.g. Thesaurus of Engineering and Scientific Terms (TEST) and that thesaurus-identified. If it is not possible to select indexing terms which are Unclassified, the classification of each should be indicated as with the title.)

Refraction, MAPTIP, maritime boundary layer, marine boundary layer, similarity theory, structure parameters